

# **EVALUATION OF HIGH TEMPERATURE GAS COOLED REACTOR FUEL PARTICLE COATING FAILURE MODELS AND DATA**



**Office of Nuclear Reactor Regulation  
U. S. Nuclear Regulatory Commission**

Available from  
National Technical Information Service  
Springfield, Virginia 22161  
Price: Printed Copy \$5.50 ; Microfiche \$3.00

# **EVALUATION OF HIGH TEMPERATURE GAS COOLED REACTOR FUEL PARTICLE COATING FAILURE MODELS AND DATA**

Michael Tokar

Manuscript Completed: October 1976  
Date Published: November 1976

Core Performance Branch  
Division of Systems Safety  
U. S. Nuclear Regulatory Commission  
Washington, D. C. 20555



### Acknowledgements

Several individuals have made significant contributions to this document. In particular, acknowledgement is due David Rubinstein for his contribution to the statistical analysis. Richard E. Ireland and Robert A. Clark deserve special credit for editing the manuscript. Denwood F. Ross, Assistant Director for Reactor Safety, provided moral support for this study from its inception.



### Abstract

HTGR fuel particle coating failure models, used to calculate fission product source terms, were evaluated in terms of the data employed in developing the models. Of the two types of reference particles, (1) TRISO UC<sub>2</sub> and (2) BISO ThO<sub>2</sub>, the TRISO particle performance has been better demonstrated, but the irradiation test data for both types of particles, for steady state as well as transient conditions, are, in general, too sparse to permit significant statistical analyses. Modifications to the models, in the form of added conservatisms to compensate for 1) uncertainties in the data and 2) lack of complete understanding of the interrelationships of coating fabrication, structure and performance in reactor, are proposed. The modified models are proffered as interim guides which can be used for scoping studies and component design until new data become available.

	<u>Page</u>
I. Introduction. . . . .	1
II. Background. . . . .	2
A. General . . . . .	2
B. History of the Derivation of Source Terms for the Design. . . . .	
Basis Fission Product Release Accident in the HTGR. . . . .	3
C. HTGR Fuel Particles . . . . .	13
1. Description . . . . .	13
2. Relationship of Coating Failure to Fission Product. . . . .	
Release Rates . . . . .	13
3. Fuel Design Approach. . . . .	17
4. HTGR Fuel Particle Failure Mechanisms and Models. . . . .	18
a. Amoeba Effect (Kernel Migration) . . . . .	21
b. Pressure Vessel Failure . . . . .	25
c. Fission Product Attack of the SiC Layer . . . . .	32
d. Defective (Imperfect As-fabricated) Fuel. . . . .	32
III. Discussion. . . . .	37
A. TRISO UC <sub>2</sub> Particles. . . . .	37
1. Defective (Imperfect As-fabricated) Fuel. . . . .	37
a. GA Model. . . . .	37
b. NRC Analysis. . . . .	37
2. Pressure Vessel Failure . . . . .	38
a. Off-Specification Fuel (Temperatures $\leq 1250^{\circ}\text{C}$ ) . . . . .	38
1) GA Model. . . . .	38
2) NRC Analysis. . . . .	39
b. Fuel at Temperatures $> 1250^{\circ}\text{C}$ . . . . .	49
1) GA Model. . . . .	49
2) NRC Analysis. . . . .	50



3.	Failure Induced by Fission Product Attack of the SiC Layer.	54
a.	GA Model.	54
b.	NRC Analysis.	57
	1) Peak Burnup Particles (78% FIMA).	58
	2) Low Burnup Particles ( $\leq 20\%$ FIMA).	59
	3) Intermediate Burnup Particles ( $>20\% < 78\%$ FIMA)	60
4.	Kernel Migration Failure	65
a.	GA Model	65
b.	NRC Analysis	65
B.	BISO ThO <sub>2</sub> Particles.	68
1.	Defective (Imperfect As-fabricated) Fuel	68
a.	GA Model	68
b.	NRC Analysis	68
2.	Pressure Vessel Failure.	69
a.	Off-Specification Fuel (Temperatures $\leq 1250^{\circ}\text{C}$ ).	69
	1) GA Model	69
	2) NRC Analysis	69
b.	Temperatures $> 1250^{\circ}\text{C}$	72
	1) GA Model	72
	2) NRC Analysis	72
	a) Peak Burnup Particles (7.5% FIMA).	72
	b) Low Burnup Particles ( $\leq 2.5\%$ FIMA and Temperatures $> 1350^{\circ}\text{C}$	76
	c) Intermediate Burnup Particles ( $> 2.5\% < 7.5\%$ FIMA) ( $> 3.0 \times 10^{21} < 8 \times 10^{21} \text{ n/cm}^2$ ).	77
3.	Kernel Migration	77
a.	GA Model	77
b.	NRC Analysis	79

IV. Proposed NRC HTGR Fuel Particle Interim Failure Model Requirements . 79

A. TRISO UC<sub>2</sub> Particles . . . . . 79

1. Defective (Imperfect As-fabricated) Fuel . . . . . 79

2. Pressure Vessel Failure . . . . . 79

a. Temperatures  $\leq 1250^{\circ}\text{C}$  (Off-Specification Fuel) . . . . . 79

b. Temperatures  $> 1250^{\circ}\text{C} \leq 1500^{\circ}\text{C}$  ( $\geq 20$  FIMA) or  $\leq 1600^{\circ}\text{C}$   
( $< 20\%$  FIMA) . . . . . 80

3. Pressure Vessel Failure and SiC-Fission Product Attack . . . . . 80

a. Peak Burnup Particles (78% FIMA and Temperatures  
 $> 1500^{\circ}\text{C}$ ) . . . . . 80

b. Low Burnup Particles  $\leq 20\%$  FIMA and Temperatures  
 $> 1600^{\circ}\text{C}$ ) . . . . . 81

c. Intermediate Burnup Particles ( $> 20\% < 78\%$  FIMA) . . . . . 81

4. Kernel Migration Failure . . . . . 82

B. BISO ThO<sub>2</sub> Particles . . . . . 83

1. Defective (Imperfect As-fabricated) Fuel . . . . . 83

2. Pressure Vessel Failure . . . . . 83

a. Temperatures  $\leq 1250^{\circ}\text{C}$  . . . . . 83

b. Temperatures  $> 1250^{\circ}\text{C}$  . . . . . 83

1) Peak Burnup Particles (7.5% FIMA) . . . . . 83

2) Low Burnup Particles ( $\leq 2.5\%$  FIMA and Temperatures  
 $> 1350^{\circ}\text{C}$ ) . . . . . 84

3. Kernel Migration Failure . . . . . 84

	<u>Page</u>
V. Application and Licensing Significance . . . . .	85
A. SORS and the MHFPR . . . . .	85
1. General Approach . . . . .	85
2. TRISO Failure Curves . . . . .	89
3. BISO Failure Curves . . . . .	90
4. Licensing Significance . . . . .	91
B. Fuel Failure Rate During Plant Operation . . . . .	93
1. General Considerations . . . . .	93
2. Fission Weighting and Effective Core Average Failed Fuel Fraction . . . . .	96
VI. Summary and Conclusions . . . . .	100
VII. References . . . . .	107-108

List of Figures

Page

1.	TRISO fuel particle coating failure diagram . . . . .	5
2.	BISO fuel particle coating failure diagram . . . . .	6
3.	Fission product release as a function of time. . . . .	
4.	TRISO (Amendment 1) fuel particle coating failure diagram. . . . .	9
5.	BISO (Amendment 1) fuel particle coating failure diagram . . . . .	10
6.	TRISO (GASSAR-6) fuel particle coating failure diagram . . . . .	11
7.	BISO (GASSAR-6) fuel particle coating failure diagram. . . . .	12
8.	Large HTGR-type fuel particles irradiated beyond peak design exposures. . . . .	14
9.	Fission product release mechanisms from fuel particle to primary coolant. . . . .	15
10.	Fission product release rate versus temperature for intact and failed fuel particles during accident conditions . . . . .	16
11.	Distributions of fuel kernel diameters and buffer coating thicknesses for a typical TRISO fissile particle batch . . . . .	19
12.	Two-dimensional distribution of kernel diameter and buffer thickness for a TRISO coated particle batch with lines of con- stant end-of-life SiC stress . . . . .	20
13.	Kernel migration coefficient versus inverse temperature ( $10^4/T$ ) determined from out-of-pile thermal gradient testing of irradiated and unirradiated UC <sub>2</sub> fuel particles . . . . .	23
14.	Amoeba lifetime as a function of temperature under a thermal gradient of 0.0104°C/cm for TRISO UC <sub>2</sub> fuel having a 100- $\mu$ m thick buffer layer . . . . .	24

15. Kernel migration coefficient versus inverse temperature  
( $10^4/T$ ) for irradiated  $\text{ThO}_2$  fuel determined from in-pile  
tests conducted by ORNL and out-of-pile thermal gradient  
tests conducted by GAC. . . . . 26

16. Amoeba lifetime as a function of temperature under a thermal  
gradient of  $0.0104 \text{ C}/\mu\text{m}$  for BISO  $\text{ThO}_2$  fuel having an  $85\text{-}\mu\text{m}$ -thick  
buffer layer . . . . . 27

17. Assumed pressure vessel failure fraction versus a) fast neutron  
fluence or b) kernel burnup for TRISO  $\text{UC}_2$  fuel. . . . . 29

18. Assumed TRISO  $\text{UC}_2$  pressure vessels failure fractions (%) at  
 $1250^\circ\text{C}$  as a function of kernel burnup and fast neutron exposure . 30

19. Effect of a rapid thermal excursion from  $1250^\circ$  to  $1425^\circ$ ,  $1600^\circ$ , or  
 $1800^\circ\text{C}$  and back to  $1250^\circ\text{C}$  on pressure vessel failure in TRISO  $\text{UC}_2$   
as a function of a) fast neutron exposure or b) kernel burnup  
for fuel experiencing 78% FIMA at a fast neutron exposure of  
 $8 \times 10^{21}$  rate - GA model . . . . . 31

20. Assumed effect of a rapid thermal excursion from  $1250^\circ$  to  $1400^\circ$ ,  
 $1550^\circ$ ,  $1700^\circ$  or  $1800^\circ\text{C}$  on pressure vessel failure in BISO  $\text{ThO}_2$   
fuel as a function of a) fast neutron exposure or b) kernel  
burnup - GA model. . . . . 33

21. Particle failure observed as a function of temperature during  
isothermal heating of irradiated TRISO carbide fuels for times  
from 16 to 200 hours . . . . . 34

22. Assumed contribution to TRISO UC<sub>2</sub> fissile fuel failure fraction from particles with defective coatings as a function of fast neutron exposure a) and kernel burnup b) for fuel experiencing a peak burnup of 78% FIMA at an end-of-life fast fluence of  $8 \times 10^{21} \text{ n/cm}^2 (E \geq 0.18 \text{ MeV})$  - GA Model. . . . . 36

23. Incremental particle failure as a function of temperature during heating of irradiated TRISO carbide fuels for times less than 16 hours . . . . . 56

24. Comparison between measured and predicted values of FGR (Kr-85 ) for P13R and S fuel cells operating continuously at peak fuel rod temperatures of 1100°C (volume average temperature 1040°C). . . . 61

25. Comparison between measured and predicted values of FGR for Cell 5 of P13S which operated continuously at a peak fuel rod temperature of 1500°C (volume average temperature 1440°C) . . . . . 62

26. Comparison of FGR measured during irradiation of the P13S thermal cycling cell (#1) and predicted using fuel performance models given in GA-A12971 . . . . . 63

27. Incremental BISO ThO<sub>2</sub> particle failure as a function of temperature 75

28. TRISO particle coating failure. . . . . 87

29. BISO particle coating failure . . . . . 88

30. Fraction of fission in the TRISO particle as a function of time in the equilibrium recycle . . . . . 98

31. Effective failure fraction versus fuel age . . . . . 99

List of Tables

Page

I.	Level of Statistical Significance of Typical Coated Particle Irradiation Tests. . . . .	42
II.	Summary of TRISO Irradiation Performance Observations. . . . .	52-53
III.	Measured and Predicted Failure Fractions for Irradiated BISO ThO <sub>2</sub> Particles Heated to 2000°C in Out-of-Pile Heating Tests . . .	74
IV.	Fluence-Burnup-Age Correlation of Worst Core Location. . . . .	86





## I. Introduction

This report discusses the review of General Atomic Co. models for large high temperature gas cooled reactor (LHTGR) fuel particle coating failure and the data which are used in support of these models. In particular the review has concentrated on the fuel failure models conceived for the maximum hypothetical fission product release (MHFPR), as presented in GASSAR-6, Section 2A (Ref. 1) and the topical report on the SORS codes (Ref. 2). Fuel failure under normal plant operation, however, has also been addressed, so that the total spectrum of potential exposure from beginning-of-life (BOL) to end-of-life (EOL) has been encompassed.

The objective of this review has been to evaluate the models and data for the purpose of determining their acceptability for safety analyses related to licensing and to determine whether modifications in the models might be required. Since the fuel particle coatings serve as the primary barrier to fission product release from an HTGR (analogous to the fuel rod cladding in LWRs), knowledge of the performance of these coatings under all reactor conditions is required as a requisite to the calculation of potential fission product release from the reactor.

This report presents the NRC analysis of the GA model and data base. An attempt has been made (1) to give a brief description of the models, and (2) to describe the guidelines used by NRC reviewers in the review and modification of the models. It should be recognized that the HTGR fuel is still under development and that new data are being generated on the existing reference fuel. Moreover, the reference fuel designs may be changed. For these reasons the review of HTGR fuel models and data base must be a continuing process, and this report does not present a final, immutable position.

## II. Background

### A. General

The review and evaluation of large high temperature gas-cooled reactor (LHTGR) fission product release models, to be used for accident analyses, siting dose calculations, and design values for sizing plant components, has been a multi-faceted effort, involving the critical study of several licensing reports and submittals (Refs. 1-9). These reports are interrelated so that the review of one report often requires the review of one or more other reports as requisites to a complete understanding of the subject matter. The analysis of the so-called "maximum hypothetical fission product release" (MHFPR), has, for example, involved the review of sections of GASSAR (Ref. 1), the Summit and Fulton preliminary safety analysis reports (PSAR's) (Refs. 8, 9) and the topical report describing the SORS codes (Ref. 2). But the SORS report uses a fuel failure model which is described in General Atomic report GA-A12971 (GA-LTR-15), (Ref. 3), and which has, in turn, been supplemented by a recent General Atomic (GA) memorandum (Ref. 4), to calculate the release of fission products from failed fuel into the coolant. Moreover, the rate of fuel failure is a function of temperature history; this is calculated by the CORCON code (Ref. 5), which is itself under review as a topical report. Since each topical report and licensing submittal is supported by numerous references, which require careful study, it becomes obvious that the review and analysis of fission product release and transport in LHTGRs is a complex process.

The fission product release model proposed by GA for LHTGRs is summarized in Chapter 5, "Fission Product Release", of the SORS topical report. The model has 4 main parts: 1) fuel particle coating failure; 2) release from fuel particles; 3) transport through graphite; and 4) release to coolant. This evaluation report is concerned primarily with the fuel particle coating failure model, since it is the lead (and most complex) portion of the overall release model. The remaining portions of the fission product release model will be dealt with in subsequent reports.

B. History of the Derivation of Source Terms for the Design Basis Fission Product Release Accident

The NRC staff first adopted an MHFPR model for the Fort St. Vrain plant. Subsequent development occurred as part of the safety evaluations of the Summit and Fulton plants. A PCRV-depressurization and concomitant loss of forced circulation of coolant accident and the resulting fission product source term that were used for these plant evaluations were presented in Appendix C of the Summit and Fulton PSARs (Refs. 8, 9). During the year 1974, the Accident Analysis and Gas Cooled Reactor Branches of AEC-Regulatory worked together to develop an appropriate fission product source term for use in the NRC staff's evaluation. The effort culminated in a meeting (Ref. 10) held between the NRC staff and representatives of General Atomic and the utilities and engineering firms associated with the Summit and Fulton plants. At the meeting the staff presented its "interim" fission product release model for the MHFPR.

For its analysis of the MHFPR the staff used figures for fuel particle coating failure (Figs. 1 & 2) which were taken from the SORS topical report (Ref. 2) and the Fulton PSAR (Ref. 9). The figures, for TRISO and BISO fuel failure, show regions of temperatures for coating failure, with no failures until a boundary representing a combination of irradiation time and temperature is reached. Across the band of temperatures and irradiation times, failure was assumed, by GA, to increase linearly with temperature until the 100% failure line is reached. The staff, in its interim model (Ref. 11), took the lowest temperature at which each age fuel would begin to fail and considered these fuel failure threshold temperatures as the temperatures at which 100% of the fuel would fail instantaneously. For example, 4-year old fuel would all fail instantaneously at ~1020°C whereas 2-year old fuel would fail at ~1190°C. These fuel failure temperatures were coupled with calculations, provided by Oak Ridge National Laboratory (Ref. 12), of the temperature history of the hottest 1/4 of the Summit core during a loss-of-forced circulation (LOFC) accident, to provide an interim model for fission product release. The resultant model assumed release to the containment of the same fractions as specified for LWR's in Regulatory Guides 1.3, 1.4, and 1.7, viz. 100% of noble gases, 50% of iodines, for which an instantaneous plateout factor of 2 is assumed, (resulting in 25% of the iodines available for leakage from the containment atmosphere), and 1% of the solids. As a simplifying approximation the time-dependent release was further assumed to occur in two distinct steps (related to fuel temperatures):

- a) the first step of 40% of the total release at one hour after shutdown and loss-of-cooling, and
- b) a second step of 60% of the total release at two hours after shutdown.

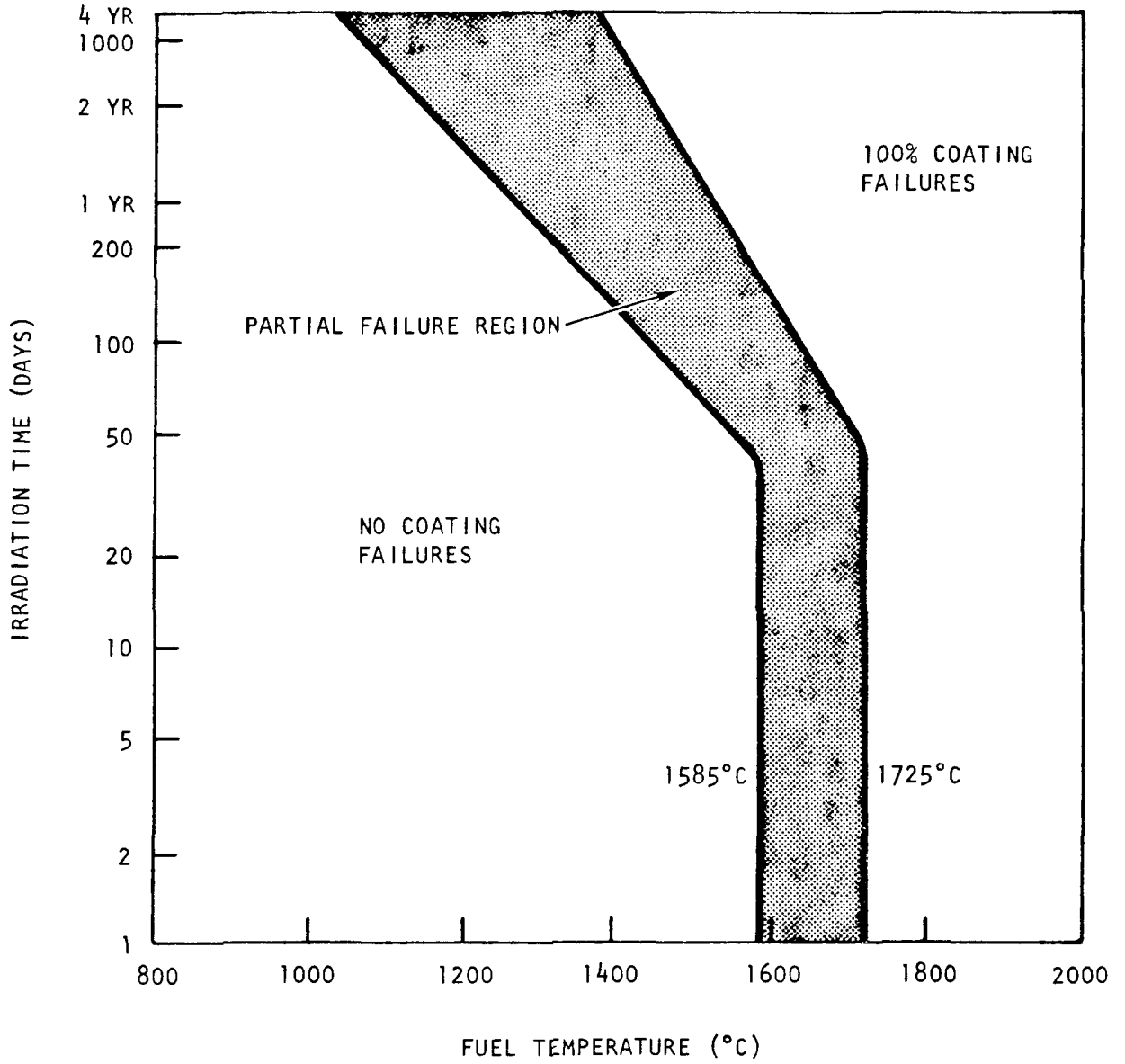


Fig. 1. TRISO fuel particle coating failure diagram (from reference 2)

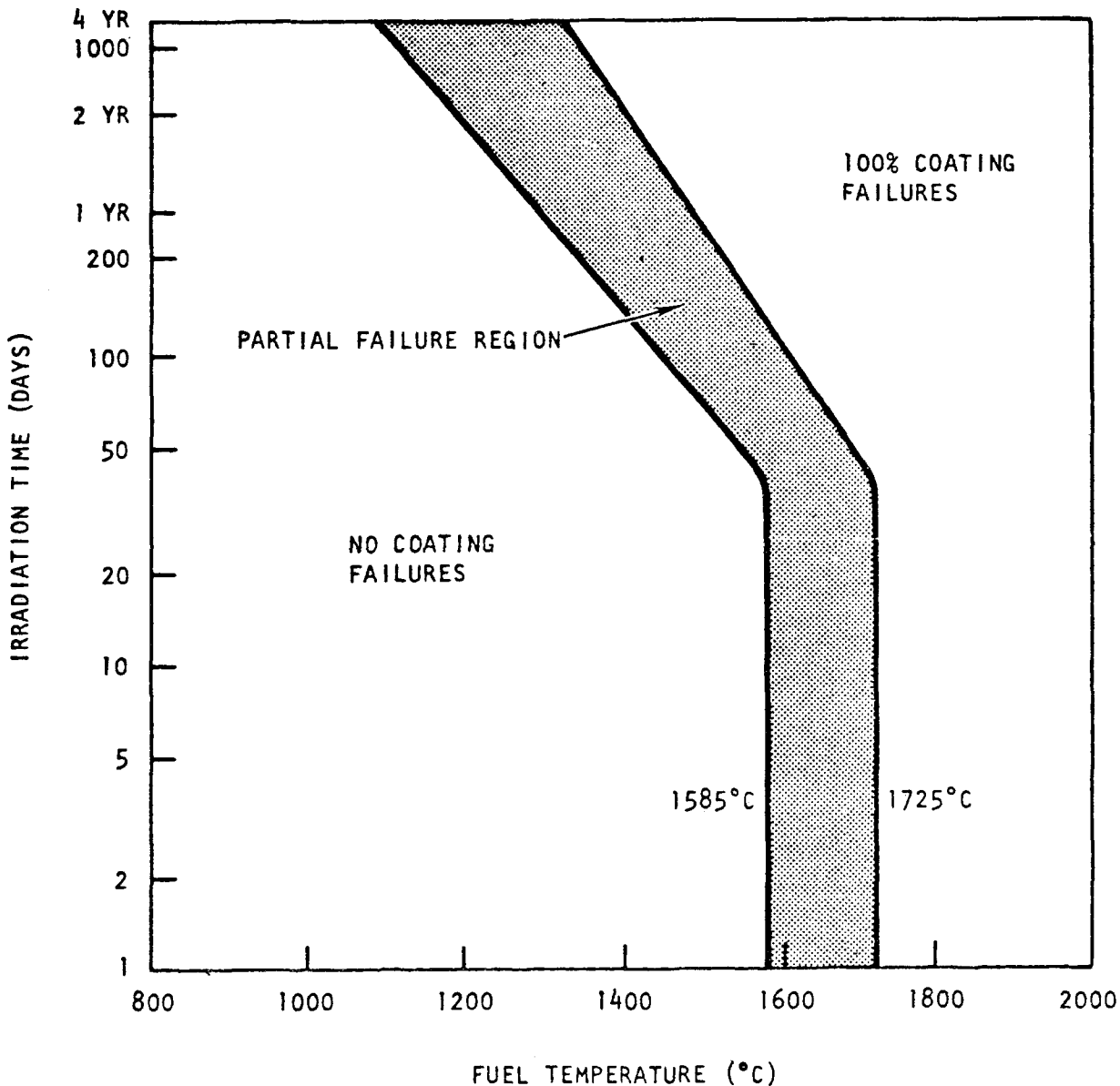


FIGURE 2. BISO FUEL PARTICLE COATING FAILURE DIAGRAM  
FROM FULTON GENERATING STATION  
UNITS 1 AND 2  
PRELIMINARY SAFETY ANALYSIS REPORT (Ref. 9)  
CHANGE 8 MAY 1974

These release assumptions are shown in figure 3, where the release curve is plotted and compared to the ORNL heat-up curves for 1/4 and 1/3 core models.

The staff's interim fission product release model resulted in a predicted 10% iodine release in 2 hours, as compared with 0.1% for the GA model for Summit and Fulton and 0.001% for the GA model in GASSAR. General Atomic has asserted (Ref. 4) that the fuel failure models presented in the Summit and Fulton PSAR's (Refs. 8 & 9, respectively) for use in the MHFPR analysis were based on early performance data on non-reference fuel, and that new fuel performance data are now available which show that the NRC "interim" model is overly conservative and results in unnecessarily restrictive requirements for HTGR siting.

The General Atomic model for TRISO and BISO fuel particle coating failure has gone through successive modifications. The original figures for TRISO and BISO coating failure (Figs. 1 & 2, respectively) were replaced in the SORS report by figure 4 for TRISO fuel, and figure 5, for BISO fuel. These figures for fuel failure as a function of temperature and age, presented in Amendment 1 to the SORS report, were purportedly based on data and models presented in the GA report on fuel particle behavior under normal and transient conditions (Ref. 3). The description of the MHFPR presented in GASSAR Appendix 2A, however, uses a third set of figures (Figs. 6 & 7). The latter figures show fuel failure rates which are considerably lower than the rates shown in the SORS Amendment 1 figures.

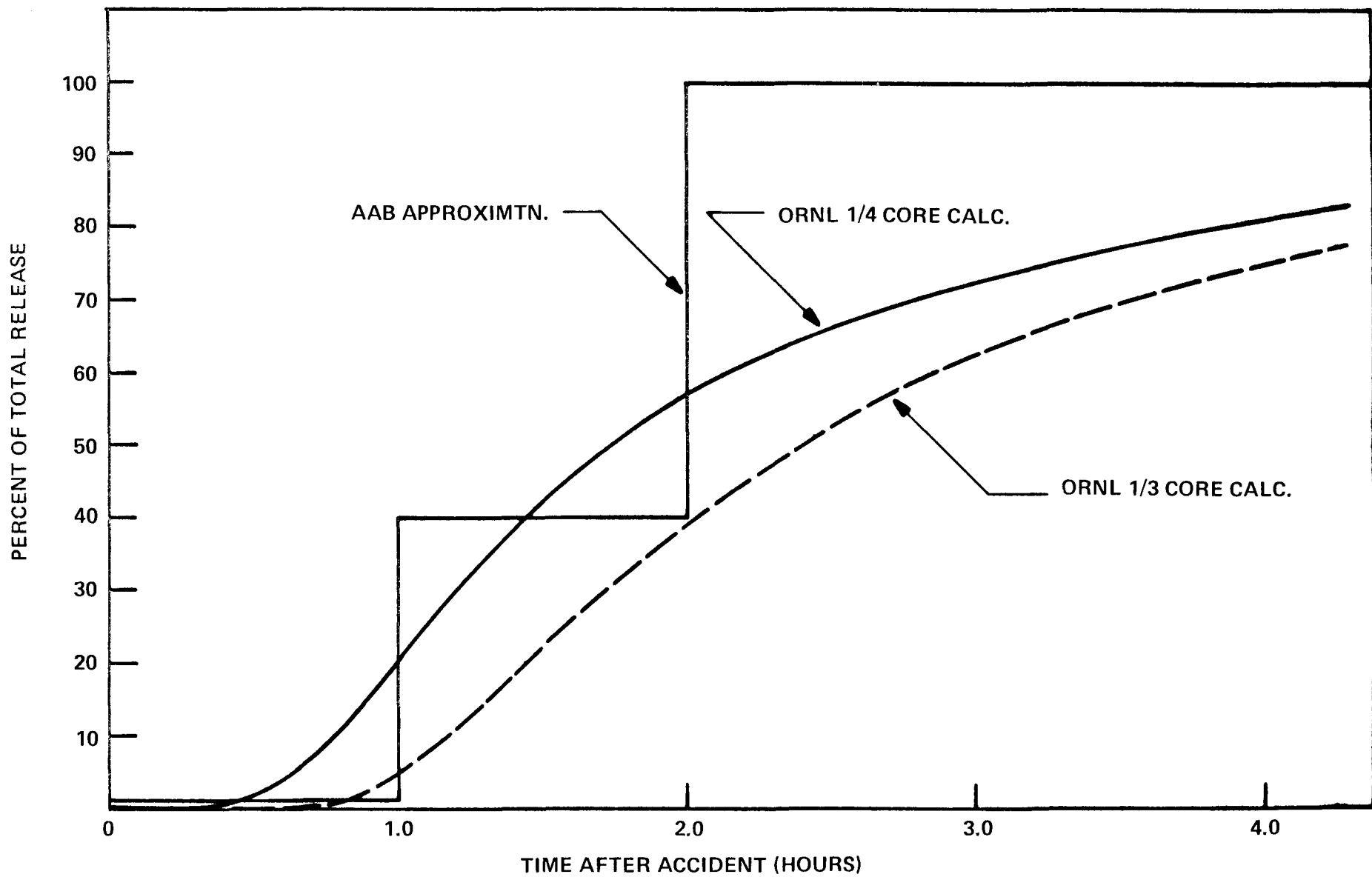


Fig. 3 Fission Product Release as a Function of Time



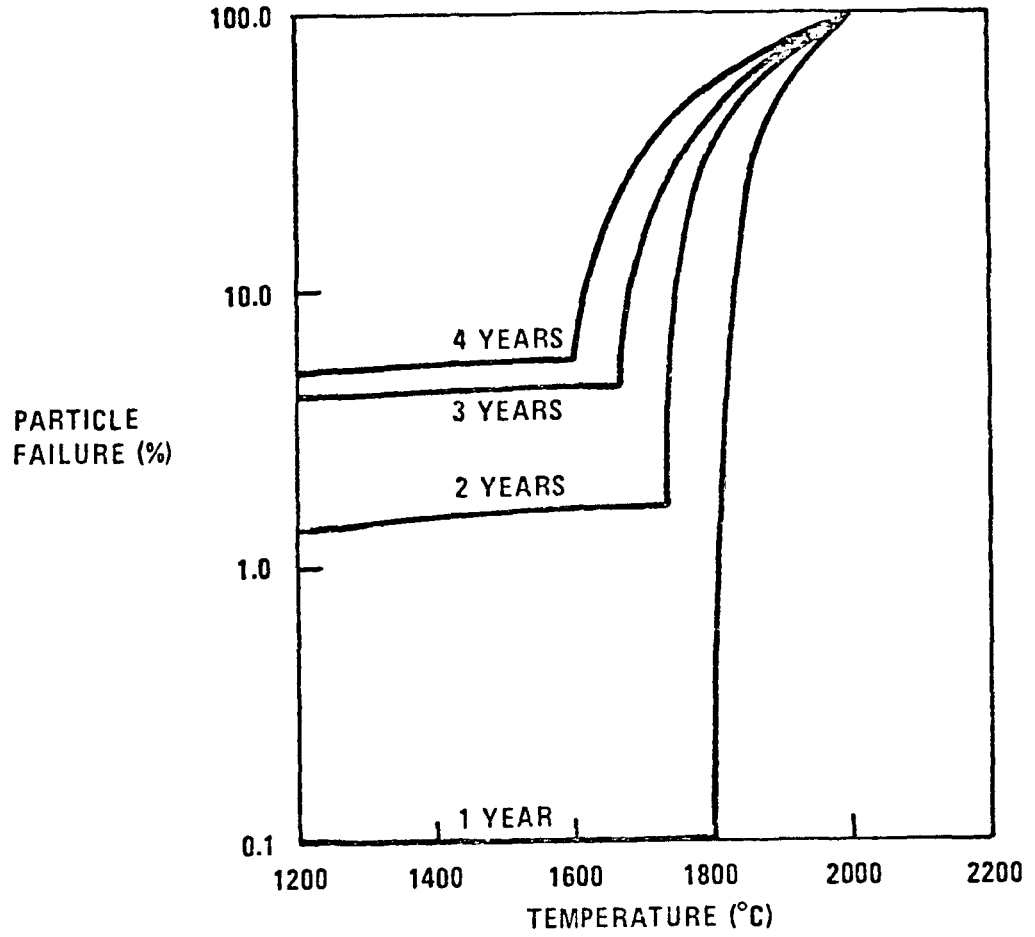


Fig. 4. TRISO fuel particle coating failure diagram

From Amendment 1, Reference 2  
February, 1975

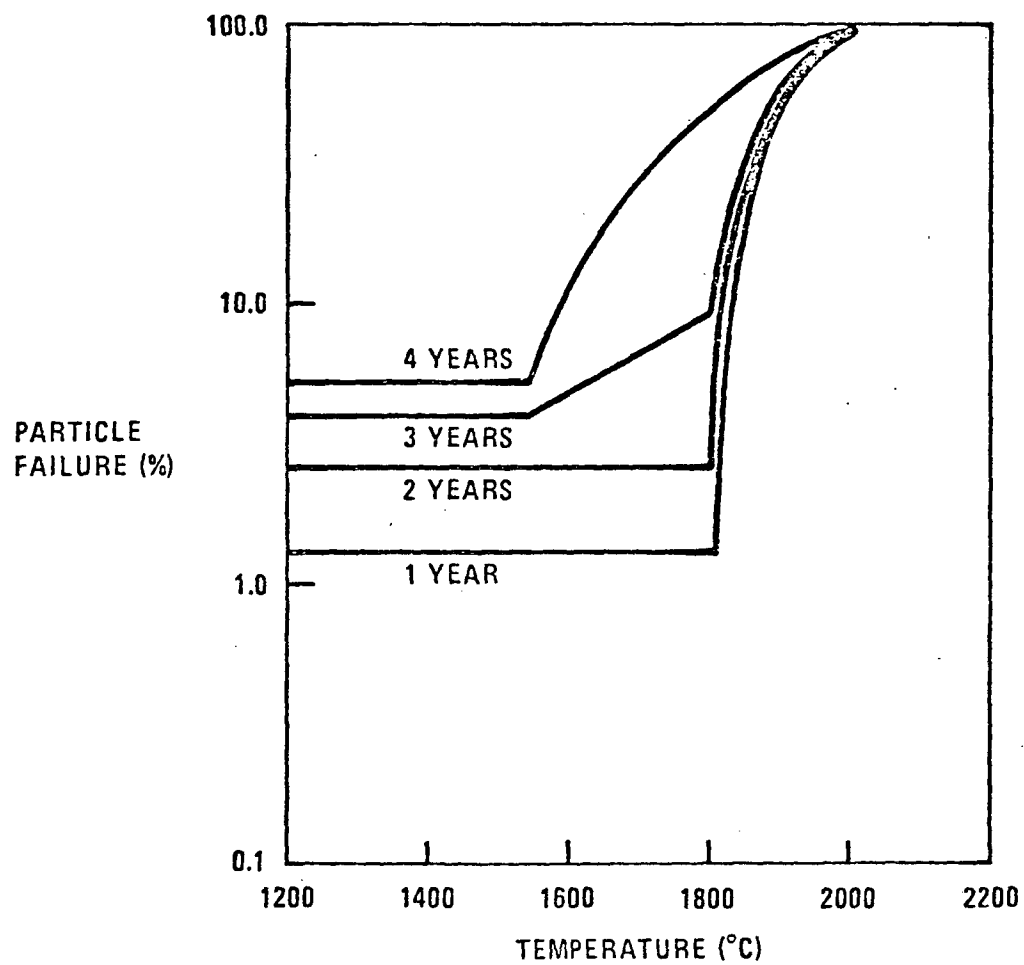


Fig. 5. BISO fuel particle coating failure diagram

From AMENDMENT 3, Reference 1  
July 18, 1975

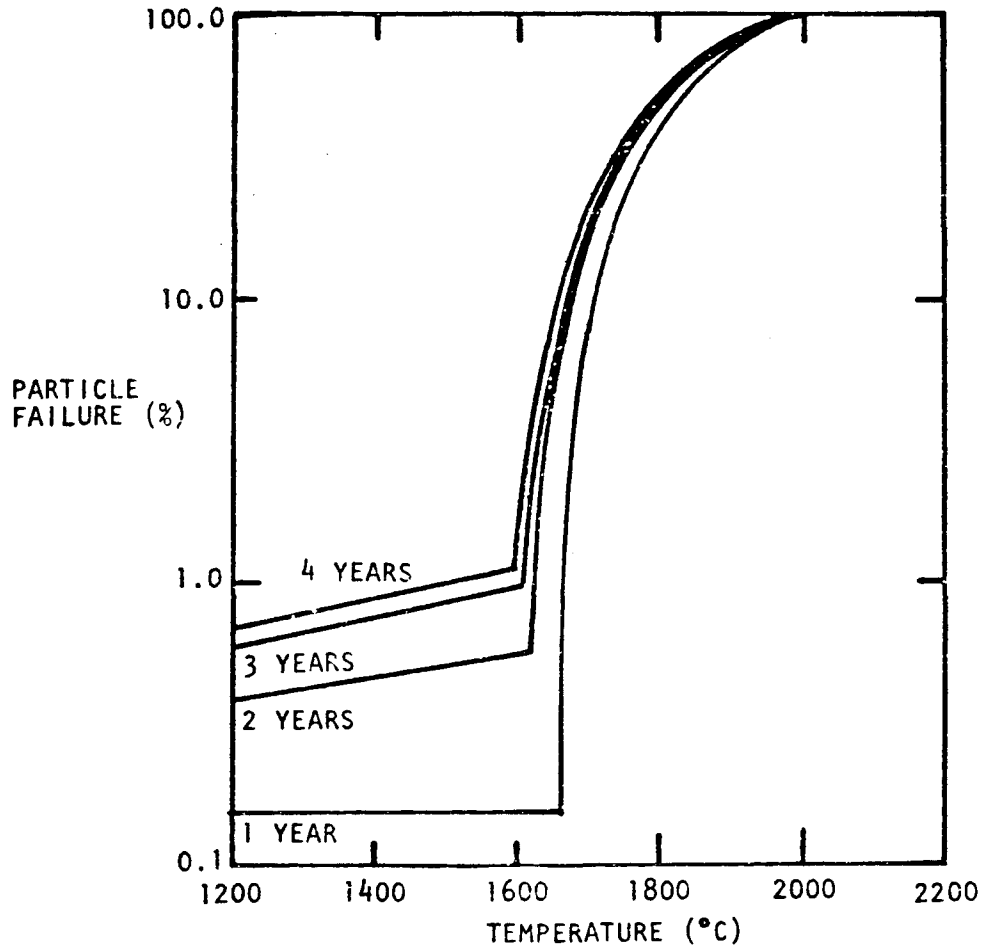


Figure 6 TRISO FUEL PARTICLE COATING FAILURE DIAGRAM

From **AMENDMENT 3**, Reference 1  
**JULY 18, 1975**

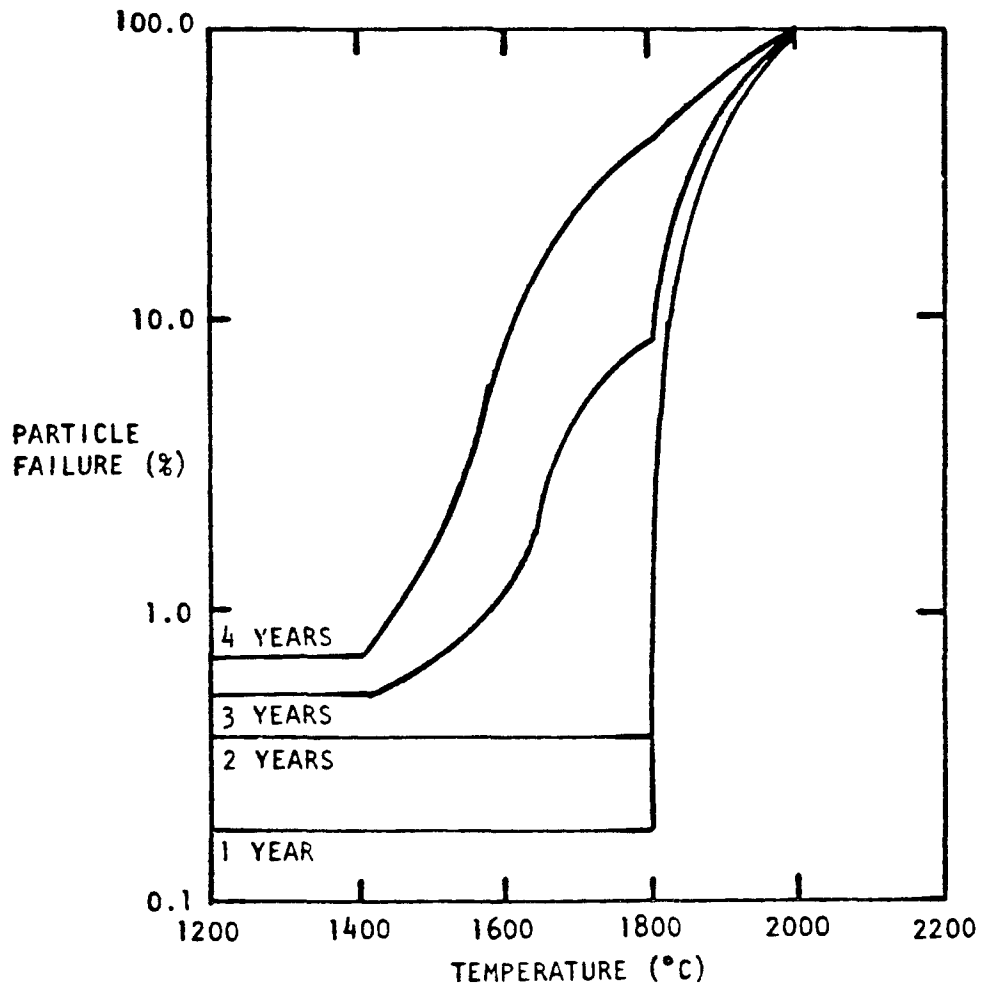


FIGURE 7 BISO FUEL PARTICLE COATING FAILURE DIAGRAM

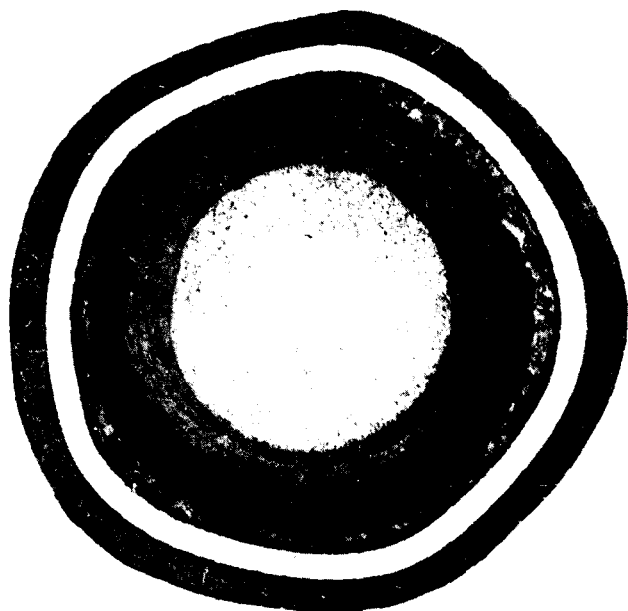
## C. HTGR Fuel Particles

### 1. Description

Examples of LHTGR fuel particles are shown in figure 8. The fertile fuel particles are BISO-coated 500  $\mu\text{m}$ -diameter  $\text{ThO}_2$  kernels. The BISO coating is made up of a low-density pyrocarbon (PyC) inner layer (buffer coat) and a higher-density PyC outer layer. The fissile fuel particles are TRISO-coated 200  $\mu\text{m}$ -diameter  $\text{UC}_2$  kernels. The TRISO coatings include a low-density PyC buffer layer, a silicon carbide (SiC) layer, and 2 higher-density PyC layers, one inside and one outside of the SiC. The buffer layer accommodates kernel swelling and provides a void volume for the accumulation of gaseous fission products. The inner dense PyC layer in TRISO coatings protects the SiC from reactions with the fuel and fission products and also provides some mechanical support. The SiC layer provides structural rigidity and a barrier to release of solid as well as gaseous fission products. The outer PyC layer of BISO coatings and the outer layer (PyC, SiC, PyC) sandwich of the TRISO coatings are essentially impermeable barriers to the release of gaseous fission products. Thus, the primary sources of release of noble gases and iodine from HTGR fuel elements are particles with failed coatings.

### 2. Relationship of Coating Failure to Fission Product Release Rates

The SORS codes developed by General Atomic model the transient process of coating failure, fission product liberation from the particles, transport through the fuel element graphite, and vaporization to the coolant channels, as illustrated in figure 9. The release characteristics of all nuclides from fuel particles, expressed as fractional release rates, are shown in figure 10. These types of fission product release functions are used by General Atomic in SORS calculations.



FISSILE PARTICLE

DESIGN

FUEL KERNEL	200 $\mu\text{m}$ $\text{UC}_2$
BUFFER	85 $\mu\text{m}$
INNER PyC	25 $\mu\text{m}$
SiC	25 $\mu\text{m}$
OUTER PyC	35 $\mu\text{m}$

IRRADIATION CONDITIONS

1350°C  
 ~70% FIMA  
 $8.0 \times 10^{21}$  n/cm<sup>2</sup> (E > 0.18 MeV)



FERTILE PARTICLE

DESIGN

FUEL KERNEL	500 $\mu\text{m}$ $\text{ThO}_2$
BUFFER	85 $\mu\text{m}$
PyC	75 $\mu\text{m}$

IRRADIATION CONDITIONS

1250°C  
 14.3% FIMA  
 $10.2 \times 10^{21}$  n/cm<sup>2</sup> (E > 0.18 MeV)

Fig. 8. Large HTGR-type particles irradiated beyond peak design exposures (From Reference 3)

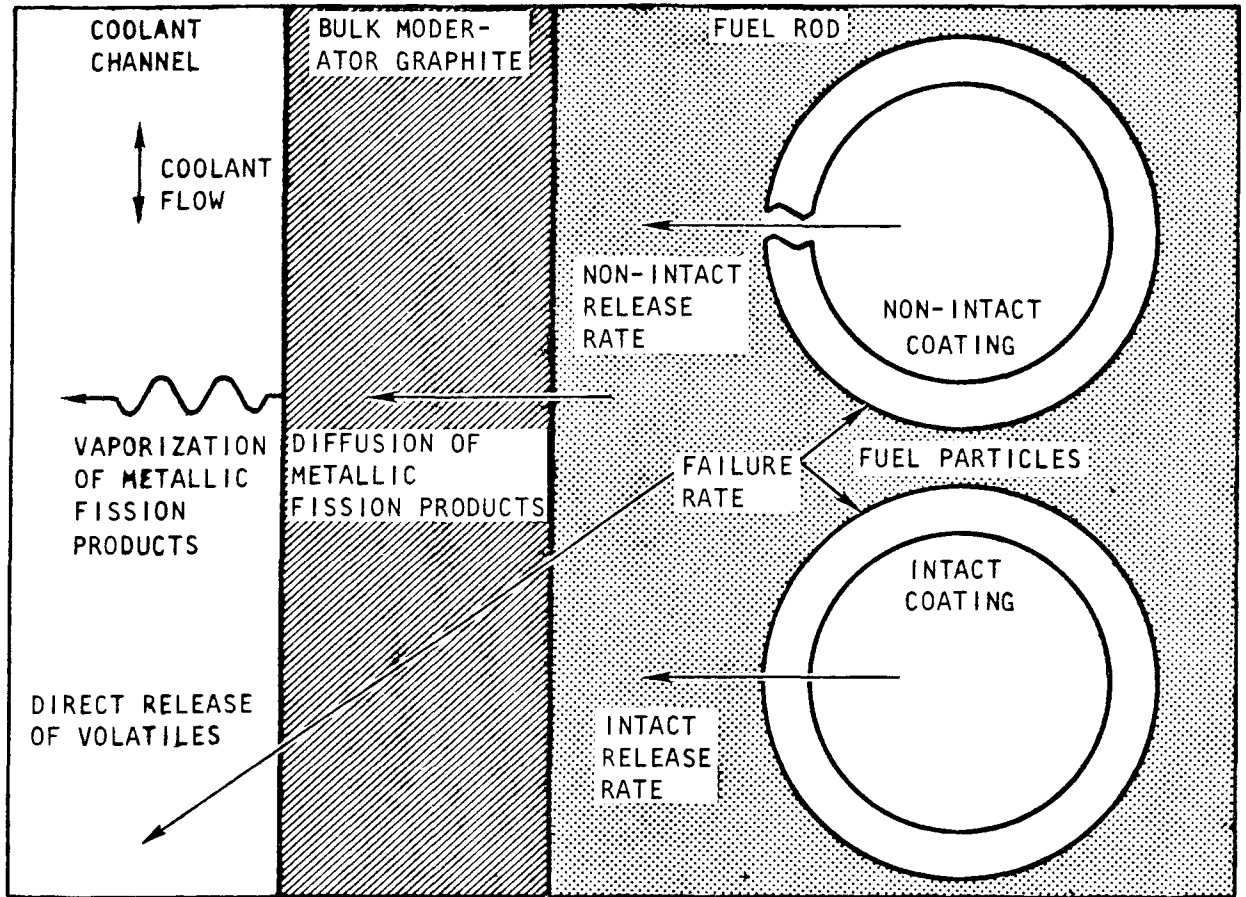


Fig. 9. Fission product release mechanisms from fuel particle to primary coolant. (From Ref. 2)

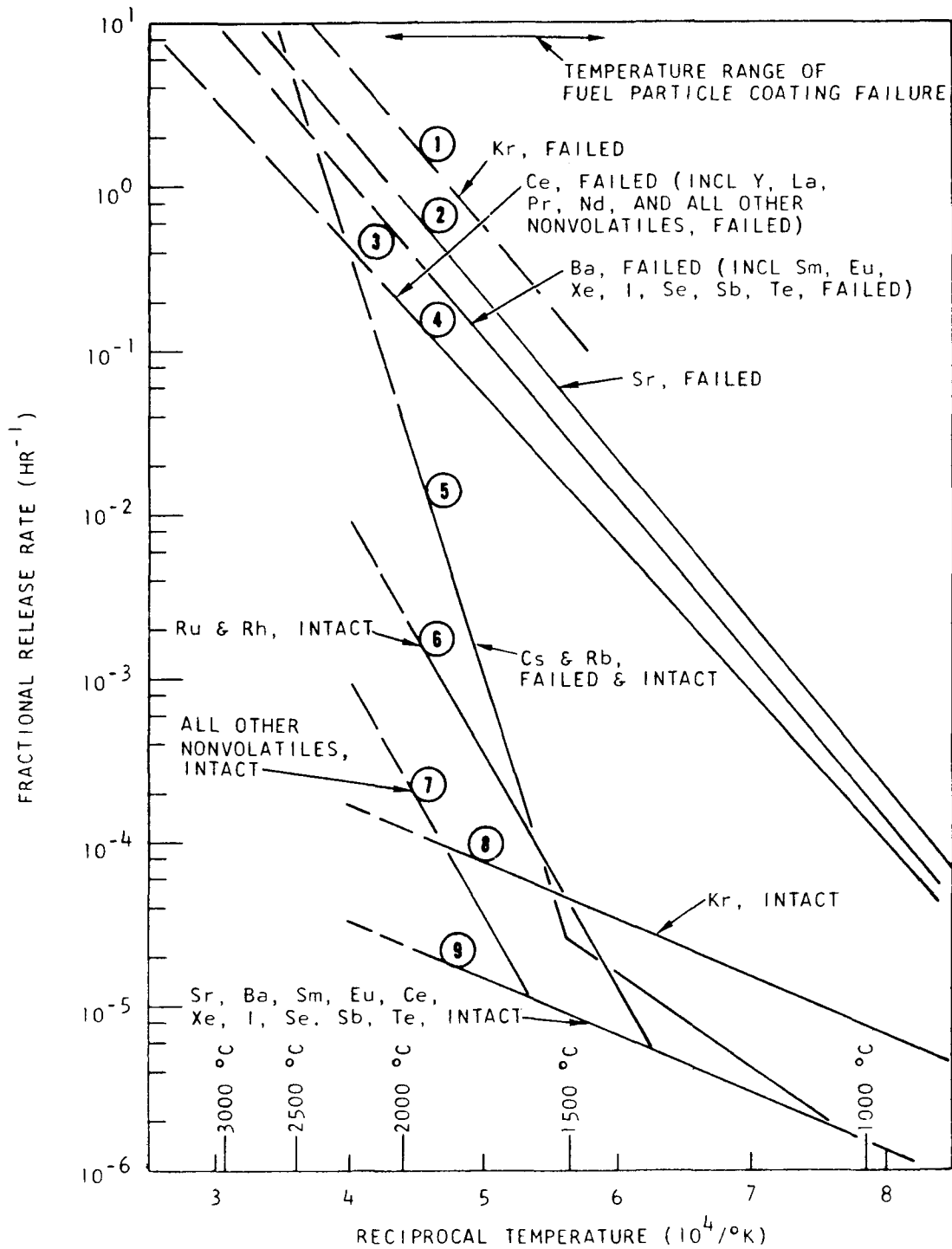


Fig. 10. Fission product release rate versus temperature for intact and failed fuel particles during accident conditions. (From Reference 2)



As shown, the fractional release of fission products from failed particles is generally an order of magnitude or more higher than from intact particles. For example, at 2000°C the fractional release of Kr is approximately 4 orders of magnitude higher than from intact particles. Accurate prediction of HTGR fuel failure, as part of the overall release model, is, therefore, of considerable importance. Its relative importance in licensing safety analysis considerations varies, however, with application and its relationship to other portions of the overall fission product release model, as discussed in a subsequent section (V) of this report.

### 3. Fuel Design Approach

The TRISO and BISO HTGR fuel particle coating designs have evolved as a result of irradiation testing of coated particles coupled with the development and application of analytical stress models (Refs. 13-16). The analytical models treat the coated particles as composite pressure vessels in which internal pressure is built up during irradiation by the accumulation of gaseous fission products in the void volume of the buffer layer. Although the models are mathematically sophisticated, they cannot be used at present as quantitative design models because of uncertainties in (1) the input data and (2) the mathematical formulation of the relationship of the precise physical mechanisms and parameter values used in the models. To compensate for these uncertainties, General Atomic adjusts the model calculations to the results of irradiation tests on fuel particles.

The analytical models indicate that fuel kernel diameter and buffer coating thickness control the fission gas pressure within a coated particle. To a first approximation, therefore, the fuel designers have assumed that these parameters control the distribution of irradiation-induced stresses in a TRISO or BISO coating layer. The distributions of fuel kernel

diameters and buffer coating thickness for a "typical" batch of coated fissile particles are shown in figure 11. This batch of coated particles reportedly had a nominal kernel diameter and buffer thickness of 200 and 100  $\mu\text{m}$ , respectively. For the same TRISO particle batch depicted in figure 11; lines of constant end-of-life SiC stress, calculated from the TRISO particle stress model (Ref. 14), are shown superimposed on a two-dimensional distribution of kernel diameter and buffer thickness in figure 12. General Atomic has reported (Ref. 15) that the irradiation performance of TRISO-coated  $\text{UC}_2$  particles correlates well with coating design when the assumption is made that only the particles with calculated SiC stresses greater than 30,000 psi have a significant probability of failure. This correlation implies that internal pressure is the dominant factor in controlling the performance of TRISO particles.

A similar approach is taken by GA with BISO particles. Estimates of BISO pressure vessel failure are made by comparing a calculated PyC coating stress distribution with an experimentally determined failure stress. As will be discussed later, however, a calculated failure stress for the outer PyC layer on BISO fuel has not been demonstrably shown to be well coupled with failure rates observed in BISO particles, particularly at high burnup.

#### 4. HTGR Fuel Particle Failure Mechanisms and Models

Other than fabrication defects, there is essentially just one dominant basic fuel failure mechanism, and that is the so-called "pressure vessel failure." This occurs when the stresses induced by fission gas pressure within the particles exceed the strength of the particle coatings. The coatings may be weakened owing to the effect of certain

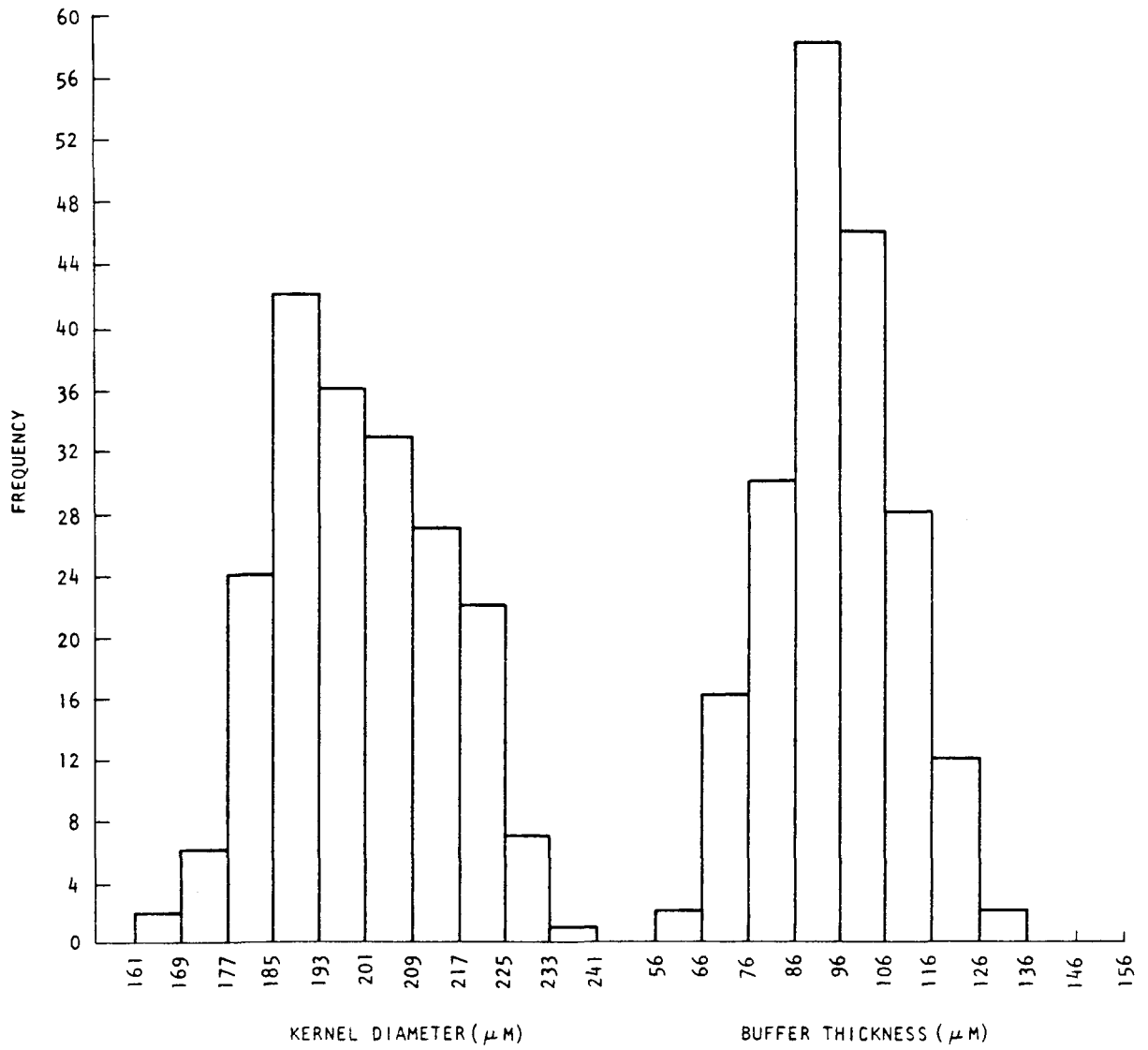


Fig. 11. Distributions of fuel kernel diameters and buffer coating thicknesses for a typical TRISO fissile particle batch (From Reference 16).

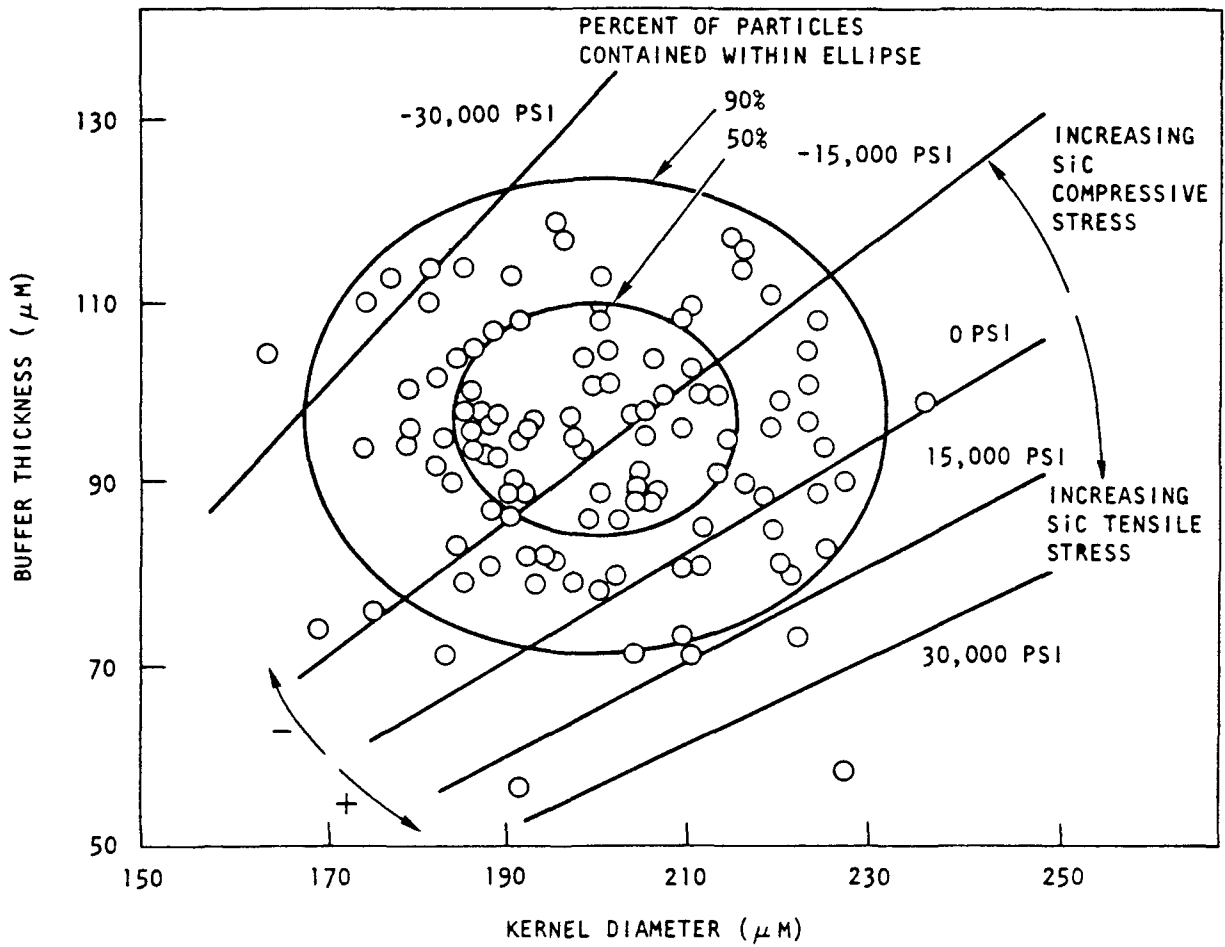


Fig. 12. Two-dimensional distribution of kernel diameter and buffer thickness for a TRISO coated particle batch with lines of constant end-of-life SiC stress (From Reference 16)

phenomena that occur during irradiation. For modeling purposes, GA treats these phenomena as independent failure mechanisms, although they are (somewhat) interrelated. Four phenomena contributing to fuel failure have been identified by GA in TRISO coatings, three in BISO coatings. These are discussed in detail in a General Atomic topical report dealing with fuel particle behavior (Ref. 3), and will be more briefly described here.

a. Amoeba Effect (Kernel Migration)

Unidirectional migration of the fuel kernel through the coatings up the temperature gradient has been observed in both carbide and oxide-coated particles. This phenomenon has been termed the "amoeba effect" or kernel migration. The amoeba effect is qualitatively similar in both oxide and carbide systems. In carbide fuel particles the amoeba effect has been shown to be a thermally activated process controlled by carbon thermal diffusion in the fuel phase (Ref. 17). It involves dissolution of carbon from the buffer layer on the hot side of the fuel kernel, carbon transport by thermal diffusion down the temperature gradient in the carbide fuel phase, and rejection of carbon as graphite at the cooler fuel kernel buffer interface. The kernel can migrate through the buffer layer apparently without significantly affecting the void volume of the buffer or interfering with particle performance. If  $UC_2$  kernel migration is allowed to progress to the point where the kernel interacts with or penetrates the outer coating layers, however, coating failure and fission product release could occur.

The rate of carbide kernel migration due to the amoeba effect is given by the expression:

$$\frac{dx}{dt} = \alpha \frac{D_c Q^*}{RT} \frac{dT}{dX} \quad (1)$$

where  $\alpha$  contains geometrical and physical constants,  $D_c$  is the carbon self-diffusion coefficient in the fuel phase,  $Q^*$  is the heat of transport for carbon thermal diffusion in the fuel phase, and the other parameters have their usual significance. The kernel migration rate can be normalized with respect to temperature and temperature gradient using Eq. 2,

$$\text{KMC} = \frac{\Delta x}{\Delta t} \cdot T^2 \cdot \frac{\Delta T}{\Delta X}^{-1} \quad (2)$$

where

$$\begin{aligned} \text{KMC} &= \text{kernel migration coefficient } (^{\circ}\text{K}\text{-cm}^2/\text{sec}), \\ \Delta x/\Delta t &= \text{migration rate (through the buffer coating (cm/sec)),} \\ \Delta T/\Delta X &= \text{temperature gradient (across the fuel particle),} \end{aligned}$$

or

$$\text{KMC} = K D_0^{\Delta H/RT} \quad (3)$$

where  $\Delta H$  is the apparent activation energy for carbon diffusion in the kernel (cal/mole) and  $K$  and  $D_0$  are constants. Using equations 2 and 3, kernel migration data are plotted as  $\log \text{KMC}$  versus  $1/T$  to obtain an empirical relationship between the normalized migration rate (KMC) and  $1/T$ . Such a plot is shown for  $\text{UC}_2$  in figure 13. The figure shows the least squares fit and the upper 95% "confidence" (percentile) limit (95% of the data fall within the 95% confidence limit) of the experimental data.

In its TRISO fuel failure model, General Atomic assumes that coating failure occurs when the migrating kernel contacts the inner PyC layer of the TRISO coating. The resulting fuel lifetime for the reference fissile particle, with a 100  $\mu\text{m}$  buffer layer, and a postulated thermal gradient of 104  $^{\circ}\text{C}/\text{cm}$  is shown in figure 14.

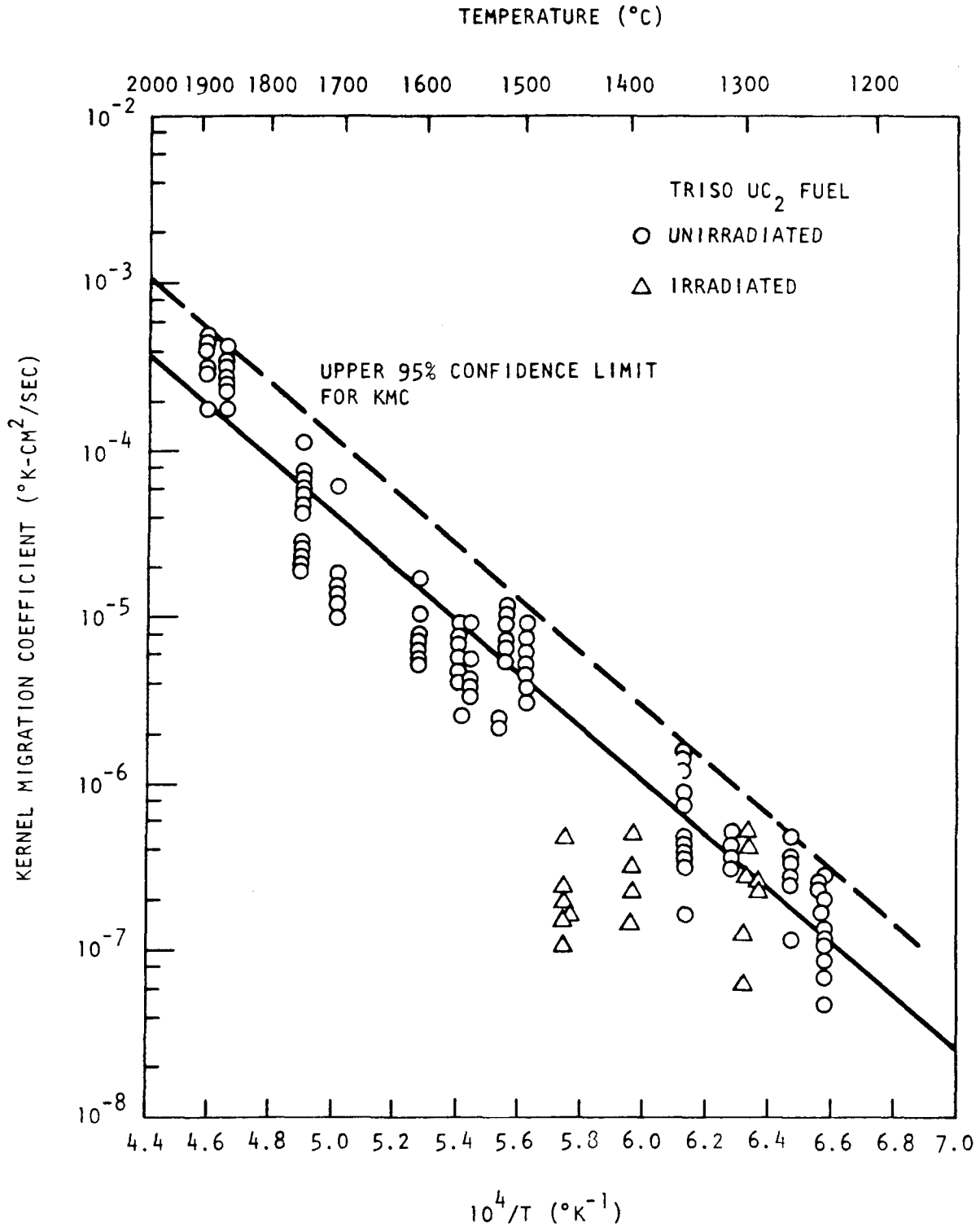


Fig.13. Kernel migration coefficient vs inverse temperature ( $10^4/T$ ) determined from out-of-pile thermal gradient testing of irradiated and unirradiated UC<sub>2</sub> fuel particles. (From reference 3)

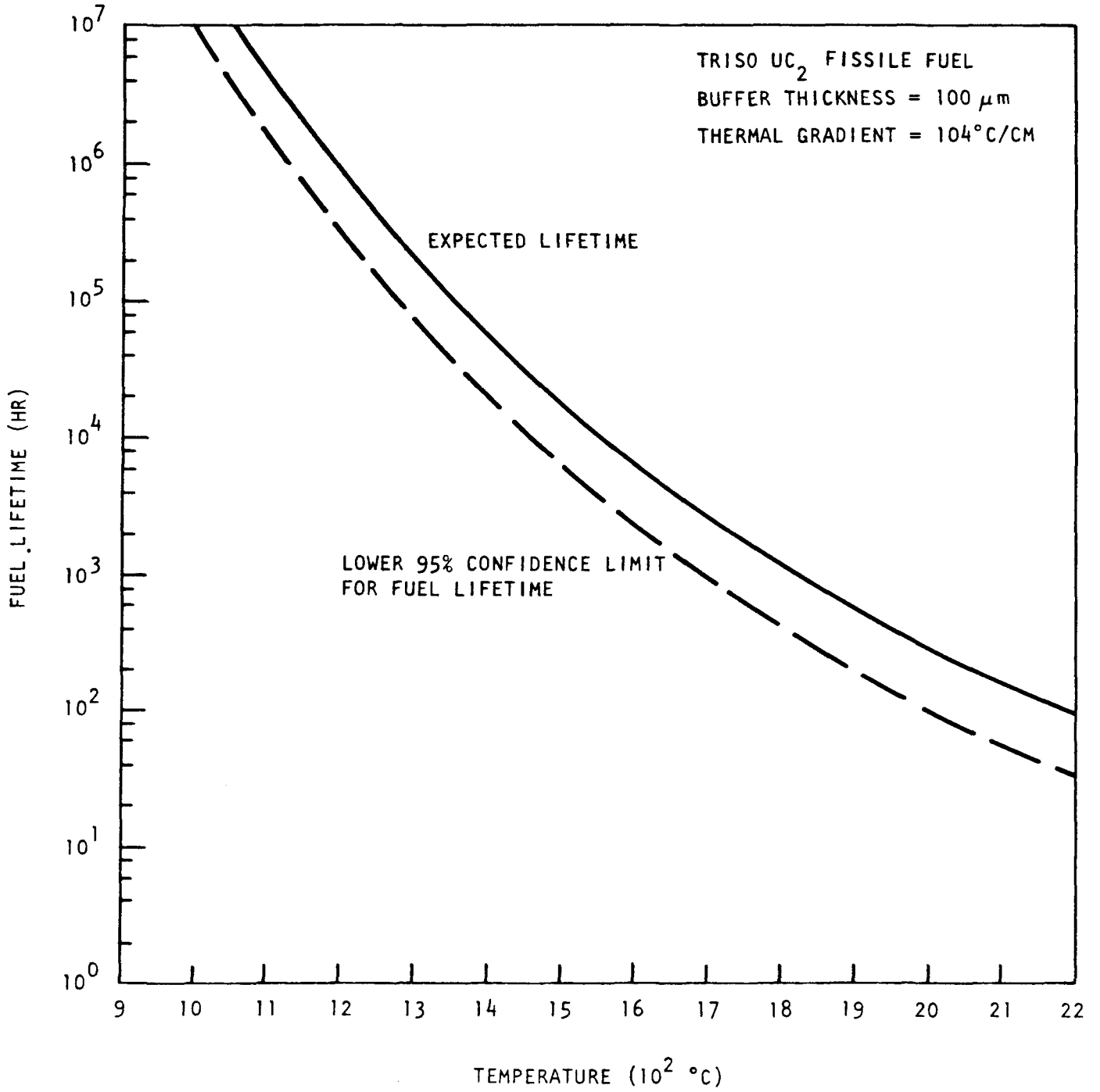


Fig. 14. Amoeba lifetime as a function of temperature under a thermal gradient of 0.0104 °C/μm for TRISO UC<sub>2</sub> fuel having a 100-μm-thick buffer layer (From reference 3).



In fertile BISO ThO<sub>2</sub> particles, the effect of amoeba migration is similar to the effect in fissile TRISO UC<sub>2</sub> particles, but the mechanism is not as well understood. Kernel migration has not been observed in stoichiometric, unirradiated UO<sub>2</sub>, but it has been observed in irradiated oxides both in-pile and out-of-pile (Ref. 18). This implies that migration may be controlled by a gas phase transport mechanism involving CO-CO<sub>2</sub> gas mixtures formed by reactions between PyC and oxygen liberated by fission processes. In spite of this as yet unresolved contradiction, the rate of kernel migration is, to date, apparently still best described by a solid-state, diffusion-controlled model similar to that which characterizes carbide kernel migration. Figure 15 shows the best fit and upper 95% confidence limit to the variation in ThO<sub>2</sub> log KMC with 1/T. The predicted amoeba lifetime under an assumed average HTGR thermal gradient of 104°C/cm is given in figure 16 for fertile particles with an 85 μm buffer layer (Ref. 3),

b. Pressure Vessel Failure

The basic performance-limiting phenomenon in both TRISO and BISO fuel particles is pressure vessel failure. As discussed in the section on "fuel design approach", the effects of irradiation temperature, neutron exposures, kernel burnup, and kernel and coating dimensions and densities on PyC and SiC coating layer stresses are estimated using coated particle stress analysis codes. Sensitivity studies performed by GA indicate that irradiation-induced stresses in the TRISO and BISO coatings are most dependent on kernel diameter and buffer thickness (Ref. 15). These two parameters, when combined with buffer layer density, define the fission gas pressure within a coated particle, according to the fuel particle stress models.

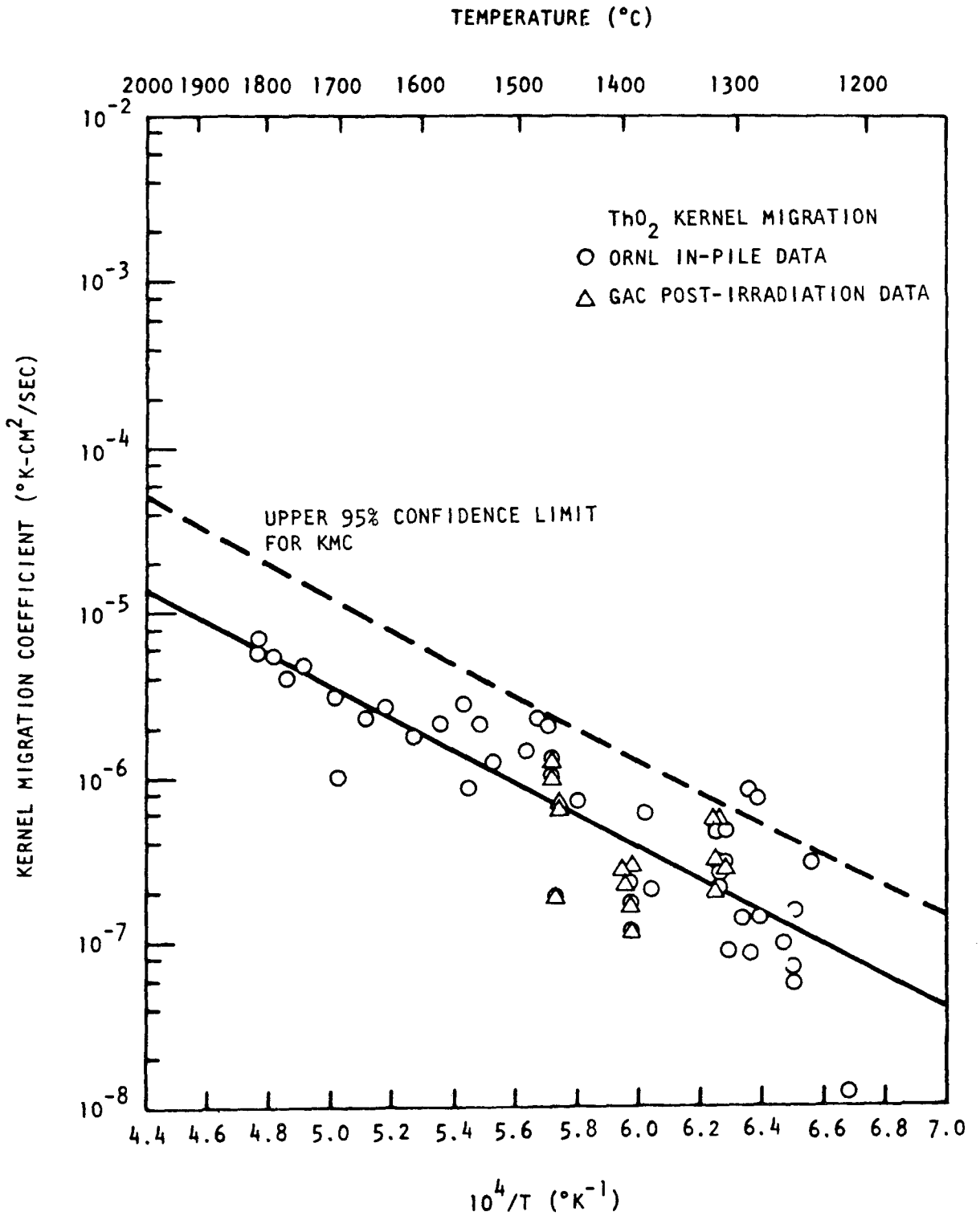


Fig. 15. Kernel migration coefficient vs inverse temperature ( $10^4/T$ ) for irradiated ThO<sub>2</sub> fuel determined from in-pile tests conducted by ORNL and out-of-pile thermal gradient tests conducted by GAC. Kernel burnups range from 0.4% to 14% FIMA. (From reference 3)

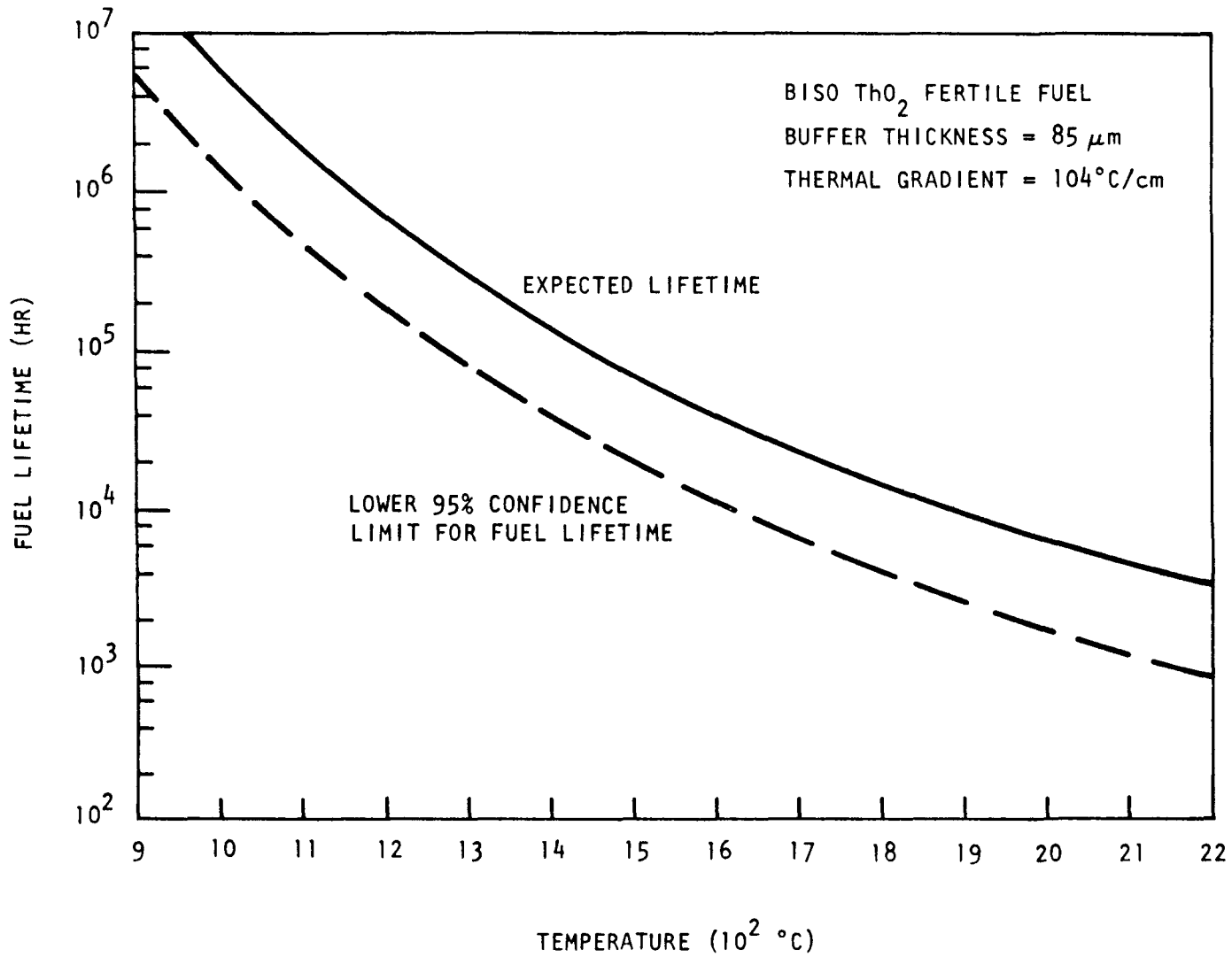


Fig. 16. Amoeba lifetime as a function of temperature under a thermal gradient of 0.0104°C/μm for BISO ThO<sub>2</sub> fuel having an 85-μm-thick buffer layer. (From Reference 3)

In its fuel particle performance model, GA treats pressure vessel failure by separating the TRISO and BISO fuel particle behavior according to temperature regime, fast neutron exposure, and burnup. For example, for reasons that are discussed in detail in a subsequent section (III) of this report, General Atomic assumes that <0.5% of the fuel operating in an HTGR at peak burnup and fluence will be subject to pressure vessel failure at 1250°C. The variation in TRISO failure fraction with fast neutron exposure and burnup at 1250°C, predicted by GA, is shown in figure 17.

Since the relationship between fast neutron exposure and kernel burnup will vary in an operating HTGR from point to point in the core as the fast-to-thermal neutron flux varies, GA proposes to predict failure over the range of expected fluence-burnup combinations by treating fluence and burnup as independent parameters, and using the largest predicted failure fraction to describe the fuel behavior. This approach is illustrated in figure 18 for TRISO UC<sub>2</sub> fuel at 1250°C.

For TRISO fuel at temperatures >1250°C GA estimates the effect of a temperature transient by superimposing the effects of an instantaneous temperature increase into the SiC layer stress calculations at any fast neutron exposure. The increased internal gas pressure that results from the internal operating temperature would cause coating stresses to increase, thereby causing an increase in failure fraction. Using the assumption of failure of 50% of the fuel particle having calculated SiC layer stresses exceeding 30,000 psi, GA obtains the TRISO UC<sub>2</sub> pressure vessel failure curves indicated in figure 19.

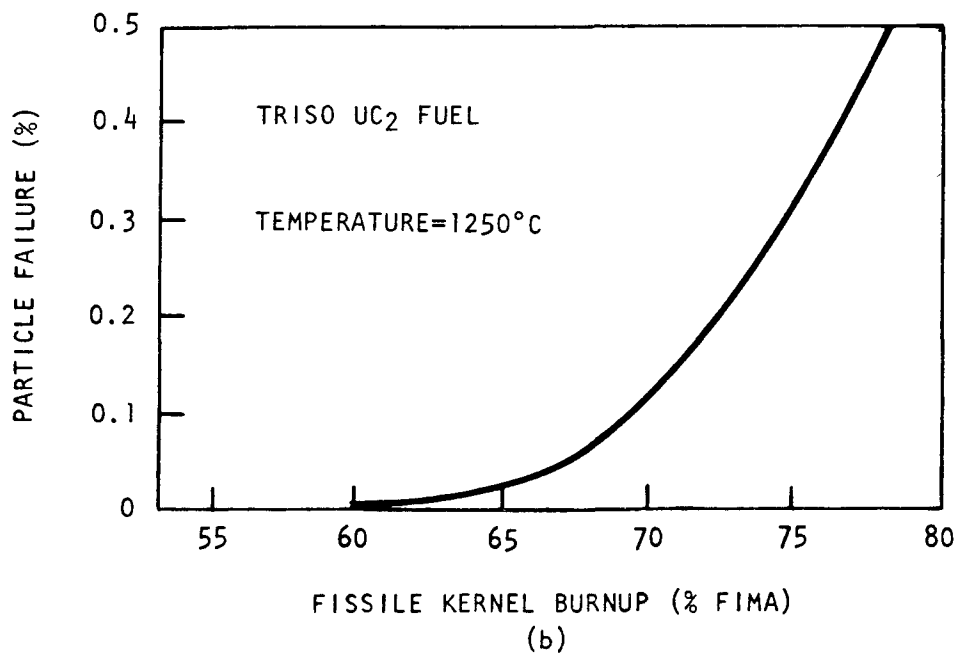
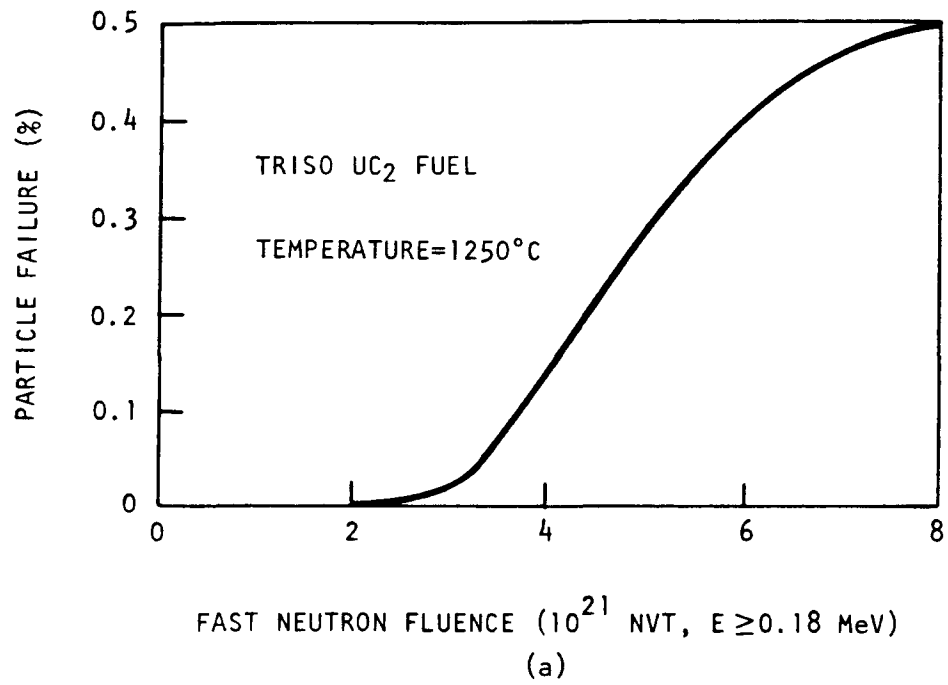


Fig. 17. Assumed pressure vessel failure fraction vs (a) fast neutron fluence or (b) kernel burnup for TRISO  $UC_2$  fuel. (From reference 3)

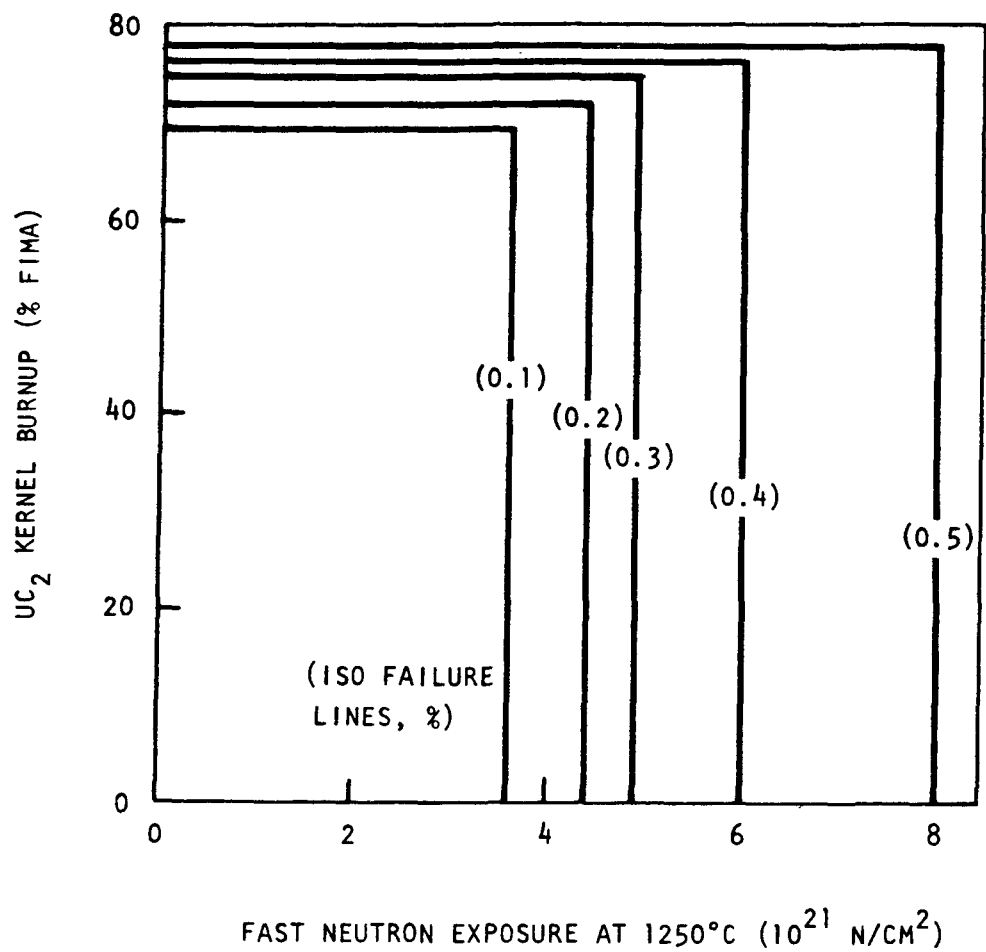


Fig.18. Assumed TRISO UC<sub>2</sub> pressure vessel failure fractions (%) at 1250°C as a function of kernel burnup and fast neutron exposure. (From reference 3)

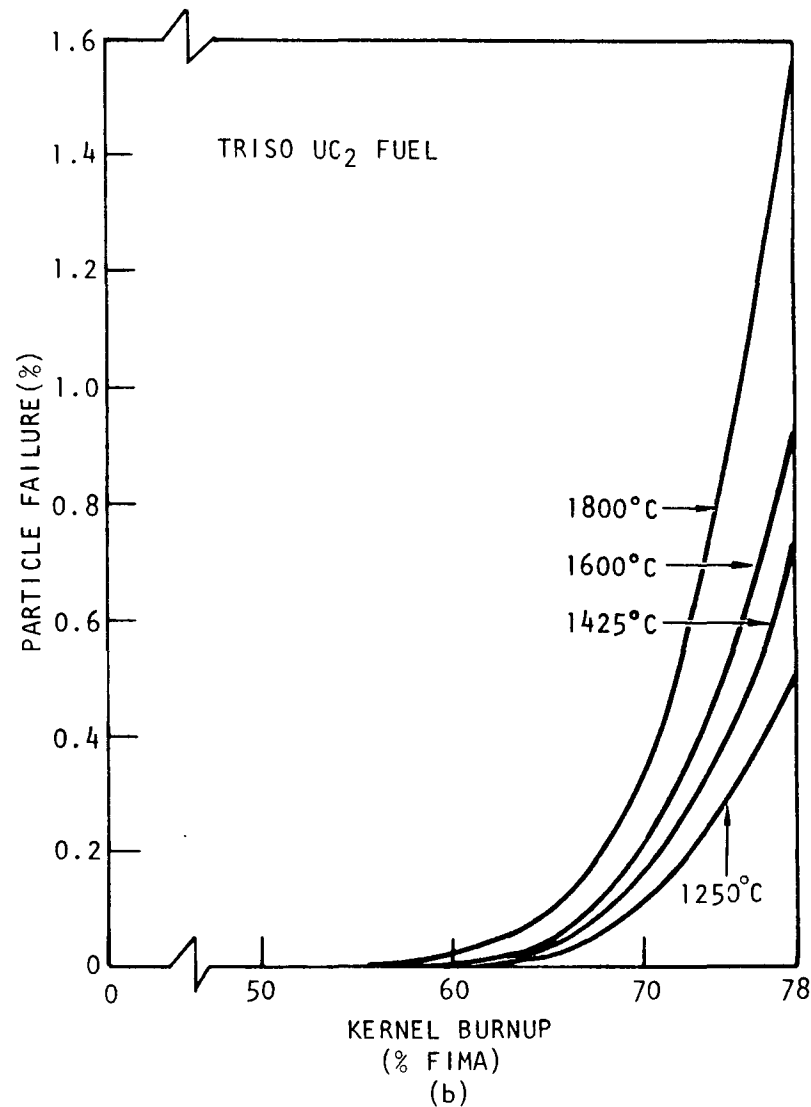
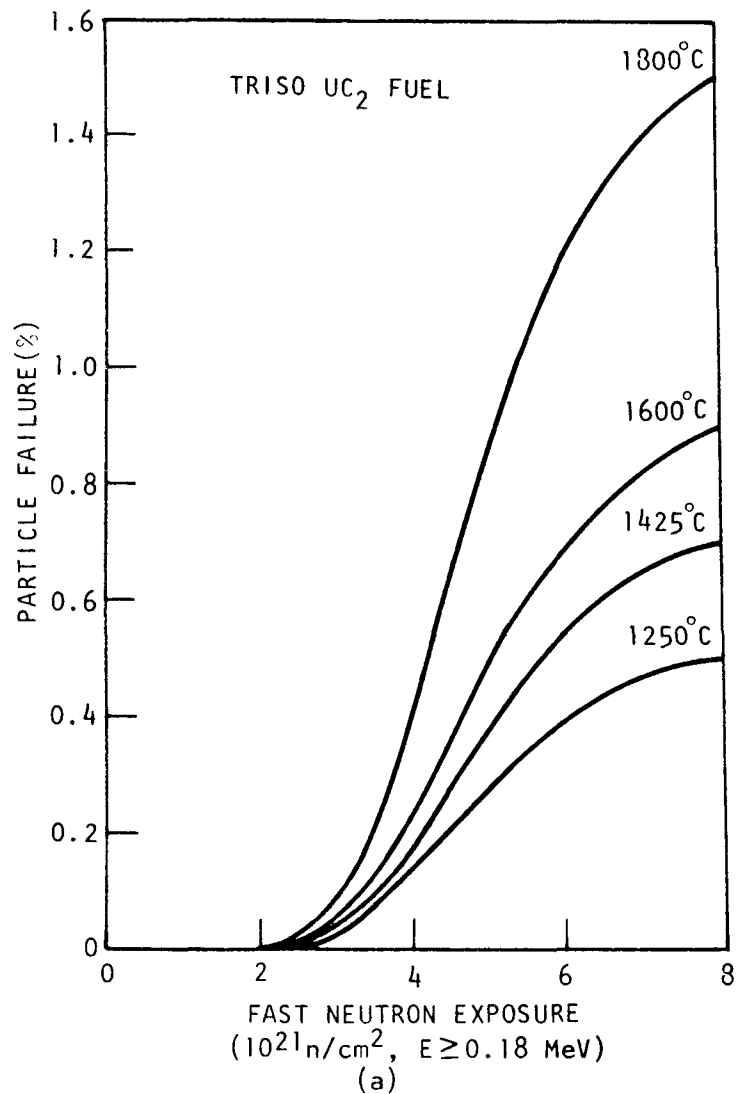


Fig. 9, Effect of a rapid thermal excursion from 1250° to 1425°, 1600°, or 1800°C and back to 1250°C on pressure vessel failure in TRISO UC<sub>2</sub> as a function of (a) fast neutron exposure or (b) kernel burnup for fuel experiencing 78% FIMA at a fast neutron exposure of  $8 \times 10^{21}$  nvt (From reference 3)

For BISO ThO<sub>2</sub> fuel, GA proposes also to use stress model calculations to estimate PyC layer stress distributions at temperatures >1250°C. Using an assumed PyC failure stress of 31,000 psi, GA obtains the BISO ThO<sub>2</sub> pressure vessel failure curves shown in figure 20.

c. Fission Product Attack of the TRISO SiC Layer

In TRISO UC<sub>2</sub> fuel particles irradiation test results have shown that rare earth fission products may migrate from the UC<sub>2</sub> fuel kernels through the buffer and inner PyC layer to the SiC layer. This may enable the fission products to react chemically with the SiC. The kinetics of migration and reaction are not presently known. Therefore, as an empirical basis for prediction of TRISO fuel failure at temperatures where SiC fission product interaction may occur, General Atomic uses the results of some out-of-pile annealing experiments. These results are plotted in figure 21. A more detailed description of these data and their interpretation is provided in a subsequent section (III.A.3) of this report. The point to be made here is simply that GA proposes to use these data to estimate fuel failure due to SiC fission product interactions at temperatures >1600°C. The methods used and their rationale are discussed in the cited section of this report.

d. Defective (Imperfect As-fabricated) Fuel

The fourth failure component for TRISO fuel (the third for BISO fuel) includes all types of fabrication defects; e.g., missing or cracked coatings. A small fraction of fuel will have defective or missing coatings. General Atomic contends that fuel particles with missing or defective coatings will not release fission gas at reactor startup, (provided that at least one coating layer is intact) but that failure of other



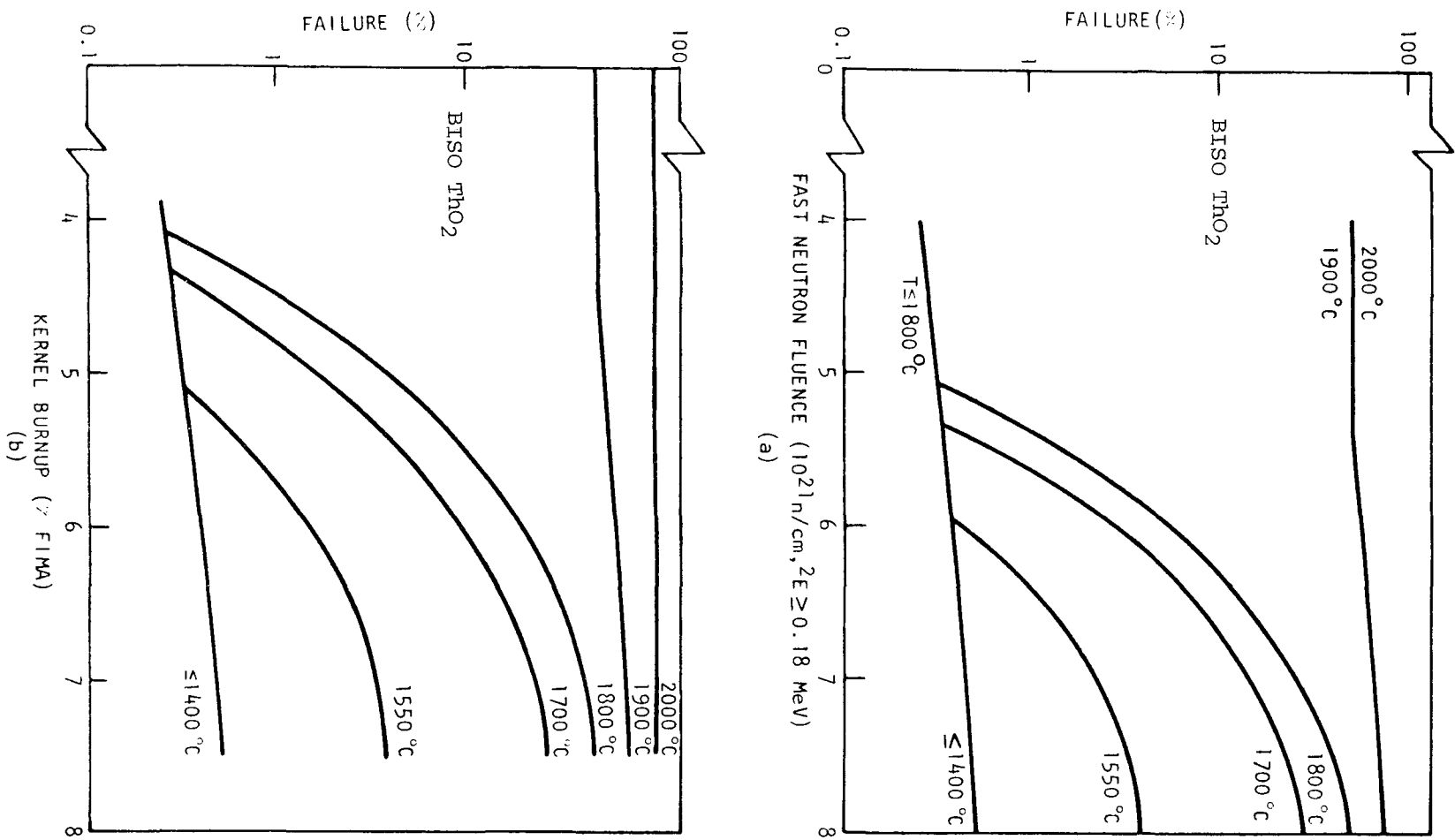


Fig. 20. Assumed effect of a rapid thermal excursion from 1250° to 1400°, 1550°, 1700°, or 1800°C on pressure vessel failure in BISO ThO<sub>2</sub> fuel as a function of (a) fast neutron exposure or (b) kernel burnup (From Ref. 3).

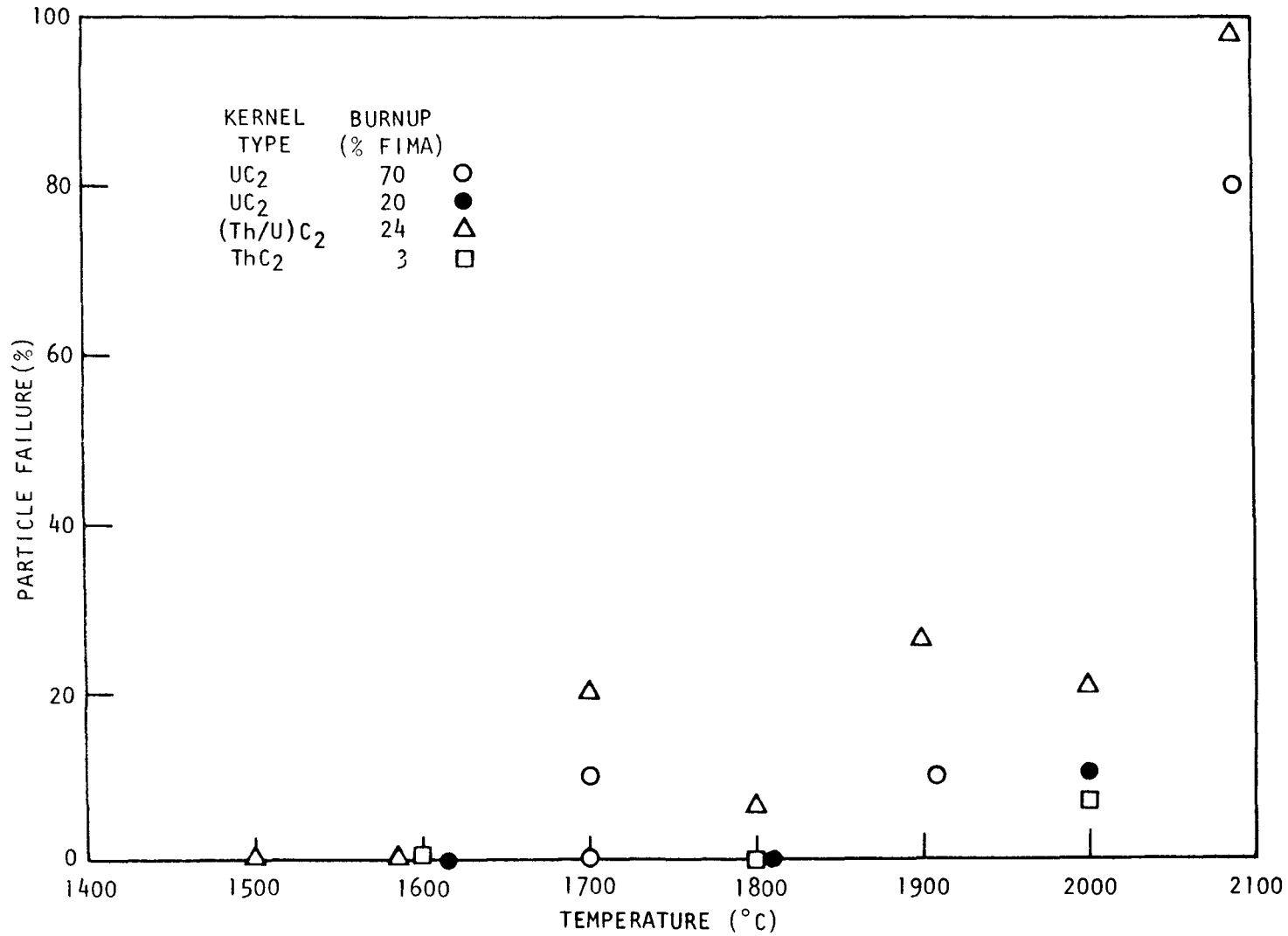
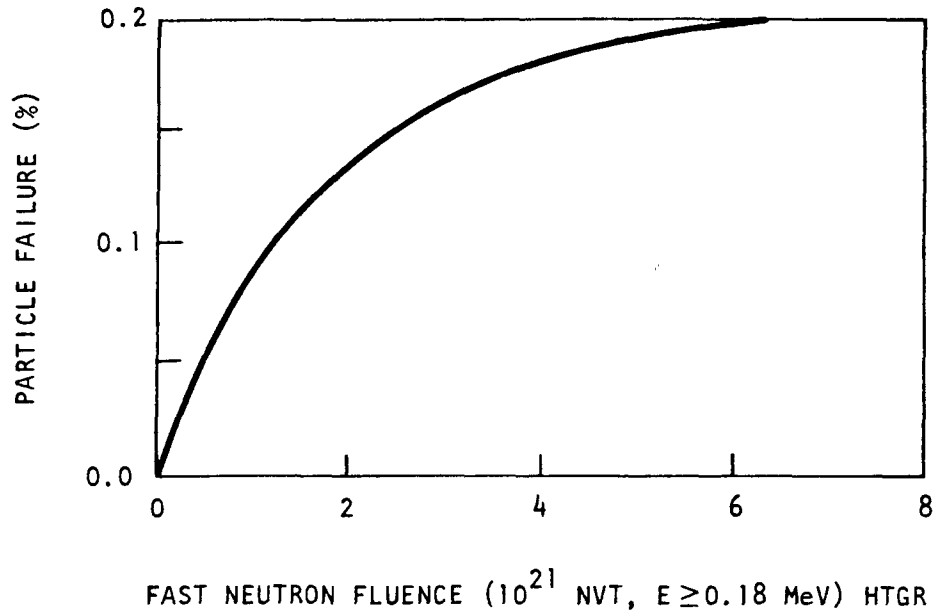


Fig. 21. Particle failure observed as a function of temperature during isothermal heating of irradiated TRISO carbide fuels for times less than 200 hr. (From reference 3)

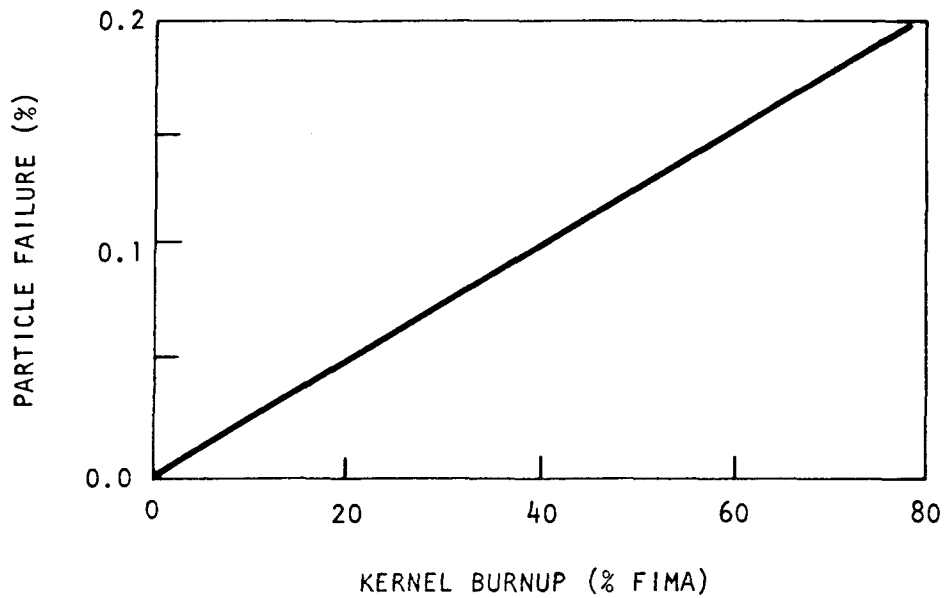
coatings on this fuel may occur as kernel burnup and internal gas pressure increase. Although GA states that the TRISO UC<sub>2</sub> fissile fuels now being tested are evaluated to ensure with 95% confidence that <0.3% of the fuel has defective (imperfect) coatings, GA assumes that the actual defective (imperfect) fraction will be 0.2% and that the failure of this fuel increases linearly with burnup from 0% at beginning-of-life (BOL) to 0.2% at 78% FIMA. The variation of failure in TRISO fuel with fabrication defects, according to the GA model, is shown in figure 22.

In the case of BISO fuel GA contends that its level of examination is sufficient to ensure with 95% confidence that <0.2% of the fuel will have missing or defective coatings. GA assumes that failure of BISO particles with defective coatings increases linearly with burnup to the 0.2% value at peak fertile fuel burnup (7.5% FIMA).

For both BISO and TRISO particles, tramp fuel in the as-fabricated coatings is tacitly included in the 0.2% failure fraction due to defective coatings.



(a)



(b)

Fig. 22. Assumed contribution to TRISO UC<sub>2</sub> fissile fuel failure fraction from particles with defective coatings as a function of fast neutron exposure (a) and kernel burnup (b) for fuel experiencing a peak burnup of 78% FIMA at an end-of-life fast fluence of 8 x 10<sup>21</sup> nvt (E ≥ 0.18 MeV). GA model. (From reference 3).

### III. Discussion

This report section contains a brief description of the proposed GA model for each fuel particle coating failure mechanism followed by a detailed description of the NRC analysis of the failure model. Suggested modifications to the GA models are presented and explained.

#### A. TRISO UC<sub>2</sub> Particles

##### 1. Defective (Imperfect As-fabricated) Fuel Particles

###### a. GA Model

General Atomic states in report number GA-A12971 (Ref. 3), on p. 31, that the presence of particles having defective coatings is accounted for by assuming that the failure of this fuel increases linearly with burnup to 100% at 78% FIMA. It is further stated that the TRISO UC<sub>2</sub> fissile fuels are being evaluated to ensure with 95% confidence that <0.3% of the fuel has defective coatings, but that the actual fraction will be assumed to be equal to 0.2% because not all defective TRISO coatings will fail in service. Thus, General Atomic proposes to estimate failure due to missing or defective coatings by

$$\frac{F}{D} = \frac{0.2\% \text{ kernel burnup} \times (\% \text{FIMA})}{78 (\% \text{ FIMA})} \quad (4)$$

###### b. NRC Analysis

While it may be true that not all defective TRISO particles will fail in service, the true fraction of defective particles which will fail is at present unquantifiable and has not been determined by experiment either for normal or transient conditions. During transients especially, defective particles may be expected to fail prematurely and unpredictably. The assumption of linear failure with burnup is arbitrary and not supported by data. Therefore, to ensure a proper degree of conservatism, and until either a sufficient amount of operating experience

with prototypic fuel is acquired or supporting experimental evidence is obtained (which might warrant adoption of the GA model for failure of defective fuel), it should be assumed that the fraction of as-fabricated, defective TRISO UC<sub>2</sub> fuel particles is 0.3% and that 100% of these particles; i.e. 0.3%, are failed at beginning-of-life (0% FIMA). Fission products released from these "failed" fuel particles must be included in any description of fuel performance. It should be noted that in this review we have not critically reviewed GA's fuel fabrication quality assurance program, but have, for the purposes of this study, accepted GA's statement regarding the 0.3% defective fuel limit. Although this limit appears achievable, General Atomic's QA program, as it applies to this value, must be reviewed and certified, since we do not presently have proof of the validity of the 0.3% defective fuel value.

## 2. Pressure Vessel Failure

### a. Off-Specification Fuel (Temperatures <1250°C)

#### 1) GA Model

According to GA, calculated SiC layer stress distributions, when compared to pressure vessel failure rates for TRISO UC<sub>2</sub> fuel irradiated (in capsule P13L) to near maximum fluence and burnup, indicated that if <1% of the fuel in an irradiation sample had calculated SiC stresses >30,000 psi, the observed SiC layer failure was 0.1% or less (Ref. 3,16). General Atomic contends that as a result of this work, the design basis and fuel specifications for TRISO UC<sub>2</sub> fuel particles ensure that <1% of the fissile fuel in an HTGR would have calculated SiC layer stresses >30,000 psi if irradiated at 1250°C to a fast neutron exposure of  $8 \times 10^{21}$  n/cm<sup>2</sup> and a kernel burnup of 78% FIMA, and that this nearly eliminates pressure vessel failure in fuel that meets specification. Since the quality control plan used to evaluate HTGR fuel is reportedly based on sampling at the 95% confidence level, small fractions of the fuel accepted for the HTGR will not meet the specification. To

account for the presence of this off-specification fuel, GA proposes that it be assumed that the SiC layer on 50% of the fuel particles having calculated SiC stresses exceeding 30,000 psi fail during operation at 1250°C. General Atomic proposes to predict the variation of pressure vessel failure with HTGR core operation by calculating the SiC layer stress distribution as a function of fast neutron exposure and by assuming that the failure fraction equals one-half of the fraction having calculated SiC stresses exceeding 30,000 psi. This leads to a predicted pressure vessel failure in 0.5% of the fuel at end-of-life (EOL).

In an operating HTGR, the relationship between fast neutron exposure and kernel burnup will vary from point to point in the core as the neutron flux varies. General Atomic, therefore, proposes to predict failure over the range of expected fluence-burnup combinations by treating fluence and burnup individually (using figures 17a and 17b) and using the largest predicted failure fraction to describe the fuel behavior. As a simplifying assumption, GA assumes that performance at operating temperatures <1250°C is the same as the performance predicted for 1250°C operation.

## 2) NRC Analysis

The assumption of 0.5% failure of fuel operated to maximum fluence and burnup ( $8 \times 10^{21}$  n/cm<sup>2</sup> and 78% FIMA) at  $\leq 1250^\circ\text{C}$  is primarily based on the results of the P13L capsule irradiation at 1250°C and the P13R and S tests at 1075°C. The P13L test included a significant number (>12,000) of particles. The particles were non-reference, however, in terms of kernel diameter ( $\sim 112 \mu\text{m}$ ) and buffer carbon thickness (49  $\mu\text{m}$ ), although the ratio of buffer

thickness to kernel diameter was roughly the same as that of reference particles (100/200). Whereas the non-prototypicality of buffer and kernel dimensions may eventually be shown to be not of major significance in terms of effect on fuel performance, the effect of particle size on TRISO failure statistics has, in fact, not yet been quantified. Moreover, the current state of knowledge of the interrelationships of fabrication, structure and performance of PyC and SiC coatings has not reached a point where coating performance can be predicted from, or correlated with, specific coating characteristics with a high degree of confidence solely from a knowledge of specified coating parameters alone. Subtle changes in fabrication methods, environment or precursors could have an effect on subsequent fuel performance.

In addition, the possible effects of irradiation time on fuel performance have not yet been completely resolved. There are no known data relative to coated-particle failure studies on HTGR fuels irradiated for a period of 4 years to a significant burnup and fast-neutron fluence (Ref. 19). Although the Peach Bottom fuel now being examined may yield some useful information, the previous tests on which the GA fuel failure model is based have been conducted under accelerated conditions. Some authorities (Ref. 19) believe that accelerated burnup might, in fact, present a harsher environment than normal reactor operation because of the higher thermal gradients and harsher neutron flux produced in the irradiation tests. On the other hand, it is also possible that irradiation creep will cause relaxation of the outer pyro-carbon under stress, which could relieve



the compressive force on the SiC layer, causing the SiC to be subjected to a higher differential pressure from the gas inside the particle. Irradiation creep phenomena in pyrocarbons are not yet well enough understood or sufficiently quantifiable to justify unqualified extrapolation of short-time-interval test results to longer irradiation times.

There are also a number of presently unquantifiable uncertainties involved in the reported failure observations which constitute the coating failure data base. For example, the method used to detect coating failures in irradiated particles is of concern. The P13L test failure detections were made visually. Visual methods of failure detection are generally not as accurate as other methods (Ref. 19); that is, a visual method of fuel failure detection may result in an underestimate of the failure fraction because some failed coatings will not be detected visually. Unfortunately, the magnitude of the error inherent in visual failure detection has not been established. Perhaps more importantly, there is a potential source of confusion and error in the reported sample sizes. For example, Table I, taken from a General Atomic report (Ref. 16), lists the number of coated particles per sample in the P13L irradiation tests which provided the initial basis and verification for the present LHTGR TRISO UC<sub>2</sub> particle design. As shown, four samples, each containing between 2600 to 3600 particles, were tested. In this particular case all of these particles were examined after irradiation. Of the 3600 particles in one sample, for instance, all were actually

TABLE I  
 LEVEL OF STATISTICAL SIGNIFICANCE OF TYPICAL  
 COATED PARTICLE IRRADIATION TESTS  
 \*(from Ref. 16)

Experiment	Number of Coated Particles per Sample	Observed Failure Fraction in Sample (%)	Predicted Failure Fraction in the Total Population	
			Most Probable Failure Fraction (%)	Failure Fraction at 95% Confidence (%)
Hypothetical	1000	0.1	0.2	0.48
Hypothetical	1000	0.5	0.61	1.05
Hypothetical	1000	1.0	1.10	1.69
Hypothetical	1000	5.0	5.1	6.33
P13L	3600	0.1	0.17	0.29
P13L	3400	0.1	0.12	0.23
P13L	3100	0.2	0.23	0.38
P13L	2600	3.7	3.73	4.38

\*Typicality as defined by GA

examined visually. But an unknown (but probably substantially smaller) number of particles were also examined metallographically and by X-ray spectroscopy. The visual method of examining the particle outer coatings with a stereomicroscope is useful mainly for detecting gross failures, and it may not detect small defects or incipient failures. Thus, although General Atomic rightly claims to have conducted "irradiation tests" on tens of thousands of coated particles, closer scrutiny shows that a relatively small number of these particles have actually been subjected to significant PIE. The coated particle test program is, therefore, not as extensive as might be inferred from the number of particles irradiated. The statistical significance of coated particle tests varies according to the number of particles examined and the error inherent in the method of examination, but although the number of particles examined, as well as the number tested, can sometimes be determined, the error in failure detection is only semi-quantifiable in most cases.

Whereas the General Atomic model for TRISO particle pressure vessel failure is tied to the 30,000 psi SiC failure stress criterion (through the P13L test), an in-depth review of the reference paper (Ref. 15) describing this test shows that the total fraction of particles with net tensile stresses in the SiC layer is another factor in the TRISO coated particle performance. This is as expected since SiC is a brittle material which has a distribution of fracture strengths determined by the flaw size distribution, rather than a unique strength value.

In the P13L particle batches which showed low coating failure ( $\sim 0.1\%$ ), about 80% of the particles had SiC coatings which were calculated to have remained in compression throughout life. The currently proposed GA model for TRISO particles pressure vessel failure does not include a provision for distribution of SiC stresses, but only an upper bound of 30,000 psi. This is an apparent weakness in the model because it is not fully consistent with the P13L test results. We believe that it is desirable to impose an additional requirement that a minimum of 80% of the TRISO particles should be fabricated with coating dimensions which will assure that the SiC layer stress will always be negative throughout life (under normal operating conditions).

It is necessary to note also that the 30,000 psi SiC layer stress is not a measured value, but is a stress model calculated number which will vary with the property values assigned to each component in the layer stress model calculation. So long as the input parameters remain consistent, comparison calculations may be meaningful. General Atomic must provide assurance, therefore, that the input parameters used in determining stress distributions (or acceptable distributions of kernel diameters and buffer thicknesses, etc.) in commercial batches of particles, and the method of stress calculation, used as part of a quality control program, are the same as those which were used for the P13L test batches. The validity of the stress model calculation must also be verified.

In essence, General Atomic's model has, as its cornerstone, the results of the so-called "P13L" capsule irradiation as reported by Gulden, et al (Refs. 15 and 16). Smith's assertion (Ref. 3) that if a batch of particles contains less than 1% of particles with calculated

SiC tensile stress in excess of 30,000 psi, then less than 0.5% of the particles will fail under normal operation, rests on Gulden, et al's work. But such an assertion, while it is a plausible hypothesis, is far from an established, incontrovertible principle. In fact, all that Gulden, et al (Ref. 15, p.108) claim toward a specification is:

"In the final particle specification, both the mean particle dimension and specifications on allowable ranges of coating parameters must be established. This will ensure that a relatively small fraction of the fuel particles have SiC coatings in tension and that there is a low probability of SiC layers exceeding tensile stress of 30,000 psi."

This statement does not claim any specific proportion of coating failure. It suggests that the proportions of particles with tensile stresses exceeding respectively 0 psi and 30,000 psi are relevant. One can take issue even with this statement for any of the following reasons, some of which are direct quotes from Reference 15.

a) (Ref. 15, p.107)

"The fracture stress of 30,000 to 40,000 psi derived from results of this analysis is in good agreement with strengths measured on SiC shells. Evans, Padgett and Davidge (Ref. 14 in Gulden's paper) using SiC shells obtained from coated particles, have reported that the mean fracture stress under internal pressure varies from about 15,000 to 80,000 psi depending upon the conditions of SiC preparation." (Emphasis added).

b) (Ref. 15, p.107)

"It appears that in spite of some uncertainties in the stress model and in the input data, the calculated end-of-life SiC stresses are probably correct within at least a factor of 2." (Emphasis added).

c) (Ref. 15, p.106)

"A comparison of the data for (batches) 4413-7 and 3516-39 suggests that both the fraction of particles with SiC stresses greater than 30,000 and 40,000 psi, and the total fraction of particles with net tensile stresses in the SiC layer are important factors in coated particle performance. This is expected since SiC is a brittle material and has a distribution of fracture strengths determined by flaw size distribution rather than a unique value of strength. The above results show that the fraction of failed particles correlates well with the fraction of particles with calculated SiC stress in excess of 30,000 to 40,000 psi. They also demonstrate that the absence of correlation between calculated stress and performance of batch 4413-7 in Figure 4 was the result of considering mean values rather than distribution of stresses within the batch." (Emphasis added).

d) Gulden et al, convey two somewhat conflicting views: 1) the importance of the fracture strength distribution, and 2) the emphasis put upon the fraction of particles above some unique critical fracture strength value between 30,000 and 40,000 psi. Characterization on the basis of a unique fracture strength must be questioned because of:

1. The wide range of mean fracture strength (or stress) reported by Evans, Padgett, and Davidge.
2. The conclusion is based primarily on three batches of particles which are different in crucial dimensions from the reference particles. Even collectively the

samples from three batches yielded only four particles with tensile stress in excess of 30,000 psi. This is not a reassuring number from the standpoint of statistics for establishing a fuel failure model. Similarly the number of failed particles (as reconstructed from Table II [Ref. 15, p. 107]), was approximately 12; again not statistically reassuring.

3. Point 2 above takes on added importance because the distribution of calculated tensile stress for batch 4413-67 is markedly different from the three above batches. For whatever reasons, batch 4413-67 with UO<sub>2</sub> kernels does not fit the pattern of the other batches.
4. The uncertainties of calculated end-of-life stresses as pointed out in Reference 15 may be considerable.
5. A variety of assertions made in Reference 15 and in subsequent publications suggest reservations. For example, (Ref. 15, p. 104)

"Variations in other coating thicknesses (inner PyC, SiC, and outer PyC) within a given coated particle batch contribute an uncertainty  $\pm 5,000$  psi to the calculated stresses which is small compared to the influence of the fuel kernel and buffer layer."

Table II and Figure 6 of Reference 15 suggest a (most likely non-uniform) shift of about 20,000 up to 30,000 psi for the no-outer PyC layer batch 3516-19. In addition, this batch has a very marked (possibly 3 fold) increase in the dispersion of coating stresses.

6. Reference 15 lacks essential information on the distribution of fracture strength and the joint distribution of fracture strength and calculated tensile stress. Without some solid information on these, the predictions relating to failure must be considered speculative in the absence of exhaustive experimentation.
7. Reference 15 is imprecise in statistical terminology in counting particles or presenting them in figures and tables.

In summation therefore, to account for the presence of off-specification fuel and to provide an added margin which will allow for the presently semi-quantifiable uncertainties mentioned above, it should be assumed that 100% of the TRISO UC<sub>2</sub> particles having calculated SiC stresses >30,000 fail, (where  $\geq 80\%$  of the particles will have calculated SiC stresses  $\leq 0$  psi throughout life) rather than 50% as GA proposes. At the end of 4 years, fuel operated to full burnup and/or maximum fluence (78% FIMA and  $8 \times 10^{21}$  n/cm<sup>2</sup>) at temperatures  $\leq 1250^\circ\text{C}$  should be considered to have a minimum pressure vessel failure of 1%, and the minimum failed fuel fraction due to pressure vessel failure of off-specification fuel should be taken to increase linearly at the rate of 0.25% per year. In other words, a calculated SiC layer failure stress of 30,000 psi may be used as an interim failure criterion when coupled to a SiC stress distribution that assures  $\geq 80\%$  of the SiC layers remain in compression throughout life. But the prediction must be given a lower bound as above to ensure that a reasonably conservative fuel failure fraction is used for source calculations for fuel of all ages.



These minimum requirements should be in effect to such time that additional test data on prototypic fuel are available to warrant further modification of the fuel failure model. Further, statistically significant test information on reference fuel particles must be obtained to validate the applicability of the proposed 30,000 psi SiC failure stress criterion before it can be accepted as a design limit for safety analyses related to licensing applications. The existing evidence is believed to be sufficient to permit use of this value for scoping studies when coupled with the above listed restraints.

b. Fuel at Temperatures > 1250°C

1) GA Model

On page 21 of report number GA-A12871 (Ref. 3), General Atomic acknowledges that predictions of the effect of continuous operation at temperatures above 1250°C are difficult owing to uncertainties in describing PyC dimensional change and creep. GA proposes, however, to estimate the effect of a rapid temperature transient by superimposing the effects of an instantaneous temperature increase on SiC layer stress calculations at any neutron exposure. GA also assumes that the pressure vessel performance criterion assumed for 1250°C operation (failure of 50% of the fuel having calculated SiC layer stresses >30,000 psi) also holds during thermal excursions. Fuel experiencing a thermal excursion at less than maximum burnup or fluence, followed by a return to normal operation, would experience no further failures until after increased kernel burnup causes gas pressures approximately equivalent to the gas pressures during the excursion.

Although GA shows plots of fuel failure (by pressure vessel effects) versus fluence and burnup (Figs. 17a and 17b) in GA-A12971 for temperatures to 1800°C (included in the report as figure 20a and 20b), GA acknowledges that above normal operating temperatures pressure vessel failure may be influenced by fission product attack of the SiC layer, resulting in an increased failure rate which cannot be correlated with the 30,000 psi SiC failure stress. At temperatures >1600°C, therefore, General Atomic proposes to augment the pressure vessel failure model by a model for fission product attack of the SiC.

2) NRC Analysis

We agree with GA that predictions of the effect of continuous operation at temperatures above 1250°C are difficult owing to uncertainties in data describing PyC dimensional change and creep. Therefore, the GA contention that the effect of a rapid temperature transient on the behavior of the fissile fuel can be estimated by superimposing the effects of an instantaneous temperature increase on the SiC layer stress calculations at any fast neutron exposure is accepted, but with certain reservations and restrictions. For example, the failure of 100% of fuel particles having calculated SiC layer stresses exceeding 30,000 psi, not 50% of these particles, should be assumed, in part, so as to be consistent with our comments on the model below 1250°C, but also due to the fact that pressure vessel performance data above 1250°C are more sparse than at lower temperatures. Since we propose to consider that the pressure vessel failure due to off-specification fuel is minimally 0.25%/year, the predicted failed fuel fraction resulting from pressure

vessel effects, at any temperature, will exceed 1% only when the calculated SiC layer stress exceeds 30,000 psi in >1% of the TRISO UC particles. For reasons to be presented in the discussion of fission product attack of the SiC layer, the effective maximum temperature for pressure vessel failure calculation via correlation with the 30,000 psi SiC failure stress criterion will be taken as 1600 C for "low-burnup" particles (<20% FIMA) and 1500 C for "high-burnup" (78% FIMA) particles.

As stated above, the data base for pressure vessel failure at temperatures above 1250 C, but below temperatures where SiC-fission product attack becomes readily observable ( 1500 to 1600 C), is quite limited, as shown in Table II. The total number of TRISO particles tested at average temperatures between 1250 and 1500 C is approximately 2500 particles, according to the list in Table II, which includes 9 samples ranging in size from 69 to 704 particles. But the number of "reference" particles, where "reference" is taken to mean prototypical in terms of type of kernels, coatings, dimensions, and method of fabrication, was 400. The relevance of applicability of test data on non-reference materials for prediction of failure probabilities on particles of different dimensions or type involves what is essentially a "judgment call" rather than a precise mathematical formulation based solely on statistics acquired on representative samples of significant population.

The problem of method of failure detection must again be considered. As noted earlier, visual examination methods are not considered accurate, and estimates of the magnitude of the error involved in each method of failure detection are not available. Thus,

SUMMARY OF TRISO UC<sub>2</sub> IRRADIATION PERFORMANCE OBSERVATIONS  
(Adopted from Ref. 4)

Sample Description			Irradiation Conditions				
Batch No.	Capsule	Position	Average Temperature (a) (°C)	Maximum Temperature (b) (°C)	Fast Neutron Exposure 10 <sup>21</sup> n/cm <sup>2</sup> E ≥ 0.18 MeV <sub>HTGR</sub>	Burnup (% FIMA)	Fission density (c) 10 <sup>21</sup> fissions per cm <sup>3</sup>
4413-5E	P13L	C1T3	1660	1660	6.3	72	1.26
4413-5E	P13L	C5T3	1405	1675	6.9	74	1.29
4413-5E	P13L	C5T3	885	895	5.2	74	1.29
4403-143	P13L	C2T3	1425	1630	6.9	73	1.28
4413-21	P13L	C2T6	1460	(k)	6.9	73	1.70
4000-304	P13M	C4T1	1300	1400	5.9	70	1.21
4000-304	P13M	C4T7	1300	1375	5.9	70	1.23
4000-325	P13M	C4T5	1300	1350	5.9	70	1.29
4161-00-023-3	P13P	1-1	1455	1735	5.9	60	1.79
4161-01-034-2	P13P	1-2	1420	1635	6.0	60	1.26
4161-032-2	P13P	1-4	1350	1630	6.1	61	2.09
4161-01-032-1	P13P	3-4	1605	1900	7.1	63	2.16
4161-034-1	P13P	3-2	1208	1360	7.1	63	1.35
4161-023-2	P13P	3-1	1085	1400	7.1	63	1.93
6151-00-035	P13R	3-4, 5	1075 <sup>(m)</sup>	(k)	12.1	74	1.79
6151-08-015	P13S	3-7, 8, 9	1075 <sup>(m)</sup>	(k)	11.7	73	1.50
6151-00-035	P13S	4-10, 11, 12	1075 <sup>(m)</sup>	(k)	10.8	72	1.74

(a) Time average fuel irradiation temperature

(b) Maximum fuel temperature during irradiation

(c) Number of fissions occurring inside the SiC layer ( $1.78 \times 10^{21}$  for reference LHTGR fuel @ 78% FIMA)

(d) Number of particles examined

(e) Determined during macroscopic examination

(f) Determined during microscopic examination

(g) Includes particles having SiC layers that are degraded by SiC-fission product interactions and particles having cracks in the SiC layer caused by pressure vessel failure

(h) Coatings having cracked SiC and PyC layers

(i) Postirradiation fission gas release (Kr-85m R/B @1100°C)

(j) Assumes  $2 \times 10^{-2}$  R/B per failed particle for Kr-85m @1100°C

(k) Not determined

(l) High FGR value is inconsistent with metallographic examinations and has been attributed to contamination during hot cell handling (Ref. 21)

(m) Design operating temperature

SUMMARY OF TRISO UC<sub>2</sub> IRRADIATION PERFORMANCE OBSERVATIONS

Batch No.	Sample Size	Results						Comments
		Macro Examination (e)		Micro Examination (f)		Fission Gas Release (i)		
		OPyC Failure (%)	Total Coating Failure (%)	SiC Coating Failure (g) (%)	Pressure Vessel Failure (l) (%)	R/B KR-85m 1100°C	Failure (%)	
4413-5E	464	0.1	0.1	0	0	(k)	(k)	Meets TRISO UC <sub>2</sub> design basis
4413-5E	582	0.1	0.1	0.3	0.3	(k)	(k)	Meets TRISO UC <sub>2</sub> design basis
4413-5E	588	0	0	0	0	(k)	(k)	Meets TRISO UC <sub>2</sub> design basis
4403-143	704	0.1	0.1	0.5	0.3	(k)	(k)	Meets TRISO UC <sub>2</sub> design basis
4413-21	477		0.2	0	0	(k)	(k)	Meets TRISO UC <sub>2</sub> design basis
4000-304	69	0.2	(k)	4.3	2.9	$1.6 \times 10^{-4}$	0.80	Meets TRISO UC <sub>2</sub> design basis
4000-304	95	0.6	(k)	1.0	1.0	$1.1 \times 10^{-2}$	(k,1)	Meets TRISO UC <sub>2</sub> design basis
4000-325	245	0	0	2.0	1.1	$8.4 \times 10^{-5}$	0.42	Meets TRISO UC <sub>2</sub> design basis
4161-00-023-3	105	0	0	11.4	0	$7.2 \times 10^{-5}$	0.36	Does not meet LHTGR TRISO UC <sub>2</sub> design basis
4161-01-034-2	199	0	0	12.0	1.0	$3.6 \times 10^{-5}$	0.18	Meets TRISO UC <sub>2</sub> design basis
4161-032-2	79	0	0	(k)	(k)	$3.6 \times 10^{-5}$	0.18	Does not meet LHTGR TRISO UC <sub>2</sub> design basis
4161-01-032-1	97	0	0	39.2	5.2	$4.7 \times 10^{-5}$	0.23	Does not meet LHTGR TRISO UC <sub>2</sub> design basis
4161-034-1	135	0	0	0.7	0	$4.7 \times 10^{-5}$	0.23	Does not meet LHTGR TRISO UC <sub>2</sub> design basis
4161-023-2	260	0	0	0	0	$6.1 \times 10^{-5}$	0.30	Does not meet LHTGR TRISO UC <sub>2</sub> design basis
6151-00-035	459	0	0	(k)	(k)	$4.5 \times 10^{-6}$	0.02	Reference LHTGR TRISO UC <sub>2</sub> fissile fuel
6151-08-015	688	0	0	(k)	(k)	$1.4 \times 10^{-5}$	0.07	Reference LHTGR TRISO UC <sub>2</sub> fissile fuel
6151-00-035	809	0	0	(k)	(k)	$4.9 \times 10^{-6}$	0.02	Reference LHTGR TRISO UC <sub>2</sub> fissile fuel

attempts to quantify fuel failure prediction are made more difficult because it is not possible to place a confidence interval on predicted failure probabilities without attaching a qualifying statement regarding the unknown magnitude of the error (due to method of failure detection) in the supporting data.

Moreover, as noted previously, in some cases the listed sample size for a test is misleading because the number of particles subjected to an irradiation test is often not the same as the number which is subjected to post-irradiation examination (PIE). Since in many cases, smaller numbers of particles undergo PIE than are irradiated, the confidence limits associated with these failures are larger than would be the case if all the irradiated particles were examined. In several cases, the numbers of irradiated particles examined via PIE methods is unknown (Ref. 19). In these cases, of course, no confidence limits may be assigned.

### 3. Failure Induced by Fission Product Attack of the SiC Layer

#### a. GA Model

General Atomic report GA-A12971 discusses the results of out-of-pile annealing experiments which were used to determine the effects of temperature above 1600°C on irradiated fuel behavior. The results are shown in a plot of particle failure as a function of heating temperature (Fig. 21). Each data point represents a sample of 5 to 23 particles and annealing times of 16 to 200 hours, and shows the first failure measurement made per

experiment. Failure was detected by visual examination and gamma counting. Comparison of the data in figure 21 with pressure vessel performance predictions, shown in figures 19a and 19b, indicates that using the pressure vessel predictions alone to predict the failure of fuel experiencing temperatures in excess of 1600°C after irradiation to nearly peak burnup/fluence conditions at a lower temperature results in an under-estimate of the fuel failure fraction. This may result from the fact that at temperatures above ~1500 to 1600°C, SiC-fission product chemical interactions weaken the SiC layer, thereby rendering it susceptible to failure at stresses below the nominal 30,000 psi failure stress. Alternatively, it may indicate that the 30,000 psi failure stress rule is not intrinsically correct.

General Atomic, therefore, proposes an envelope of failure values to be assumed for fuel operation at temperatures exceeding 1600°C, as shown in figure 23. At peak burnup (78% FIMA) it is assumed that failure increases linearly from the pressure vessel failure value at 1600°C to 100% at 2000°C. Failure in fuel having burnups <20% is assumed to increase linearly from the pressure vessel value at 1800°C to 100% at 2000°C because unirradiated TRISO UC<sub>2</sub> fuel particles can be heated above 1800°C without failure and because TRISO UC<sub>2</sub> particles irradiated to 20% FIMA did not fail until test temperatures exceeded 1800°C. Failure estimates at intermediate burnups are to be made, according to the proposed GA model, by estimating the critical temperature ( $T_{crit}$ ) at which failure by SiC-fission product interactions exceeds failure predicted from the pressure

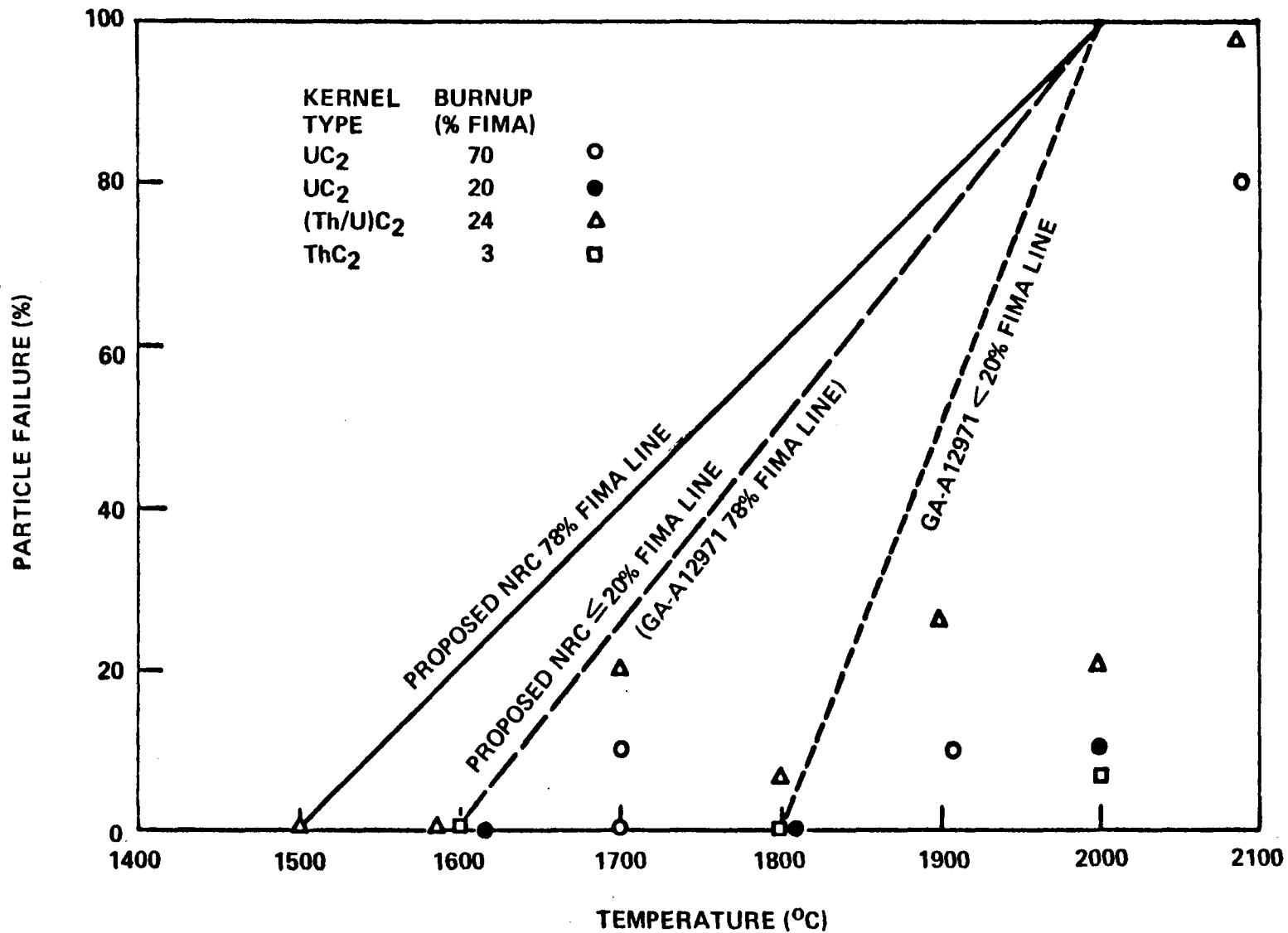


Figure 23 Incremental particle failure as a function of temperature during heating of irradiated TRISO carbide fuels for times less than 16 hours



vessel (30,000 psi SiC failure stress) correlation. The critical temperature is assumed to vary linearly from 1600°C at 78% FIMA to 1800°C at 20% FIMA and is given by

$$T_{\text{crit}} = -3.45 (\text{BU}) + 1869$$

where

$$\begin{aligned} T_{\text{crit}} &= \text{critical temperature (}^{\circ}\text{C)} \\ \text{BU} &= \text{kernel burnup (\% FIMA)}. \end{aligned} \quad (5)$$

It is further assumed by GA that the SiC-fission product interaction mechanism covers a new increment of failure each 100 hours. That is, it is assumed that the "instantaneous" failure fraction remains constant for 100 hours and is increased at the end of each 100-hour period by adding the product of the unfailed fuel fraction and the failure fraction determined by using Eq. 5 and figure 21.

b. NRC Analysis

We agree with General Atomic that there are insufficient data at present to provide a description of the SiC-fission product reaction kinetics. Using the body of data presented in figure 12 of reference 3 (also presented in attached Fig. 21), we have, therefore, attempted to bound the data in a suitably conservative way, taking into account the nature of the failure mechanism, the existing sparsity of data, and the gaps in knowledge in current understanding of the exact failure mechanism in terms of the chemical and physical phenomena involved. As discussed below, we have subdivided the failure model into three parts, dealing with peak burnup (78% FIMA), "low burnup" (<20% FIMA), and intermediate burnup (>20<78% FIMA) particles.

1) Peak Burnup Particles (78% FIMA)

We agree with GA that predictions of TRISO UC<sub>2</sub> particle failure due to SiC-fission product interactions cannot be made via coupling with a calculated SiC layer stress; e.g., 30,000 psi, since it is not possible to quantify the extent of weakening of the SiC coatings which occurs as a result of the SiC-fission product chemical interaction. Thus, pressure vessel failure predictions, alone, cannot be used to predict failures in the temperature regime where SiC-fission product interactions occur. As does GA, we propose to assume that failure increases linearly from the pressure vessel (+ defected fuel + amoeba effect) value at the lower end of the temperature regime for fission product attack to 100% at 2000°C, but we would shift the low temperature end from 1600°C to 1500°C, as shown in figure 23. The reason for the change is that, whereas there are no fuel failures shown at 1600°C, neither are there any high burnup ( $\geq 78\%$  FIMA) data. The highest burnup for particles tested at 1600°C was 24% FIMA [for some (Th/U)C<sub>2</sub> particles]. Hence, to provide added assurance that high burnup particles which might fail at temperatures  $< 1600^\circ\text{C}$  are accounted for in the failure prediction, the 78% FIMA failure line is shifted to 1500°C, and it is assumed that at temperatures  $> 1500^\circ\text{C}$ , the fraction of peak burnup fuel which fails instantaneously during any temperature excursion can be taken from the 78% FIMA line in figure 23.

It should be assumed that the "instantaneous" incremental failure fraction remains constant over a 16-hour period, and that the total failure fraction is increased at the end of each 16-hour period,

by adding the incremental 16-hour failure fraction to the previous total. A time interval of 16 hours is used instead of 100 hours as recommended by GA, because 5 of the 17 data points in Figures 21 and 23 represent failures detected after 16 hours. The new incremental failure fraction is obtained from the product of the unfailed fuel fraction and the failure fraction determined from Figure 23.

At present there are not enough data to determine the kinetics of fission product-SiC interaction-induced failure. Moreover, the effects of cycling are not well quantified and it is possible that fatigue effects could accelerate fuel failure. A possible weakness of the GA fuel particle coating failure models is that the potential existence of synergistic effects is not explicitly addressed.

2) Low Burnup Particles (<20% FIMA)

For "low-burnup" (<20% FIMA) TRISO UC<sub>2</sub> particles, we assume that failure increases linearly from the pressure vessel (+ defected fuel + amoeba affect) failure value at 1600°C to 100% at 2000°C, as shown in Figure 23. The lower end of the temperature regime is shifted to 1600°C from the 1800°C advocated in GA-A12971 so as to bound the data for failure of the (Th/U)C<sub>2</sub> particles at 1700 and 1800°C. These data points, the triangles in figures 19 and 23, represent failure of 24% FIMA particles, and should, therefore, be bounded by the line for "low burnup" fuel. In a manner similar to that described in the previous discussion on 78% FIMA fuel, a new increment of failure is assumed to occur each 16 hours, the new failure increment is assumed to occur instantaneously, (i.e., at the beginning of each 16-hour period), and the failure increment is added to the previous total to get the "instantaneous" total.

3) Intermediate Burnup Particles (>20%<78% FIMA)

By a means similar to the GA model, failure at intermediate burnups is to be predicted by estimating the temperature  $T_{crit}$ , at which failure by SiC-fission product interaction exceeds failure predicted from the pressure vessel (30,000 psi failure stress) correlation, but the critical temperature is assumed to vary linearly from 1500°C at 78% to 1600°C at 20% FIMA and is given by

$$T_{crit} = -1.72 (BU) + 1634 \quad (6)$$

where

$T_{crit}$  = critical temperature (°C)  
and BU = kernel burnup (%FIMA).

The same rules for imposing the intermediate burnup model should be used as are used in the 78% FIMA and  $\leq 20\%$  FIMA cases; e.g., a new increment of failure each 16 hours, etc.

These modifications to the GA model for SiC-fission product, reaction-induced failure should remain in effect until there is sufficient test data to warrant further change. In this regard the information contained in sections 5.1 and 5.2 of GA memorandum "CLS:030:FM8:75 (Ref. 4) is considered useful, but insufficient. The predictions of fission gas release using the existent GA model are not conservative over the full range of fluence, as evidenced in figures 24, 25 and 26. Although the predicted fission gas release is shown (in these figures) to be generally conservative in the middle range of exposures, the low and high exposure regimes are not conservative. Moreover, since the fission gas

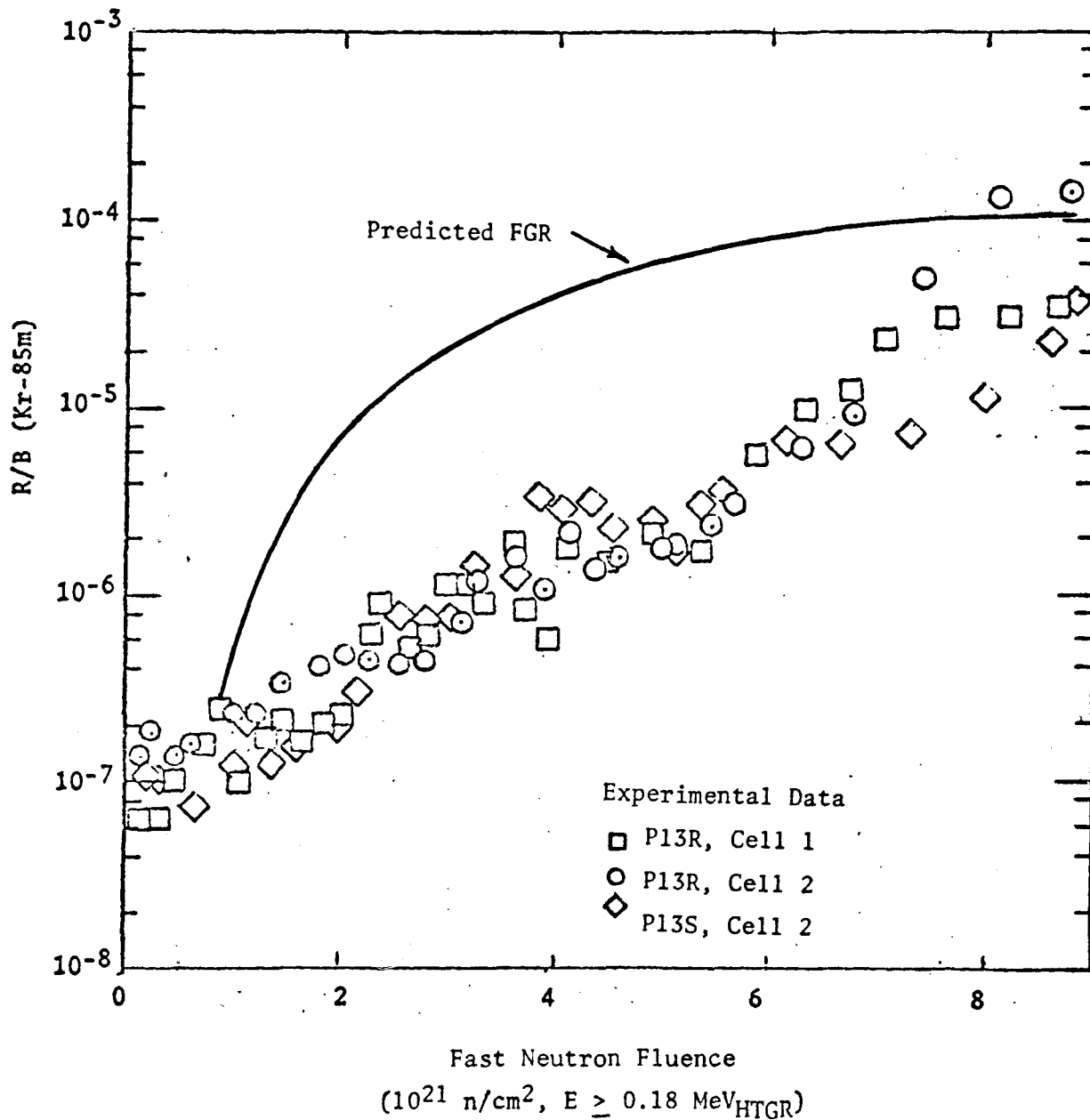
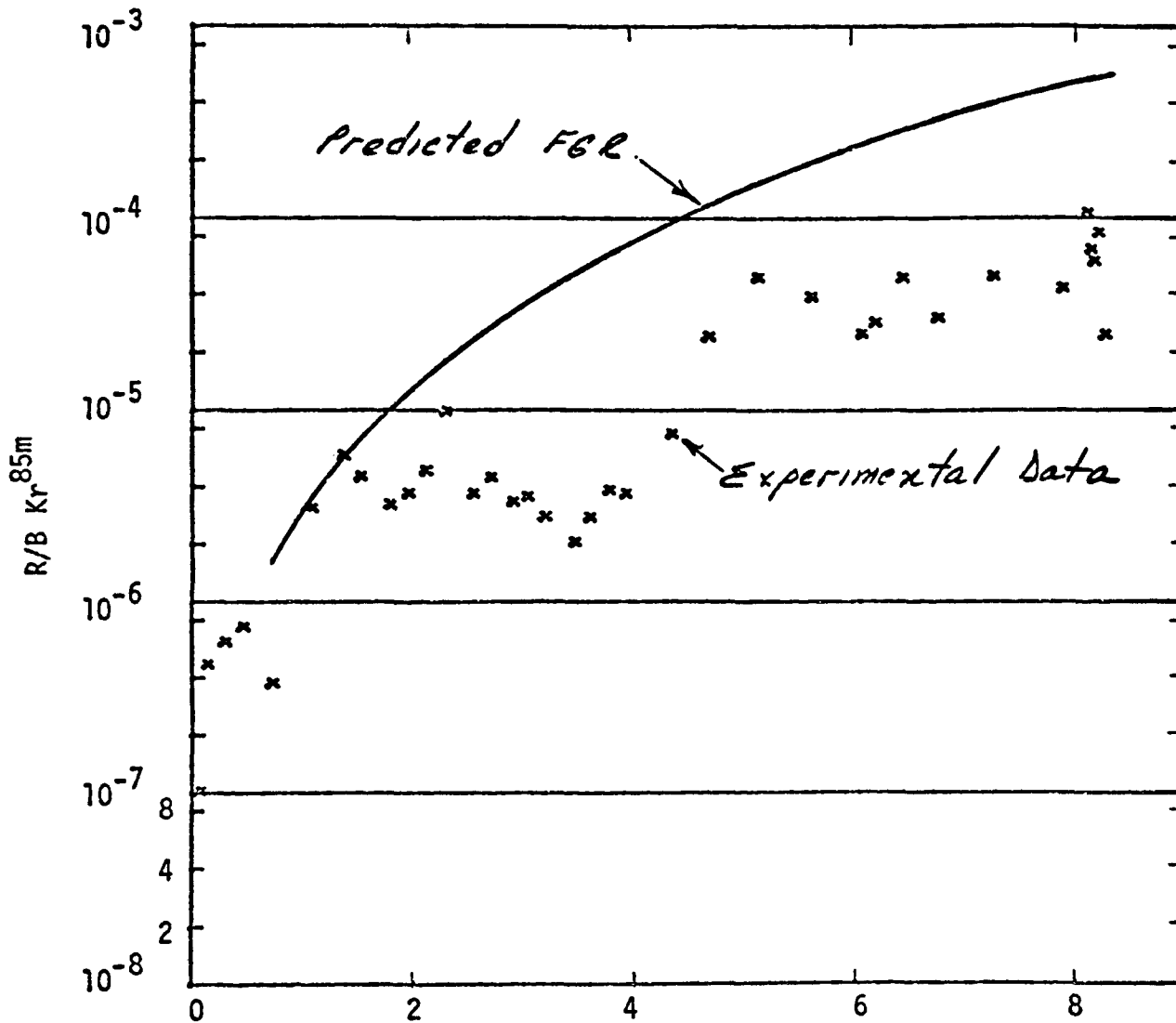


Fig. 24. Comparison between measured and predicted values of FGR (Kr-85m) for P13R and S fuel cells operating continuously at peak fuel rod temperatures of 1100°C (volume average temperature 1040°C). (From reference 4)



Fast Fluence  $\times 10^{21} \text{ n/cm}^2 \text{ (E > 0.19 MeV) HTGR}$

Fig. 25. Comparison between measured and predicted values of FGR (Kr-85m) for Cell 5 of P13S which operated continuously at a peak fuel rod temperature of  $1500^{\circ}\text{C}$  (volume average temperature  $1440^{\circ}\text{C}$ ) (From reference 4)

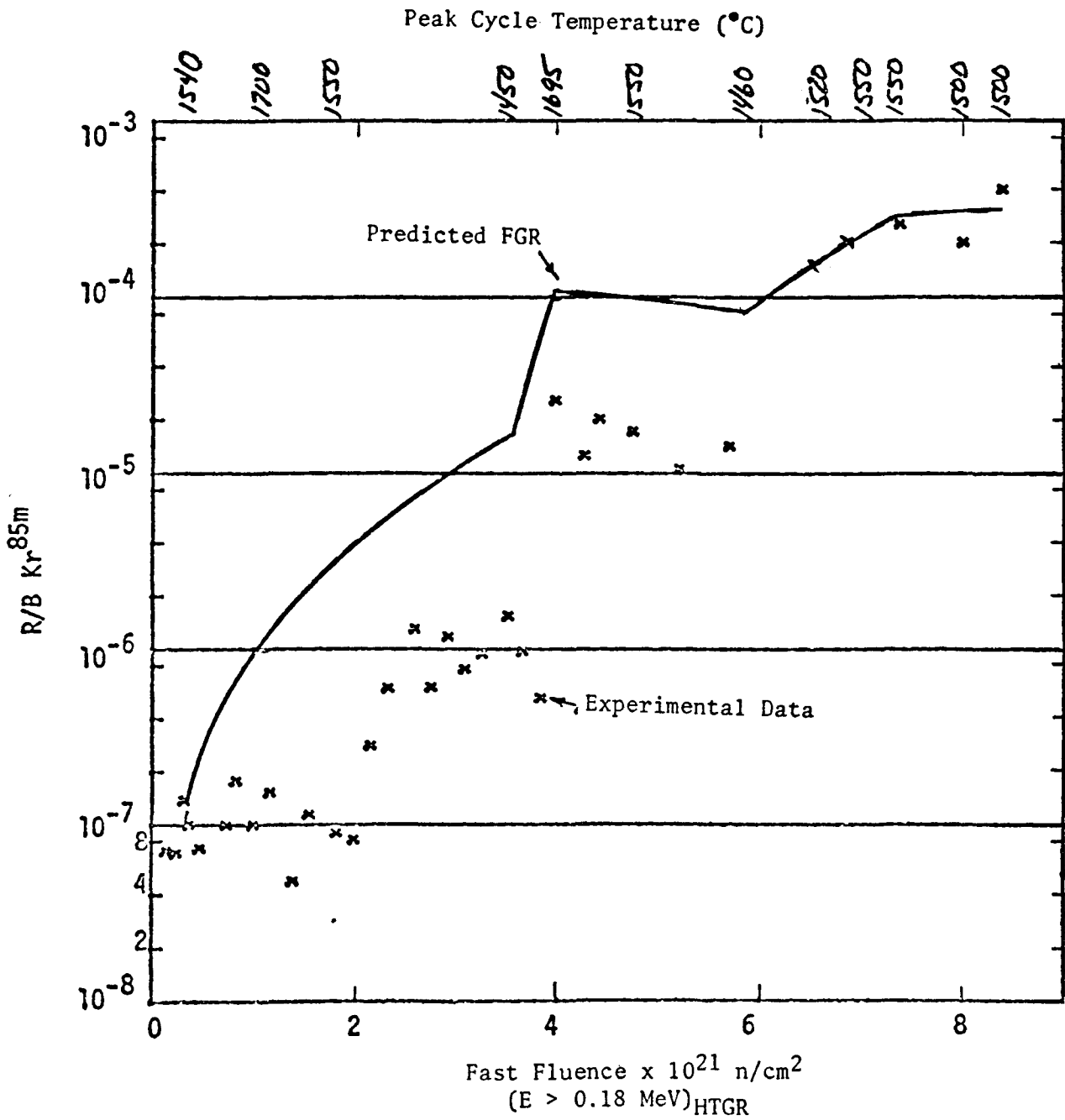


Fig. 26. Comparison of FGR measured during irradiation of the P13S thermal cycling cell (#1) and predicted using fuel performance models given in GA-A12971. (From reference 4).

release was used to estimate fuel failure, by back-calculating and using assumptions for release rate as a function of temperature, fuel failure per se was not measured directly. The errors involved in the calculations are not presently quantifiable. Nor is it possible to determine whether the predicted fission gas releases were conservative due to conservative fuel failure models or due to conservatisms associated with other aspects of the calculation (such as the release constants). The data shown in figure 21, therefore, are more directly applicable in the determination of a fuel failure model in our opinion, although the fission gas release data provide useful back-up information.

We do not intend to imply, however, that the data, as presented in figure 21 and described in reference 3 are not without question. Although the data as originally presented was supposed to represent tests conducted at 24 to 100 hours, subsequent discussion with GA revealed that the test intervals were actually 16 to 200 hours. Some samples were heated for 16 hours, examined, reheated, examined, and reheated. The  $UC_2$  1700° sample, however, was not tested at any other temperature. The 1600, 1800, and 2000 °C samples were heated for 200 hours at 1600°C, 100 h at 1800 °C, and 100 h at 2000 °C. Whereas there were only 5 particles per sample tested at 1500, 1700, 1900 and 2100 °C (16 hours), there were 23 (Th, U)C<sub>2</sub> and 28 UC<sub>2</sub> particles tested at 1600, 1800, and 2000°C. Under these circumstances, it is virtually impossible to treat this type of information in a meaningful statistical analysis since the sample populations and test conditions vary markedly and the sample sizes are so small. It is evident that these tests could not have been originally conceived with the purpose of providing statistically meaningful test data for performance modeling.



4. Kernel Migration Failure

a. GA Model

General Atomic assumes that fuel failure occurs when the migrating kernel contacts the inner PyC layer of the TRISO coating, even though experimental observations have shown that the coating failure does not occur until the fuel kernel migrates well into the structural coating layers. It is further assumed that the fuel operates at a constant temperature under a core average thermal gradient of  $104^{\circ}\text{C}/\text{cm}$ . A lower 95% confidence limit for fuel lifetime is used; i.e., the upper 95% confidence limit to the fit of kernel migration data is used to obtain the kernel migration coefficient.

b. NRC Analysis

The assumption of fuel failure when the migrating kernel contacts the inner PyC layer of the TRISO coating is conservative, as is the use of a lower 95% confidence limit for fuel lifetime. Subject to the results of our continued review of GASSAR (Ref. 1) and GA-LTR-17 (Ref. 6), the use of a core average fuel thermal gradient of  $104^{\circ}\text{C}/\text{cm}$  in exemplar calculations is also acceptable.

General Atomic does not, however, make allowance for irradiation induced dimensional changes in the TRISO-coated particles as is done in the analysis of the amoeba lifetime of BISO particles. In BISO particles the total particle diameter decreases about 5% and this reduction is accommodated by the buffer layer. A 5% shrinkage as the allowable kernel migration distance in a reference BISO  $\text{ThO}_2$  fertile particle corresponds to a reduction in the buffer

thickness from 85  $\mu\text{m}$  to 65  $\mu\text{m}$ . If a similar relative shrinkage occurs in the TRISO buffer layer, (the TRISO SiC layer is dimensionally stable), the allowable kernel migration distance would be reduced by  $(20/85) \times 100 \mu\text{m}$ , or 23.5  $\mu\text{m}$ . Hence, the allowable kernel migration distance in TRISO  $\text{UC}_2$  particles is  $100 - 23.5 = 76.5 \mu\text{m}$ . The reduced migration distance should be used in calculating the kernel migration lifetime.

General Atomic contends in GA memorandum #CLS:030:FMB:75, (Ref. 4) that there is no thermal gradient during an MHFPR event because the graphite moderator and fuel equilibrate at the same temperature during the event, which assumes complete loss of core cooling (adiabatic heatup). The CORCON code, which provides the input temperatures to the SORS code, which is used to calculate fission product release, is still under review, however, and it is presently undecided whether to accept the assumption of no thermal gradient. Regardless of the applicability of the amoeba failure model during an MHFPR event, the assumption of a reduced buffer coating thickness during irradiation may affect the calculation of allowable fuel lifetime for fuel at the upper end of the range of operating temperatures (1250 to 1300°C). Evaluation of the core thermal design methods and analysis should show if this is, indeed, the result of the assumed reduction in buffer coating thickness. It should be noted that section 4-4.3, "Evaluation of Design," of the Fulton Generating Station PSAR contains the statement "The thermal design is based on no particle damage from kernel migration...".

If this design criterion is to be upheld, it may be necessary to modify the core design to effect a reduction in operating temperatures or to modify the fuel design by increasing the buffer coating thickness.

As shown in GASSAR figure 4.2-12, the diametral shrinkage in BISO and TRISO particles reaches a maximum at a fast fluence of 4 to 5 n/cm<sup>2</sup> (for peak burnup fuel). Therefore, for simplicity in the model, we propose that it should be assumed that the TRISO buffer layer densifies linearly as a function of neutron exposure to a maximum shrinkage of 23.5 μm at 5 x 10<sup>21</sup>n/cm<sup>2</sup>.

B. BISO ThO<sub>2</sub> Particles

1. Defective (Imperfect As-fabricated) Fuel

a. GA Model

General Atomic states, in report number GA-A12971, that the level of examination of fertile fuel particles is sufficient to ensure with 95% confidence that <0.2% of the fuel will have missing or defective coatings. The GA model assumes that failure increases linearly with burnup in the particles with defective coatings to 100% at peak fertile fuel burnup (7.5% FIMA). This is expressed by

$$F_D = \frac{\text{fertile fuel burnup (\% FIMA)}}{7.5 (\% \text{ FIMA})} \times 0.2\% \quad (7)$$

where  $F_D$  is the failure fraction attributed to defective coatings.

b. NRC Analysis

As in the case with TRISO particles, there is no experimental evidence that failure increases linearly with burnup in BISO particles with defective coatings. The true failure rate in defective BISO particles might, in fact, be greater than for TRISO particles in view of the fact that the BISO particles have only one stress-bearing layer whereas the TRISO particles have three (2 pyrocarbon, 1 SiC). The General Atomic model also does not acknowledge the normal observation of "infant mortality." Hence, to ensure an appropriate degree of conservatism, it should be assumed that 100% of the defective BISO particles (i.e., 0.2%) are failed at beginning-of-life until either a sufficient amount of operating experience with prototypic fuel is acquired or other experimental evidence is

obtained which would provide a correlation of failure of defective fuel with service. As in the case of TRISO particles GA must provide evidence that its quality control program will provide the claimed limits on defective BISO particles.

## 2. Pressure Vessel Failure

### a. Off-Specification fuel (Temperatures <1250°C)

#### 1) GA Model

General Atomic uses the same arguments as used in the discussion of pressure vessel performance of TRISO fuel to show that small quantities of off-specification BISO fertile fuel are expected in an HTGR. To account for this fuel, GA assumes that 0.5% of the BISO fertile fuel will be subject to pressure vessel failure when irradiated to a fast neutron exposure of  $8 \times 10^{21}$  n/cm<sup>2</sup> and a kernel burnup of 7.5% FIMA at temperatures  $\leq 1250^\circ\text{C}$ . It is further assumed that pressure vessel failure in BISO ThO<sub>2</sub> particles increases linearly with kernel burnup and fast neutron exposure from 0 at startup to 0.5% at a burnup of 7.5% FIMA or a fast neutron exposure of  $8 \times 10^{21}$  n/cm<sup>2</sup>. In contrast to the TRISO particle failure model the BISO particle failure model for off-specification fuel is not, at present, tied to a particular failure stress in any coating layer, (although it is stated on page 38 of GA-A12971 that the expected failure stress in the outer PyC layer on BISO fuel is 31,000 psi).

#### 2) NRC Analysis

In general, the pressure vessel failure model used by General Atomic to predict fuel failure in BISO ThO<sub>2</sub> fertile fuel particles has much weaker support, in terms of experimental data

of statistical significance and correlation with a failure stress, than does even the TRISO fuel model. The irradiation performance of TRISO particles has been, at temperatures  $\leq 1250^{\circ}\text{C}$ , at least tenuously coupled to an analytical stress model, mainly through the results of the P13L test which showed that the fuel performance could be related to particle coating and kernel dimensions by coupling these dimensions to a calculated SiC layer failure stress. But BISO fuel performance, while also theoretically amenable to prediction via pressure vessel model stress calculations, has not been at all verified through experiment. Thus, it is not presently possible to directly relate calculated OPyC (outer pyrocarbon) layer stress distributions to pressure vessel failure rates in BISO  $\text{ThO}_2$  particles. One problem is that the true failure stress for the BISO OPyC is not known, although GA has reported on-going work to determine this stress. Moreover, final fuel specification limits for BISO  $\text{ThO}_2$  fuel have apparently not yet been established, as indicated by the description of the irradiation performance of unbonded BISO  $\text{ThO}_2$  fuel particles, provided in section 5.2 of General Atomic memorandum #CLS:030:FMB:75 (Ref. 4). In the referenced memorandum, the results of irradiation tests on some unbonded BISO  $\text{ThO}_2$  particles are described (23,000 particles irradiated at  $1075^{\circ}\text{C}$  in capsules P13R and S). Preliminary results indicated very low failure ( $\sim 0.05\%$ ) for samples which reportedly satisfied specification limits, but in five other samples which had outer PyC layers whose properties were "slightly

outside current guide lines" for the specification limits, the gaseous fission product release measured during PIE was reportedly equivalent to 0.6% particle failure.

If one takes the quoted 0.6% particle failure for the five nonspecification samples ( $\sim 5000$  particles) literally, then one obtains 30 failed particles. On the further assumption that the number of failed particles follow a Poisson distribution one obtains 0.81% as the upper 95% confidence limit for the proportion of failed particles. Besides the possible uncertainties in the numbers; i.e., 0.6 (possibly rounded) and  $\sim 5000$ , the fission gas release per particle of  $2 \times 10^{-2}$  for Kr-85m at  $1100^{\circ}\text{C}$  may be in error. At least one would expect the fission gas release to vary in a statistical fashion from particle to particle.

Another seeming contradiction occurs in Table 3 of the Smith memorandum. Table 3 of the memorandum lists the computed failure fractions for each of the three samples that were within specifications; the values are 0.12, 0.01, and 0.01%. The last two percentages are not readily reconciled with the given sample sizes of 1000 or 3000. For example, a single failed fuel particle in a sample of 3000 yields a failure fraction of 0.033%, clearly larger than the reported 0.01%.

Until the BISO particle fuel failure rate has been more directly coupled to statistically based calculations of stresses in the OPyC coating, the prediction of failure rates for "off-specification" fuel will remain essentially arbitrary. GA's assumption of a linear increase in failure rate with kernel burn-up and fast neutron exposure is completely arbitrary. In order to provide an interim working model, therefore, and until sufficient data are obtained to verify the BISO particle failure model, it will be assumed that the minimum BISO ThO<sub>2</sub> failure fraction, resulting from pressure vessel failure, should be assumed to increase linearly at the rate of 0.5% per year to 2% at end-of-life (4 years). It is stressed that this should be an interim model which ultimately should be superseded by an analytical model, based on data on prototypic fuel, which can directly relate BISO particle kernel and coating characteristics and specifications to coating irradiation performance.

b. Temperatures >1250°C

1) GA Model

General Atomic proposes to make predictions of pressure vessel failure during temperature transients using stress model calculations in which a PyC failure stress of 31,000 psi is assumed (Ref. 3). The results of the calculations are given in figure 20 as a function of fluence, burnup and temperature. In addition, GA assumes that pressure vessel failure increases linearly from the estimated value at 1800°C to 100% at 2000°C.



Out-of-pile heating tests used to support GA's BISO fuel model are described in section 5.4.2 of GA memorandum #CLS:030:FMB:75 (Ref. 4). Failure values measured during the tests and values predicted using GA's models are included in Table III. Whereas the low burnup (<2% FIMA) fuel had very low failure rates (as predicted) the high burnup fuel experienced significantly greater failure rates than predicted except at 2000°C, where the model predicted 100% failure.

2) NRC Analysis

a) Peak Burnup Particles (7.5% FIMA)

The results of the BISO ThO<sub>2</sub> fuel particle out-of-pile tests, described in GA memorandum #CLS:030:FMB:75, are plotted for high burnup (6.8 - 7.8% FIMA) in figure 27 along with the values predicted by the GA model for BISO fuel. As indicated in the previous discussion, the GA model underpredicted the failure rate except at 2000°C. Hence, to provide a reasonably conservative estimate of BISO ThO<sub>2</sub> fuel failure at high burnup, as a lower bounding set of values, it is proposed that the pressure vessel failure value be assumed to increase linearly from the value for off-specification fuel at 1250°C to 100% at 2000°C. This proposed linear relationship of fuel failure with temperature has a slope nearly parallel to a line drawn through the high-burnup data points at 1400, 1600 and 1800°C (see Fig. 27), and using a confidence coefficient of 97.5%, the 7.5% FIMA line closely follows the 97.5% confidence limit values obtained from the HT-18 capsule irradiation test described in reference 4.

TABLE III

Measured and Predicted Failure Fractions for  
Irradiated BISO ThO<sub>2</sub> Particles Heated to 2000°C in  
Out-of-Pile Heating Tests

Irradiation Conditions		Failure Values <sup>(a)</sup> (%) at			
Fast Neutron Exposure ( $10^{21}$ n/cm <sup>2</sup> , E ≥ 0.18 MeV HFIR)	Kernel Burnup (% FIMA)	1400°C	1600°C	1800°C	2000°C
		2.8 - 3.7	1.7 - 2.2 <sup>(b)</sup>	0, (0.1)	0, (0.1)
6.4 - 7.5	6.8 - 7.8 <sup>(c)</sup>	2.5(0.5)	30(10)	58(40)	60(100)

(a) Values not in parenthesis are experimental; those in parenthesis are predicted; predicted values are based on kernel burnup.

(b) Burnup value used for failure predictions was 2%.

(c) Burnup value used for failure predictions was 7.3%.

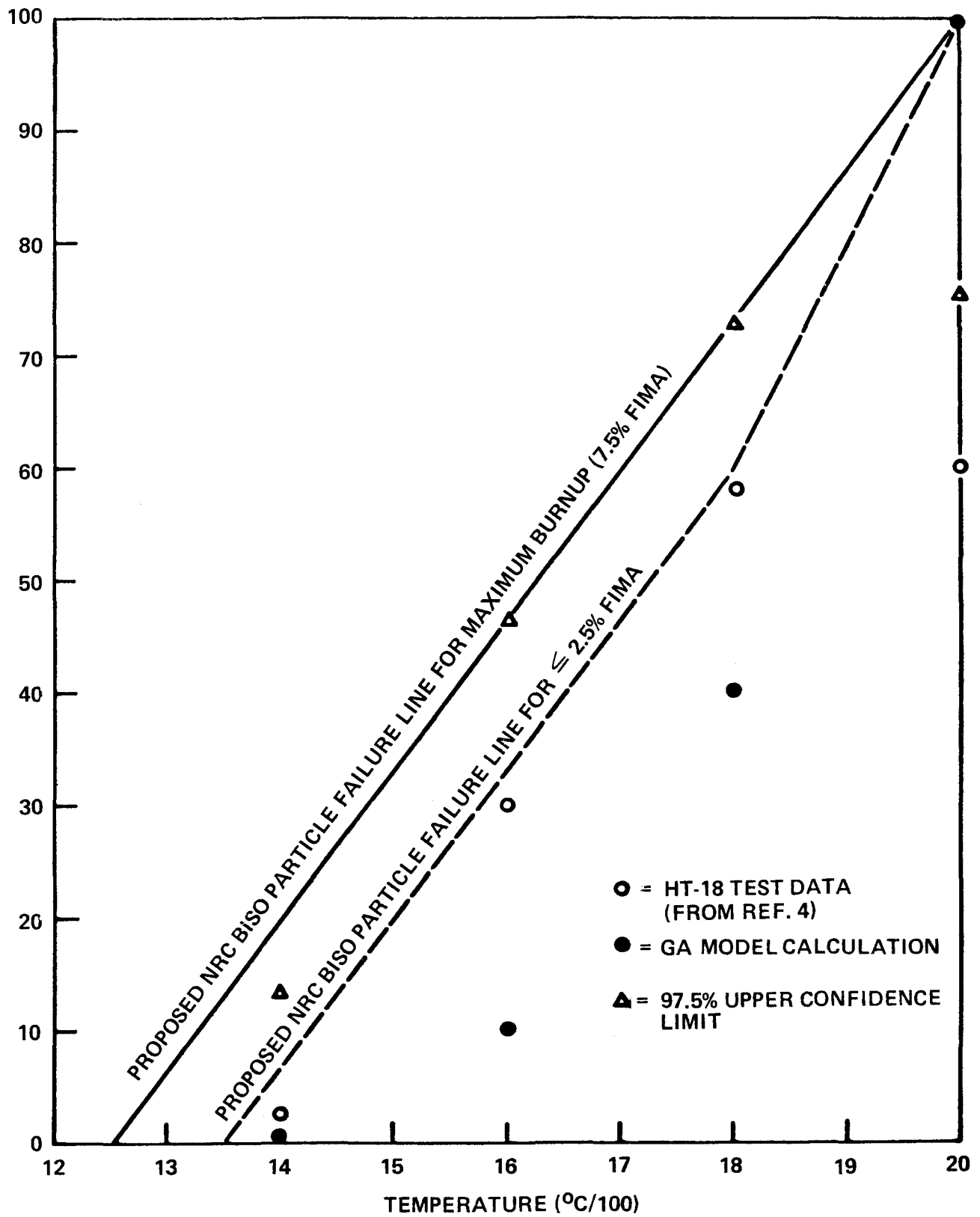


Figure 27 Incremental BISO ThO<sub>2</sub> Particle Failure as Function of Temperature

The 7.5% FIMA failure line bounds the data by a substantial margin because the data represent a total of only 40 particles, an average of 10 particles per data point. Until further information is obtained on the effects of transients on BISO fuel it would be unwise to modify the high burnup line to predict lower failure rates. In using figure 27 to predict BISO particle failure it is assumed that failure occurs instantaneously at a given temperature. For the purpose of providing a bounding calculation, it is also assumed that maximum burnup occurs at an exposure of  $8 \times 10^{21} \text{n/cm}^2$ .

b) Low Burnup Particles (<2.5% FIMA and Temperatures >1350°C)

To model BISO particle fuel failure at low burnup ( $\leq 2.5\%$  burnup) it is proposed that the pressure vessel failure value remain constant at 0.5% failure to 1350°C. At temperatures  $>1350^\circ\text{C}$  the pressure vessel failure is assumed to increase linearly with temperature to 60% at 1800°C, followed by a further but more rapid linear increase with temperature, from 60% failure at 1800°C to 100% at 2000°C.

The failure model is represented in figure 27 by the dashed line for  $\leq 2.5\%$  FIMA fuel. The line from 1350°C to 1800°C just bounds the high burnup data points and has a slope which parallels the 7.5% FIMA line. For simplicity in the model, it should be assumed that the  $\leq 2.5\%$  FIMA burnup line corresponds to a fast fluence of  $3 \times 10^{21} \text{n/cm}^2$ . Thus, fuel having exposure  $< 3 \times 10^{21} \text{n/cm}^2$  should be treated as fuel with  $\leq 2.5\%$  FIMA in predicting BISO fuel failure unless another correlation is provided, as in GASSAR Section 2A (Ref. 1). (See Table IV).

c) Intermediate Burnup Particles (>2.5%<7.5% FIMA)  
( $>3.0 \times 10^{21} < 8 \times 10^{21} \text{ n/cm}^2$ )

To obtain estimates of incremental failure at intermediate burnups and fluences, it is proposed that the pressure vessel failure rate increases linearly between the values at 2.5% and 7.5% FIMA, or  $3$  and  $8 \times 10^{21} \text{ n/cm}^2$ , (see Fig. 27). The value for failure used should be the maximum value determined using fluence and burnup independently.

The models proposed here for BISO  $\text{ThO}_2$  fertile particle pressure vessel should be used until sufficient data are available to provide confirmation of the BISO particle analytical stress model advocated by GA. At present, this stress model does not result in conservative values for pressure vessel failure at high burnups and at temperatures  $< 2000^\circ\text{C}$ , and thus it cannot be used to predict BISO  $\text{ThO}_2$  particle failure probabilities for safety analyses related to licensing concerns.

### 3. Kernel Migration

#### a. GA Model

The effect of kernel migration on fertile fuel particle performance is handled the same way as for TRISO particles. General Atomic assumes that fuel failure occurs in BISO particles when the migrating kernel contacts the OPyC layer. A core average gradient of  $104^\circ\text{C/cm}$  is used, along with the upper 95% confidence limit for the variation in  $\text{ThO}_2$  KMC as a function of inverse temperature, to determine the migration distance for a specific temperature. (A calculated gradient is used for each core location in the design calculations, however.)

GA does take account of neutron induced density and dimensional changes in the outer layer PyC of the BISO particles in determining the allowable kernel migration distance. As discussed on pages 36 and 38 of GA-A12971, experimental measurements on particles before and after irradiation have demonstrated a maximum reduction in diameter of approximately 5%. The decrease in particle diameter is applied to the buffer layer, resulting in a reduction in the allowable kernel migration distance to 65  $\mu\text{m}$ .

b. NRC Analysis

The assumption of fuel failure when the migrating kernel contacts the OPyC layer of the BISO coating is reasonably conservative as is the use of a lower 95% confidence limit for fuel lifetime (upper 95% confidence limit on KMC). Subject to the results of our review of GASSAR and GA-LTR-17 (Ref. 6), the use of a nominal HTGR fuel thermal gradient of 104<sup>o</sup>C/cm in the calculation is also acceptable, as is the allowance of 20  $\mu\text{m}$  shrinkage of the buffer layer during irradiation. For simplicity, it should be assumed that the buffer layer shrinks linearly at the rate of 4  $\mu\text{m}/(1 \times 10^{21} \text{ n/cm}^2)$  to a maximum of 20  $\mu\text{m}$  at  $5 \times 10^{21} \text{ n/cm}^2$ . The assumption of no thermal gradient during an MHFPR event, and concomitant lack of amoeba migration, is being addressed as part of the CORCON code review. An evaluation of the consequences of MHFPR event amoeba failure will, therefore, be deferred, pending resolution of the CORCON review.

#### IV. Proposed NRC HTGR Fuel Particle Interim Failure Model Requirements

This report section contains a summation of the HTGR fuel particle failure model elements that we believe must be included, for reasons discussed in Section III, in a current interim HTGR fuel failure model. The model suggested here is intended as an interim guide, which may be used for scoping studies and plant component design work. The term "interim" is stressed. Permanent endorsement of these model requirements for safety analyses related to licensing concerns is not intended. The model requirements listed here are provided simply as conservative guidelines which should be followed until sufficient data are obtained to either permit their unqualified endorsement and adoption for licensing or to warrant their modification.

##### A. TRISO UC<sub>2</sub> Particles

##### 1. Defective (Imperfect As-Fabricated) Fuel

To account for the presence of particles with as-fabricated defective coatings, it will be assumed that the fraction of TRISO UC<sub>2</sub> fuel particles with defective as-fabricated coatings is 0.3% and that these particles are failed at beginning-of-life (0% FIMA). General Atomic must provide a detailed quality assurance program which will assure that the fraction of as-fabricated defective coatings will not exceed 0.3%.

##### 2. Pressure Vessel Failure

##### a. Temperatures <1250°C (Off-Specification Fuel)

To account for the presence of off-specification fuel it will be assumed that 100% of the TRISO UC<sub>2</sub> particles having SiC stresses >30,000 psi fail. The minimum failed fuel fraction at temperatures  $\leq$  1250°C will

be taken to increase linearly at the rate of 0.25% per year; i.e., 1% failure at the end of 4 years (78% FIMA,  $8 \times 10^{21}$  n/cm<sup>2</sup>). The minimum total fraction of failed TRISO UC<sub>2</sub> fuel particles due to the combination of defective as-fabricated coatings and off-specification coatings and kernels is, therefore, to be taken as  $\geq 1.3\%$  at 78% FIMA and  $1 \times 10^{21}$  n/cm<sup>2</sup> and temperatures to 1250°C.

b. Temperatures >1250°C <1500°C (>20% FIMA) or <1600°C (<20% FIMA)

In this temperature range, failure of 100% of the fuel having calculated SiC layer stresses exceeding 30,000 psi is assumed to occur via pressure vessel rupture of the SiC layer. The effect of a rapid temperature transient can be estimated by superimposing an instantaneous temperature increase on the SiC layer stress at any fast neutron exposure. The minimum failed fuel fraction resulting from pressure vessel effects will, therefore, exceed 1% only when the calculated SiC layer stress exceeds 30,000 psi in >1% of the TRISO UC<sub>2</sub> particles.

3. Pressure Vessel Failure and SiC-Fission Product Attack

a. Peak Burnup Particles (78% FIMA and Temperatures >1500°C)

For particles at peak burnup (78% FIMA) and at temperatures >1500°C, it will be assumed that failure occurs by pressure vessel failure of coatings which have been weakened by chemical reaction with fission products. It will be assumed that prediction of fuel failure cannot be made via coupling with a calculated SiC layer stress; e.g., 30,000 psi, since it is not possible to predict the extent of weakening of the SiC coatings resulting from chemical attack. An incremental increase in failure of TRISO UC<sub>2</sub>



particles at 78% FIMA will, therefore, be assumed to occur for each 16 hours of exposure to temperature in excess of 1500°C. The increment in failure (above the previous total value for fabrication defects and pressure vessel failures) will be assumed to increase linearly from 0% at 1500° to 100% at 2000°C (see Fig. 23). It will be assumed that a new increment of failure occurs each 16 hours unless the temperature increases above the previous value (in which case the increment corresponding to the higher temperature is used). The total failure fraction is increased at each 16-hour period by adding the new incremental 16-hour failure fraction to the previous total.

b. Low Burnup Particles (<20% FIMA and Temperature >1600°C)

For low burnup particles (<20% FIMA) it will be assumed that fission product attack of the SiC layer does not effectively weaken the coatings until a temperature >1600°C is reached. At  $\leq 1600^\circ\text{C}$  fuel failure prediction will be derived from pressure vessel failure calculations based on a SiC layer failure stress of 30,000 psi, but above 1600°C, fuel at  $\leq 20\%$  FIMA will simply be assumed to undergo a new increment of failure each 16 hours. The increment of failure will be assumed to increase linearly from 0% at 1600°C to 100% at 2000°C (see Fig. 23).

c. Intermediate Burnup Particles (>20% FIMA)

Incremental failure estimates at intermediate burnups will be made by estimating the "critical" temperature ( $T_{\text{crit}}$ ) at which fission product - SiC interactions effectively weaken the SiC layer and by assuming that the incremental failure increases from the pressure vessel value at  $T_{\text{crit}}$  to 100% at 2000°C. The "critical" temperature is assumed to vary linearly from 1500°C at 78% FIMA to 1600°C at 20% FIMA and is given by:

$$T_{\text{crit}} = -1.72 (\text{BU}) + 1634 \quad (8)$$

Where:

$$T_{\text{crit}} = \text{critical temperature } (^\circ\text{C}),$$

and,

$$\text{BU} = \text{kernel burnup } (\% \text{ FIMA}).$$

When estimating fuel performance it will be assumed that figure 23 and Eq. 8 can be used to determine the incremental fraction of fuel failure occurring instantaneously during any temperature excursion. It will be assumed that a new increment of failure occurs each 16 hours and that the total fuel failure fraction is increased at the end of each 16-hour period by adding the incremental failed fuel fraction determined by using figure 23 and Eq. 8 to the previous total.

#### 4. Kernel Migration Failure

It will be assumed that fuel failure occurs when the migrating kernel contacts the inner PyC layer of the TRISO coating. A lower 95% confidence limit for fuel lifetime will be used. Subject to the results of the continued review of GASSAR, GA-LTR-17, and other licensing submittals, a core average fuel thermal gradient of  $104^\circ\text{C}/\mu\text{m}$  may be used in the calculation of  $\text{UC}_2$  migration. To account for densification of the porous buffer carbon layer, a reduction of  $23.5 \mu\text{m}$  will be used in calculating the kernel migration lifetime of the TRISO  $\text{UC}_2$  particles. The reduction should be assumed to occur linearly with fluence to a maximum shrinkage of  $23.5 \mu\text{m}$  at  $5 \times 10^{21} \text{ n/cm}^2$ . For a given temperature and temperature gradient, the migration distance,  $x$ , can be calculated using Eq. 2 and KMC as determined from figure 13 (for  $\text{UC}_2$  kernels).

B. BISO ThO<sub>2</sub> Particles

1. Defective (Imperfect As-Fabricated) Fuel

It is assumed that 0.2% of the as-fabricated BISO fuel will have defective coatings and 100% of these defective particles are failed at beginning-of-life (0% FIMA). General Atomic must provide a detailed quality assurance program which will assure that the fraction of as-fabricated defective BISO fuel particles will not exceed 0.2%.

2. Pressure Vessel Failure

a. Temperature <1250°C

To account for the presence of off-specification fuel it will be assumed that 2% of the BISO particles fail at end-of-life (7.5% FIMA) as a result of pressure vessel rupture. The minimum failed fuel fraction resulting from pressure vessel failure should be taken to increase linearly at the rate of 0.5% per year (from 0% at beginning-of-life). The total fraction of failed BISO ThO<sub>2</sub> fuel particles resulting from defective coatings and off-specification components is, therefore, 2.2% at 7.5% FIMA and temperatures to 1250°C.

b. Temperatures >1250°C

1) Peak Burnup Particles (7.5% FIMA)

For particles at peak burnup (7.5% FIMA), pressure vessel failure is assumed to increase linearly from the value for off-specification fuel (2% at 1250°C) to 100% at 2000°C. The increase in pressure vessel failure will be taken from figure 27 from the 7.5% FIMA line and will be added to the sum of the defective and off-specification fuel failure fractions (2.2% at <1250°C) to get the total failed fuel fraction.

2) Low Burnup Particles (<2.5% FIMA) and Temperatures <1350°C

For low burnup particles (<2.5% FIMA) it will be assumed that the pressure vessel failure value remains constant at 0.5% failure to 1350°C. At temperatures >1350°C the increase in pressure vessel failure is assumed to increase linearly from 0% (2.2% at EOL when off-specification and defective fuel are included) at 1350°C to 60% at 1800°C. At temperatures >1800°C the failure fraction will increase from 60% at 1800°C to 100% at 2000°C.

3) Intermediate Burnup Particles (>2.5% <7.5% FIMA)

Incremental pressure vessel failure estimates at intermediate burnups will be made by the interpolation. For a given temperature, the pressure vessel failure increment will be taken from figure 27 by assuming that the failure rate increases linearly between 2.5% to 7.5% FIMA (or 3 to  $8 \times 10^{21}$  n/cm<sup>2</sup>, if the neutron fluence exceeds burnup).

3. Kernel Migration Failure

It will be assumed that fuel failure occurs when the migrating kernel contacts the inner PyC layer of the BISO coating. A lower 95% confidence limit for fuel failure will be used. Subject to the results of the continued review of GASSAR, GA-LTR-17, and other licensing submittals, a core average fuel thermal gradient of 104°C/μm may be used in the calculation of ThO<sub>2</sub> migration. To account for densification of the porous buffer carbon layer, a reduction of 20 μm in buffer thickness (from 85 to 65 μm) will be used in calculating the kernel migration lifetime of the BISO ThO<sub>2</sub> particles. For a given temperature and thermal gradient history, the migration distance can be calculated using Eq. 2 and the KMC determined from the "upper 95% confidence internal curve" in Fig. 15 (for ThO<sub>2</sub> kernels).

V. Application and Licensing Significance

A. SORS and the MHFPR

1. General Approach

As stated in GASSAR-6, Chapter 2A, for fuel performance calculations and the MHFPR, General Atomic assumes that (1) all refueling regions are at end of cycle (to maximize fluence and burnup) and (2) that all core locations experience the fluence and burnup of the worst core location; i.e., those locations of 1, 2, 3, and 4-year-old fuel representing <1% of the core. This correlation is shown in Table IV, taken from GASSAR-6, Chapter 2A. These assumptions concerning end of cycle and worst core location resulted in the curves for fuel failure as a function of temperature and fuel age given in figures 6 and 7, for TRISO and BISO fuel particles, respectively. These figures were, as indicated earlier, also taken from GASSAR-6, Section 2A (Ref. 1).

In a manner similar to the approach used by General Atomic in the GASSAR-6 analysis, fuel failure curves were drawn for TRISO and BISO fuel particles (Figs. 28 and 29, respectively) by incorporating the above assumptions for end of cycle and worst core location in the modified fuel failure model; i.e., the model containing the requirements and assumptions discussed in the preceding section of this report. To provide better insight into the workings and logic of the NRC-modified model, the derivation of the curve in figures 28 and 29 is discussed in the following sections.

TABLE IV  
FLUENCE-BURNUP-AGE CORRELATION OF  
WORST CORE LOCATION\*

Age (yr)	Fluence ( $10^{21}$ nvt)	Burnup (% FIMA)	
		TRISO	BISO
1	2.4	59.	1.2
2	4.4	72.	3.4
3	6.2	77.	5.5
4	8.0	78.	7.5

\*From GASSAR-6 Chapter 2A (Ref. 1)

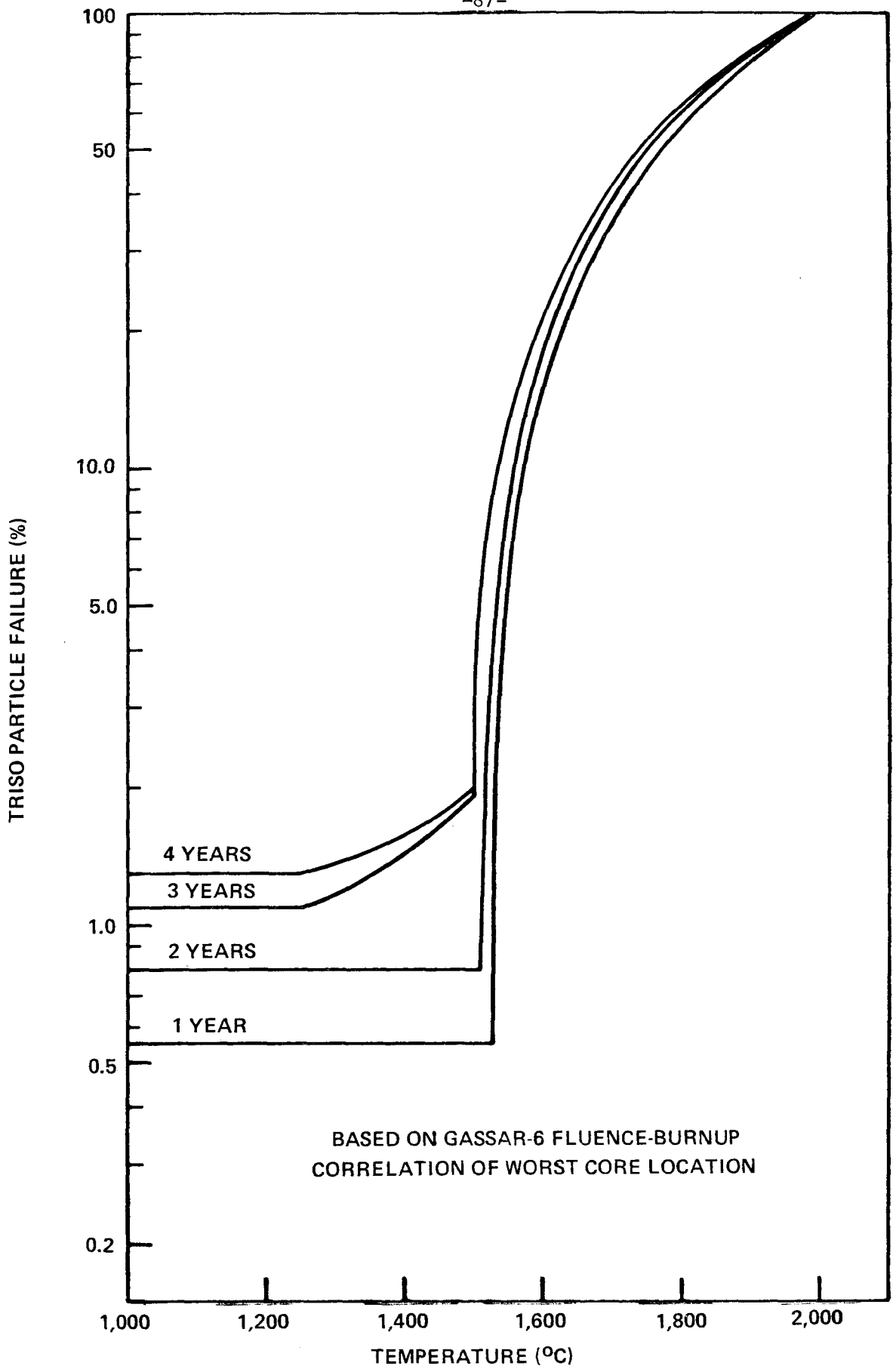


Figure 28 TRISO Particle Coating Failure

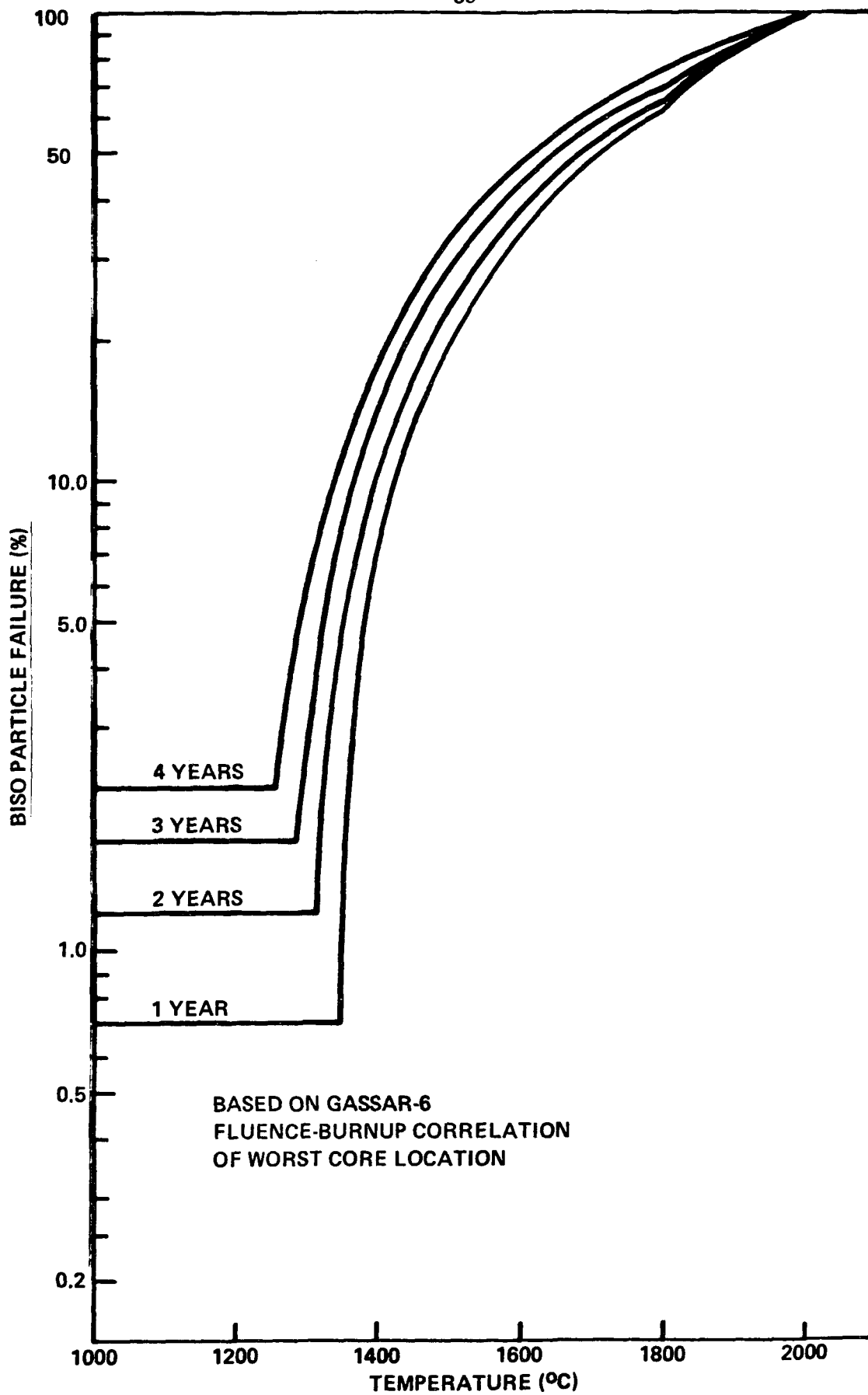


Figure 29 BISO Particle Coating Failure



## 2. TRISO Failure Curves

The horizontal portions of the curves for each fuel age shown in figure 28 were obtained from the sums of the failed fuel fractions for defective and off-specification fuel (see Sections III.A and IV.A). The defective fuel fraction is taken as 0,3% at BOL. Since a minimum failed fuel fraction due to off-specification fuel at temperatures  $\leq 1250^{\circ}\text{C}$  is taken to be 0.25%/year, the 1, 2, 3, and 4-year defective and off-specification fuel failure fractions are 0.55, 0.80, 1.05, and 1.30, respectively.

For estimates of pressure vessel failure at temperature  $>1250^{\circ}\text{C}$ , figure 19 was used along with the fluence and burnup values for each fuel age, provided in Table IV. For example, from Table IV it is seen that 3-year-old TRISO fuel at the worst core location has a fluence of  $6.2 \times 10^{21} \text{ n/cm}^2$  and a burnup of 77% FIMA. From figure 19 it is seen that at  $1500^{\circ}\text{C}$  (interpolating between the  $1425^{\circ}\text{C}$  and  $1600^{\circ}\text{C}$  curves), the plot of particle failure vs fluence yields a value of  $\sim 0,7\%$  at  $6.2 \times 10^{21} \text{ n/cm}^2$ , whereas the plot for failure vs burnup yields a value of  $\sim 0.8\%$ . Taking the higher value (0.8%) and multiplying by 2 (to account for the fact that GA assumed that only 50% of the TRISO particles having SiC layer stresses of 30,000 psi would fail), one obtains a pressure vessel failure value of 1.6% at  $1500^{\circ}\text{C}$ . Adding 0.3% for defective fuel to this value yields the total fuel failure (neglecting amoeba effects) of 1.9% for 3-year-old fuel at  $1500^{\circ}\text{C}$ . For 1- and 2-year-old fuel the failed fuel fraction is shown to remain essentially constant until a temperature is reached where SiC-fission product interaction becomes important, because the pressure vessel failure value obtained from figure 19, when added to the defective fuel value, is not greater than the assumed

total (0.55 and 0.80% for 1- and 2-year-old fuel, respectively).

The fuel particle failure curves show a very rapid increase in failure with temperature at the so called "critical" temperature, where SiC-fission product interaction becomes readily detectable. This temperature is obtained for each fuel age from Eq. 6, which related the critical temperature to burnup. Using Table IV again to correlate fuel age with burnup, one obtains a critical temperature of 1532, 1510, 1502, and 1500°C for 1, 2, 3, and 4-year fuel, respectively. The increase in fuel failure with temperatures above these "critical" temperatures is then obtained from figure 23. In the regime of SiC-fission product attack, the fuel failure is assumed to be incremental in the sense that a new increment of failure, to be obtained from figure 23, is added to the previous total for each 16 hours at temperature.

### 3. BISO Failure Curves

The curves for BISO ThO<sub>2</sub> fertile particle failure as a function of age and temperature are shown in figure 29. As with the TRISO fuel, the horizontal portions of the curves represent the totals for defective fuel plus off-specification fuel. As indicated in Sections III.B and IV.B the defective fuel fraction is assumed to be 0.2% at BOL, according to the proposed NRC model. The off-specification fuel is assumed to fail at the rate of 0.5%/year.

The assumed incremental BISO ThO<sub>2</sub> particle failure fraction is then obtained from figure 27. Since only the 1 year fuel has <2.5% FIMA burnup (as indicated in Table IV), only the 1 year fuel maintains a constant failure rate to 1350°C. The increment in failure, at temperatures above the constant failure rate line, is added to the previous total to get the "instantaneous" failure rate for BISO fuel.

#### 4. Licensing Significance

For a given location and time the SORS codes determine, in subroutine FKCALC, the percentage of failed TRISO and BISO particles based on the temperature and fuel age. Since the CORCON and SORS codes subdivide the core into radial nodes, each of which may represent many refueling regions of varying ages, a composite fuel failure fraction is calculated as the sum of the products of the failure fraction and the volumetric fraction for each age.

As shown in a comparison of the NRC-derived failure curves for TRISO fuel (Fig. 28) with the GASSAR-6 curves (Fig. 6), the curves have the same shape and form, as could be expected since the fundamental basis for the curves is the same. The major difference in the sets of curves, other than the slightly higher failure rates in the NRC-modified model at or near normal operation temperature, is the temperature at which there is a rapid increase in failure rate (due to the effect of SiC-fission product interaction). In the GASSAR-6 model, this occurs at roughly 1600-1650°C whereas in the NRC-modified model the rapid increase in failure rate occurs at approximately 1500°C. Hence, although the NRC-modified failure rates are more conservative than GASSAR-6, the difference is small when compared to the difference between this latest NRC proposed model and the original GA model shown in figure 1, or the early NRC-modification of figure 1 (which assumed, for example, that all the 4-year-old fuel failed at ~1020°C). If all other considerations remain unchanged, therefore, and also if the remaining portions of the GA model for fission product release are accepted (including dispersal from the particles, transport through the graphite, etc.), the fission product release from

TRISO fuel during an MHFPR event based on the fuel failure rates in figure 28, would not be appreciably changed from the GASSAR-6 model.

A comparison of the new proposed NRC-derived curves for BISO particle failure (Fig. 29) with the GASSAR-6, Chapter 2A curves (Fig. 7) reveal that the difference between the two are significantly greater than is the case for the TRISO failure models just discussed. The main reason for the greater difference in the BISO curves, as compared to the TRISO, is that whereas the TRISO fuel performance is fairly well coupled to a SiC layer failure stress analytical model, the BISO fuel performance has not been as well verified through experiment; thus, it was necessary to choose a more arbitrary and conservative fuel failure rate for the BISO fuel as an added safety margin to account for the increased uncertainty. The result is that the fission product release from BISO fuel will be significantly greater when using the newly proposed NRC model than is currently obtained by using the GASSAR-6, Chapter 2A method.

The relative effect of the newly-proposed fuel failure rate on the MHFPR calculation, and subsequent effects on siting considerations for the HTGR, depends on how the curves are used relative to other portions of the overall model. Thus, in the NRC safety evaluations used for Summit and Fulton, it was assumed that the fission products are released instantaneously from the fuel particles at the moment the coatings fail. The only delay in the release, according to that model, results from the delay time required during core heatup to reach the temperature at which the particles fail. In the GA approach described in SORS, however, the effects of time of fuel failure on, for example, the fraction of  $I^{131}$  released from the core during a LOFC accident, are negligible because the release from the failed fuel particles is governed by the release constants,

not by the integrity of the fuel particles as shown by a sensitivity study performed at the Los Alamos Scientific Laboratory (LASL) (Ref. 20).

The degree of importance of the fuel failure model thus depends upon the relative weight of each MHFPR model segment; i.e., it depends upon whether the GA model for fission product release (dispersal) from the fuel particles is accepted "as is", or whether this release model also requires modification (and to what degree). If, for safety analyses related to licensing concerns, the fission products are assumed to be released instantaneously from failed fuel particles, then the fuel failure rate is rate limiting in the fission product release calculation.

#### B. Fuel Failure Rate During Plant Operation

##### 1. General Considerations

The foregoing discussion has centered principally on the calculation and prediction of failed fuel fractions during accident conditions, such as the MHFPR event. There is a need, however, to have a capability for prediction of fuel failure taking into account all normal and off-normal conditions which might be expected during plant life. This is fundamentally coupled to the thermal design of the core since fuel performance limitations determine the thermal design, while in turn, the thermal design determines the fuel failure rate. The curves presented for TRISO and BISO fuel failure (Figs. 28 and 29) are, therefore, intended to provide conservative values of fuel failure for normal operation, as well as transients and accidents, for all failure mechanisms except kernel migration. The relationship of kernel migration considerations to core thermal design warrants further study, for reasons to be outlined below.

The application of the fuel failure curves given in figures 28 and 29 to normal operation is here directed toward yielding fuel failure fractions

which will lead to conservative values of fission product release for analysis of accident scenarios which follow normal operation. It must be tempered with the realization that further review of GA thermal design methods may require additional modification to the curves so as to ensure that their use will always lead to conservative estimates of fission product release. The problem is complicated by the fact that GA has not been consistent in the presentation of information dealing with fuel failure modeling. For example, as indicated in Section II.B of this report, the curves used for TRISO and BISO fuel failure presented in Section 2A of GASSAR-6 (Ref. 1) are not the same as those in the latest version of the SORS topical report (Ref. 2). Moreover, in the GA topical report dealing with "HTGR Core Thermal Design Methods and Analysis," GA-LTR-17 (Ref. 6), it is stated that the "subordinate limit" supporting the fuel failure design basis is an annual core average of 0.25% of failed BISO coatings and 0.3% of failed TRISO coatings, whereas in GA-LTR-15 (Ref. 3) it is stated that "the total coating failure predicted by the performance-limiting mechanisms described is less than 0.7% for the fuel in an HTGR during steady state operation". Elsewhere in GA-LTR-17 the statement is made that ". . . limits are set to control the total coating failure to a fuel volume fraction of 2.5% which is consistent with not exceeding the design activity level," whereas in GASSAR-6, Section 11.1, the "design" core average failed fuel fraction is listed as 2.6% (the "expected" value is given as 0.268%). On page 11.1-7 of GASSAR-6 the "maximum failed fuel particle coating fraction" is given as 10%, while the "maximum expected failed fuel fraction" is set at 1%. In another GA topical report (Ref. 7)

the EOL failed fuel fraction is stated to be 5.6% for "design" cases and 0.56% for "expected cases" . . .for KR-85 and stable gaseous species".

Several examples of the confusing and apparently conflicting sets of values for failed fuel coatings can be added to those cited above. The point to be considered is that until the confusion is eliminated, as a result of our review of GASSAR-6 and the cited topical reports, the curves given in figures 28 and 29 represent an attempt to impose a unified approach to the fuel failure analyses for all temperatures, so that reasonably conservative estimates of fission product release can be made for all HTGR conditions which may lead to off-normal operation. It should be recognized that these curves may require modification as the relationship of fuel performance to thermal design is clarified and as new test data are obtained.

As noted earlier, the fuel failure curves provided in figures 28 and 29 do not incorporate kernel migration, at least directly. For normal plant operation, however, kernel migration must be addressed, even if it is not a concern during a LOFC (MHFPR) event (as contended by GA). In this regard, in the Summit and Fulton PSARs and GA-LTR-17, GA has treated kernel migration by assuming that 40% of the buffer coating is available for normal operation while 60% is available for transients. This means, for example, that for BISO fuel,  $0.40 \times 85 \mu\text{m}$ , or  $\sim 34$  microns, of the buffer carbon is available for kernel migration during normal operation. This calculation, however, ignores the densification of the buffer, which, as indicated in the discussion in Section III.B3, can reduce the available buffer thickness by  $20 \mu\text{m}$ . A similar argument can be made for the TRISO fuel. This issue has been raised as part of the review of GA-LTR-17

(Ref. 6). It has not yet been resolved. It may be of significance in the calculation of failed fuel fraction and concomitant fission product release during normal operation. It is notable that in the GASSAR-6 application, GA no longer proposes to use the 40/60 normal operation/transient buffer thickness ratio allowance.

The fuel failure curves in figures 28 and 29, because of the conservatisms discussed earlier, should bound the effects of kernel migration, but a more precise estimate cannot be made until the core thermal analysis is evaluated. This results from the fact that the migration is a function of both temperature and thermal gradient, the values of which are estimated by the thermal analysis.

## 2. Fission Weighting and Effective Core Average Failed Fuel Fraction

The calculation of failed fuel fractions to be used to determine primary coolant source terms is further complicated by the introduction of fission weighting to determine an "effective core average failed fuel fraction." This concept, which is described in Section 11.1.1.5 of GASSAR-6 (Ref. 1) takes into account the fact that the fraction of fissions in TRISO versus BISO fuel changes during the lifetime in reactor. This is shown schematically in figure 30 for TRISO fuel; although the fraction of fissions occurring in TRISO fuel is high at BOL, the fraction of failed particles is low, and the resultant "effective core average failed fuel fraction," including the TRISO fuel contribution to this fraction will be low. This is illustrated in figure 31, which is a plot of effective failure fraction versus fuel age.

Figure 31 (from GASSAR-6, Section 11) was obtained in the following way. The effective failure fraction corresponding to a reload segment may be written as:



$$F_h = \sum_{i=1}^n \frac{1}{V_j} \sum [F_T (nvt) V_{ij} (nvt)] f_j + [F_B (nvt)] \quad (9)$$

Where  $F_h$  = fraction of fissions in fuel particles with failed coatings  
at a given nvt for reload segment j,

$$V_j = \sum_{i=1}^n V_{ij} = \text{volume of the fuel reload segment j,}$$

$V_{ij}$  = an incremental volume of the reload segment, j, which has  
experienced a fluence of "nvt",

$F_T(nvt)$ ,  $F_B(nvt)$  = TRISO and BISO failed coating fractions

$f_j$ ,  $(1-f_j)$  = the fraction of fissions occurring in TRISO and BISO  
particles, respectively) as obtained from Fig. 30.

Since at any time, there is fuel in the core from four different reload segments, ranging from 1 to 4 years in age, a core average failed fuel fraction may be obtained by evaluating  $\bar{F}_j$  in the above equations for a reload segment of each core region and determining the average of the reload segment failed fuel fraction.

The effective core average failed fuel fraction,  $F$ , was then obtained from the "sum" curve in Fig. 31 by applying the normal averaging technique of:

$$F = \frac{1}{T} \sum_{i=1}^n F_i(t) \Delta T \quad (10)$$

This resulted in an "expected effective core average failed fuel fraction" of 0.268% (for GASSAR-6). General Atomic has defined a "design" EOL failure limit which is 10 times the expected limit; therefore, this design effective core average failed fuel fraction, based on figure 31 analysis, was 2.68%.

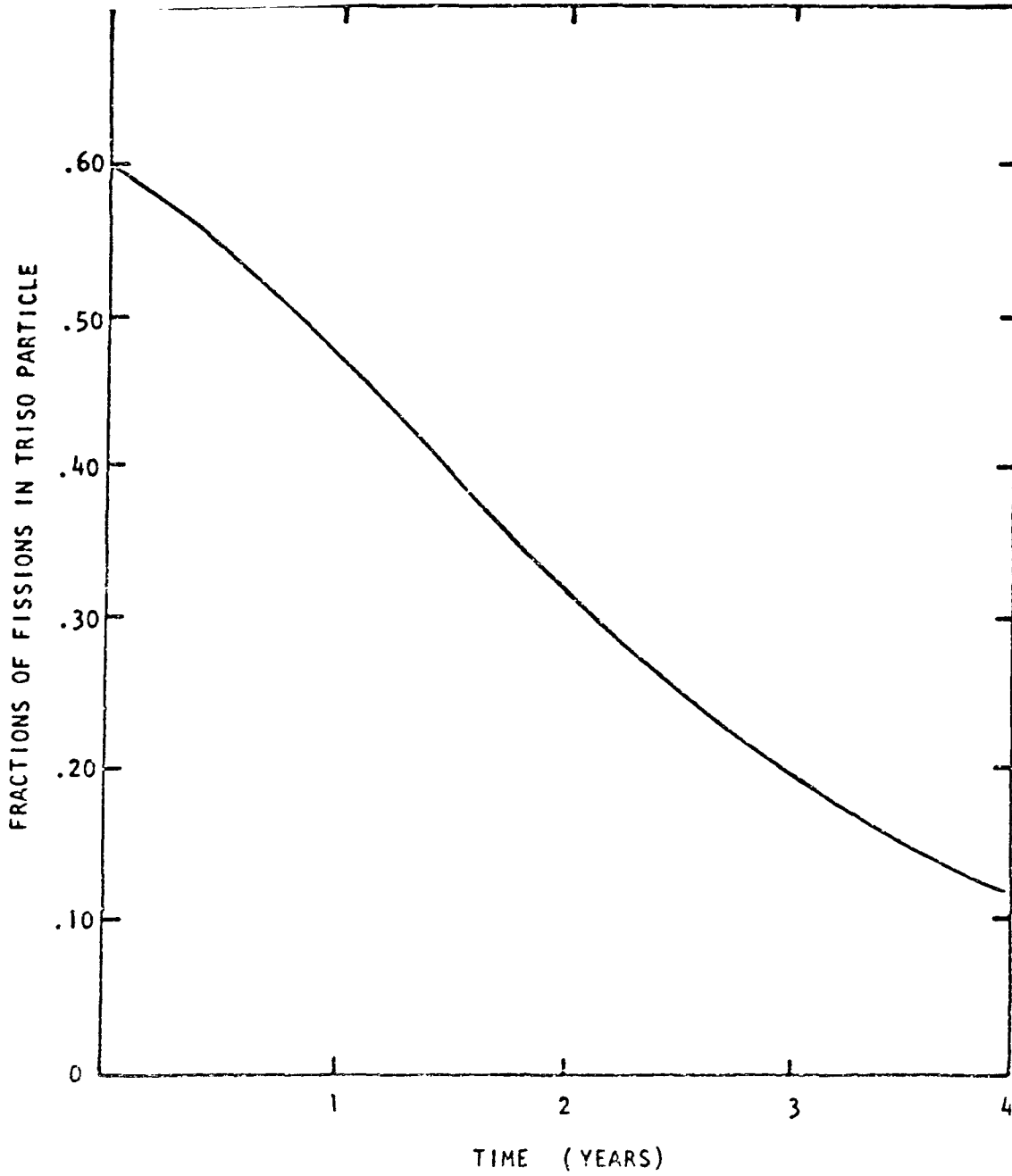


Fig. 30. Fraction of Fissions in the TRISO Particle as a Function of Time for the Equilibrium Recycle

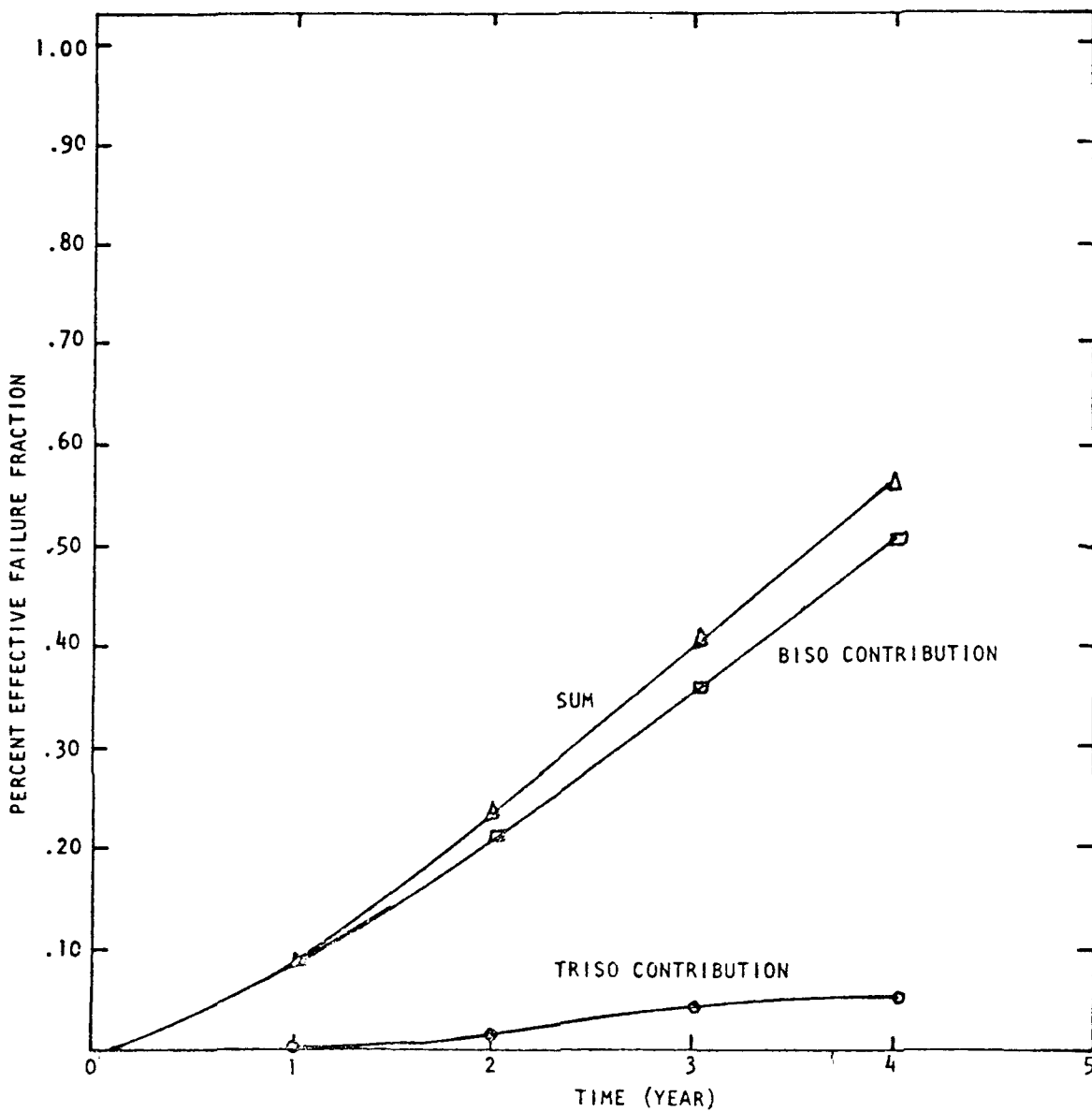


Fig. 31. Effective Failure Fraction Versus Fuel Age

It should be noted that the curves in figure 31 were based on values of  $F_t$  (nvt) which were obtained from an "old" GA fuel failure model (Ref. 8) which resulted in assumed pressure vessel failure fractions which were approximately twice those for the present GA model (Ref. 1) for temperatures  $\leq 1250^\circ\text{C}$ . Use of the new GA fuel failure model would reduce the effective expected fuel failure fractions somewhat. On the other hand, utilization of the proposed NRC guidelines for fuel failure, as illustrated in figures 28 and 29, would result in higher values for effective failed fuel fraction than shown in figure 31. This could have an effect on some aspects of accident analysis and design of some plant components, since as stated in Section 4.4.3 of the Fulton PSAR (Ref. 9), "accident analysis and plant system design are based upon a continuous core average failed fuel fraction of 2.68%". This value of 2.68% as previously stated, is 10 times the GASSAR-6 "expected" continuous core failed fuel fraction (effective) value. Multiplying the "expected" effective core average failed fuel fraction, obtained through use of the proposed NRC guidelines, by a factor of 10 might result in a higher design value than 2.68%, but the impact of this change has not yet been evaluated. Nor has it been established that the "factor of 10" is a necessary or proper approach to conservatism in establishing design values for fuel failure, accident analyses or plant system design.

#### VI. Summary and Conclusions

General Atomic has identified phenomena that contribute to coating failure in HTGR fuel particles and has proposed multi-piece models for predicting the contribution from each of these phenomena to the total failure fraction. Each of these model segments has been reviewed and evaluated in terms of the supporting data and the uncertainty associated

with the data. Some modifications to parts of the model have been proposed. These modifications are primarily based upon our judgments of the conservatism required. The magnitude of the conservatism imposed by our model modification is a function of (1) weaknesses in the as-proposed models and supporting data base, and (2) assessments of the relative impacts of the uncertainty and conservatism to the overall HTGR fuel particle coating failure model (and related fission product release model). A portion of the added conservatism was considered essential because the fundamental interrelationships of coating fabrication parameters, structure, and performance are not fully understood and are still the subject of considerable research and study. For example, it is an acknowledged fact that comparison of BISO particle irradiation behavior with model calculations is not as advanced as similar work with TRISO particles. For this reason our proposed modification to the BISO particle failure model segment presented by GA is more extensive and severe than our proposed changes to the TRISO particle coating model segment. These changes or bounds on the fuel particle coating model are, however, intended to be interim; further modifications may be required as more applicable data on reference fuel are acquired.

The review of LHTGR fuel particle coating failure models and test data has shown that these particles can be expected to perform adequately. The basic fuel design concept is sound, as is proven by the excellent performance of coated fuel particles in the Peach Bottom 1 reactor (now decommissioned) and the Dragon reactor in England. Operation of the Fort St. Vrain reactor may also yield further supporting evidence that the fuel and thermal design concepts are satisfactory. A distinction must be

made, however, between (generally) satisfactory performance and totally predictable performance. The LHTGR fuel particle qualification program has suffered from the fact that there are insufficient irradiation data on the reference fuel to permit development of failure models incorporating confidence intervals. Although the test program has yielded useful information on failure mechanisms and has shown in general how these failure mechanisms can be accommodated by specific fuel particle design features, the irradiation test program has not yet provided statistically adequate information on the reference design fuel to permit development of fuel failure probability predictions which can be accepted without qualification for safety analyses related to licensing concerns. Even for normal operation, the data base for reference design fuel particles is sparse; there are in fact no data at present for reference fuel irradiated to the design lifetime and maximum fluence and burnups.

Having determined that the LHTGR reference fuel irradiation test data base is not sufficient to permit a statistical treatment, our review of the GA models for fuel failure centered on a determination of how the models could be modified to incorporate suitable conservatism to permit their use for limited applications such as scoping studies. The models were broken down to their component parts, and each part was modified as deemed appropriate considering the existing data or lack thereof, keeping in mind that while applicable data on reference fuel might be lacking, other data of a supportive nature were available on non-reference fuel,

The LHTGR fuel particle coating performance models are, when modified according to our interim guidelines, acceptable for scoping studies. The coupling of irradiation behavior of the coating with a specific failure stress cannot be accepted without reservation, however, for reasons detailed

in Section III of this report. The BISO particle PyC coating performance, in particular, has not been demonstrably shown to be coupled to a specific failure stress. General Atomic predictions of failure probability in BISO particles at high burnups have been shown to be, in general, non-conservative and are, therefore, **unacceptable**. Further work remains to be done to qualify the BISO particle.

The coupling of TRISO coating performance to a specific failure stress (30,000 psi) in the SiC layer, while better documented than the BISO PyC case, also requires additional support, in the form of data of statistical significance on reference fuel, before it can be accepted without condition for safety analyses related to licensing. At temperatures where fission product-SiC interaction is a problem, the current data base is too sparse to permit statistical correlation of data with failure curves.

In its future efforts in fuel particle coating performance model development, General Atomic should strive to demonstrate a clear relationship between fuel particle fabrication methods and precursors, particle coating design, irradiation test results, and performance predictions. The structure and properties of carbonaceous materials are extremely dependent on the methods and nature of precursors used in fabrication, yet a clear coupling between these important parameters and the performance predictions for fuel particle coating behavior has not been demonstrated. It appears that the lack of an identifiable and unmistakable tie between fabrication parameters and performance models to a large degree results from the fact that the irradiation tests were conducted on a wide range of particles of varying design, fabricated under different conditions.

The irradiation test results, therefore, are in most cases not directly applicable to the so called "reference" design and are in almost all cases not easily traceable to particular fabrication methods and precursors. For future safety analysis reports used in licensing, fuel performance models should show a clear connection between fabrication, quality assurance, irradiation test results, and model predictions.

In retrospect it appears that the fuel particle irradiation test program was not designed and conducted for the primary purpose of qualifying a reference particle design, but was instead conceived for the purpose of checking general fabrication parameters and for screening of materials and designs. The creation or production of an adequate data base to qualify a "reference" fuel design, in terms of statistically significant numbers of samples and specimens, tested not only to the design maximum conditions of thermal/irradiation exposure but beyond as well to temperatures at which all the particles are failed (to provide a data base for the MHFPR), was apparently not identified early enough in the test program as a desirable feature for safety analyses. Consequently, at this time the need has not been satisfied. Future experiments should be designed with the primary objective of meeting this requirement. Moreover, future LHTGR fuel particle R&D should attempt to reduce the current uncertainty with respect to fuel particle failure detection. As noted in the discussion, some methods of failure detection appear to be more accurate than others. Unfortunately, the visual methods upon which General Atomic has relied heavily, are among the most inaccurate, but the degree of error in each method has not yet been determined quantitatively. Such an assessment must be made in judging



the worth of the data used in safety analyses. Therefore, it is suggested that future fuel particle development programs should be designed keeping in mind the need to provide better quantified data with respect to fuel failure detection error.

An attempt has been made in this study of General Atomic's LHTGR fuel particle coating failure models and data base to provide a fairly comprehensive evaluation. Because of observed weaknesses in the existing data base and models proposed by GA, suggested guidelines have been presented for an interim model. This review, however, is not intended as an all-encompassing work. Because of the ambiguities and uncertainties cited above and also because the connection between the fuel design and thermal design has not yet been completely established, this study is not all-inclusive. Also we have not intended to imply that the fuel failure mechanisms identified and treated by the failure models presented in this report are all-inclusive. General Atomic has, for example, inadequately addressed fuel rod matrix-coating interaction although it is known to be a potential problem when the fuel rod fabrication method known as "in-block carbonization" is used. This example again illustrates the potential coupling of fabrication methods and precursors with failure mechanism and probability. It also illustrates the problem of qualifying a reference fuel design, when the fuel performance is dependent upon fabrication parameters which must be evaluated by complicated, lengthy, and expensive irradiation tests. Again, the method of failure detection plays a potential major role in connection with this particular failure mechanism because fuel rod matrix-particle coating interaction is not easy to detect and can only be identified by tedious metallographic examination of individual fuel particles. We have not attempted in this study to

critique the applicability and relevancy of the different types of tests used in the HTGR fuel particle irradiation test program. This is, itself a complex issue and should be the subject of a separate study. We do believe, however, that the testing to date has been conducted within the state-of-the-art at the time.

We believe that, the weaknesses in the current data base and models notwithstanding, General Atomic's approach to the design and modeling of LHTGR fuel particles is basically sound; that is, considering the fact that there are approximately  $10^{11}$  fuel particles in a large HTGR core, it is not possible to inspect each particle individually to ensure that it is perfect and that it will not fail in service. A quality assurance program that will provide assurance that a predictable number of unsatisfactory particles is not exceeded is needed, coupled to fuel performance models that will predict failure probabilities with reasonable confidence. Improvement in the data base and models are needed, however, for licensing purposes.

For consistency, it is believed that there should ultimately be a single fuel failure model for the HTGR, that the model should accurately describe the relevant phenomena, and that this model should be applicable to all conditions; thus the same basic fuel failure model should be used for the accidents as well as for normal operation. It should only be necessary to change the input to the model; e.g., temperatures for different operating conditions, or to moderate the output as is proposed, for example, by the use of fission weighting for steady-state operation.

VII, REFERENCES

1. General Atomic Standard Safety Analysis Report (GASSAR), GA-A13200, Docket No. STN 50-535.
2. M. H. Schwartz, D. B. Sedgley, and M. M. Mendonca, "SORS" Computer Programs for Analyzing Fission Product Release from HTGR Cores During Transient Temperature Excursions, " GA-A12462 (GA-LTR-10), April 15, 1974.
3. C. L. Smith, "Fuel Particle Behavior Under Normal and Transient Conditions," GA-A12971 (GA-LTR-15), October 21, 1974.
4. C. L. Smith, "In Support of LHTGR Fuel Performance Models for MHFPR Studies," General Atomic Memorandum #CLS:030: FMB:75, Submitted to NRC on October 21, 1975.
5. K. E. Schwartztrauber and F. A. Silady, "CORCON": A Program for Analysis of HTGR Core Heatup Transient," GA-A12868 (GA-LTR-13) July 15, 1974.
6. A. S. Shenoy and D. W. McEachern, "HTGR Core Thermal Design Methods and Analysis," GA-A12985 (GA-LTR-17), December 1974.
7. M. J. Haire and D. W. McEachern, "Gaseous Radioactivity Levels in the Primary Coolant of an HTGR." (GA-LTR-14), October 1, 1974.
8. Summit Power Station, Unit 1 & 2, Preliminary Safety Analysis Report, Docket No. 50-450/451.
9. Fulton Generating Station, Units 1 & 2, Preliminary Safety Analysis Report, Docket No. 50-463/464.
10. NRC Memorandum, V. A. DeLiso, "Summary of Meeting Held February 6, 1975, to Discuss the Source Term and Dose Calculations of the MHFPR for the HTGRs.
11. Safety Evaluation - Summit Power Station, Units 1 & 2, October 1974.
12. "HTGR Safety Studies Progress Report for the Period Ending June 30, 1974," GCR-DL674-2, August 21, 1974.
13. J. W. Prados and J. L. Scott, "Mathematical Model for Predicting Coated Particle Behavior," Nuclear Applications 2, 402 (1966).
14. J. L. Kaae, K. W. Stevens, and C. S. Luby, "Prediction of the Irradiation Performance of Coated Particle Fuels by Means of Stress Analysis Models," Nuclear Technology 10, 44 (1971).
15. T. D. Gulden, C. L. Smith, D. P. Harmon, and W. W. Hudritsch, "The Mechanical Design of TRISO-Coated Particle Fuels for the Large HTGR," NUCL, Technol. 16, 100-9 (1972).

16. T. D. Gulden, D. P. Harmon, and O. M. Stansfield, "Design and Performance of Coated Particle Fuels for the Thorium Cycle HTGR," GA-12628, January 24, 1974.
17. T. D. Gulden, "Carbon Thermal Diffusion in the  $UC_2C$  System," J. Am. Ceram. Soc., No. 1. 14-18 (1972).
18. "HTGR Base Program Quarterly Report for the Period Ending November 30, 1973, GA-A12818, December 28, 1973.
19. M. T. Morgan, "Review of HTGR Coated Fuel Particle Stability," ORNL-TM-4882, August, 1975.
20. John E. Foley, " $^{131}I$  Release from an HTGR During the LOFC Accident," LA-5893-MS, March 1975.

1

2

3  
4  
5  
6  
7  
8  
9  
10  
11  
12  
13  
14  
15  
16  
17  
18  
19  
20  
21  
22  
23  
24  
25  
26  
27  
28  
29  
30  
31  
32  
33  
34  
35  
36  
37  
38  
39  
40  
41  
42  
43  
44  
45  
46  
47  
48  
49  
50  
51  
52  
53  
54  
55  
56  
57  
58  
59  
60  
61  
62  
63  
64  
65  
66  
67  
68  
69  
70  
71  
72  
73  
74  
75  
76  
77  
78  
79  
80  
81  
82  
83  
84  
85  
86  
87  
88  
89  
90  
91  
92  
93  
94  
95  
96  
97  
98  
99  
100

